Comparative study on the molecular structure of ethylene/1-octene, ethylene/1-heptene and ethylene/1-pentene copolymers using advanced analytical methods

by

Anthony Ndiripo

Thesis presented in partial fulfilment of the degree of
Master of Science (Polymer Science)

at the

University of Stellenbosch

Supervisor: Professor Harald Pasch   March 2015

Declaration

By submitting this thesis electronically, I declare that the entirety of the work contained therein is my own, original work, that I am the sole author thereof (save to the extent explicitly otherwise stated), that reproduction and publication thereof by Stellenbosch University will not infringe any third party rights and that I have not previously in its entirety or in part submitted it for obtaining any qualification.

Anthony Ndiripo   March 2015

Abstract

Linear low density polyethylene (LLDPE), one of the fastest growing types of polyethylene, is made from the copolymerisation of ethylene and higher 1-olefin comonomers. 1-octene is the comonomer of choice as it gives mechanically better LLDPEs as compared to other 1-olefins. Recently, a shortage of 1-octene has been observed in the global market. Considering the fact that ethylene/1-heptene (EH) copolymers may have properties that are very similar to those of ethylene/1-octene (EO), replacing 1-octene with 1-heptene as the comonomer in the manufacture of commercial linear low density polyethylene (LLDPE) is a viable option.

In order to do so, evaluation of microstructural and mechanical properties of both types of resins and their comparison were carried out first. Several LLDPE resins were synthesised using Ziegler-Natta (ZN) and metallocene type catalysts. The LLDPE resins were made using varying amounts of the comonomer to obtain copolymers of different compositions. Ten of the ZN-LLDPE resins became the core focus of the present study. Carbon-13 nuclear magnetic resonance spectroscopy (^{13}C NMR) showed the differences in the compositions of both the EH and EO resins. Crystallisation analysis fractionation (CRYSTAF), differential scanning calorimetry (DSC) and high temperature high performance liquid chromatography (HT-HPLC) revealed the presence of at least two fractions within the EH and EO copolymers which varied in quantity and chemical composition as the comonomer content was increased. The fractions were identified as being the copolymer (of ethylene and the comonomer) and polyethylene. Comparisons of the EH and EO CRYSTAF and HPLC data showed similarities in the microstructures of the resins. Preparative-temperature rising elution fractionation (prep-TREF) was used to obtain several fractions from each resin for quantification and analyses. DSC, HT-HPLC, CRYSTAF, and ^{13}C NMR revealed close similarities in the fractions of EH and EO copolymers with comparable comonomer contents. It also was revealed that TREF fractionations are influenced by the bulk resin comonomer content.

EH and EO copolymers demonstrated high similarities in tensile strength and Young's modulus at comonomer contents of < 3 mol %. Minor differences in the mentioned properties at comonomer content of > 3 mol % were attributed to the slightly better ability of 1-octene at reducing crystallinity as compared to 1-heptene as well as small differences in the comonomer contents of the test samples. The results of the study suggest that 1-heptene can be used in the place of 1-octene in the commercial manufacture of LLDPE.

Opsomming

Lineêre lae digtheid poliëtileen (LLDPE), een van die vinnigste groeiende poliëtileen tipes, word produseer deur die ko-polimerisasie van etileen en 'n hoër 1-olefien ko-monomeer. 1-okteen is die ko-monomeer wat die meeste gebruik word aangesien dit LLDPE met die beste meganiese eienskappe produseer. Daar is egter 'n tekort aan 1-okteen in die globale mark. Aangesien etileen/1-hepteen (EH) kopolimere moontlik soortgelyke eienskappe het as etileen/1-okteen (EO), kan 1-okteen moontlik vervang word deur 1-hepteen as 'n komonomeer in die produksie van LLDPE.

Om dit te doen is die meganiese en mikrostrukturele eienskappe van beide polimere geëvalueer. Verskeie LLDPE polimere is gesintetiseer met behulp van Ziegler-Natta (ZN) en metalloseen kataliste. Die komonomeer inhoud is gevarieer om LLDPE polimere te produseer met verskillende komposisie. Tien van die gesintetiseerde ZN-LLDPE polimere is gekies en is die kernfokus van die huidige studie. ^{13}Koolstof kern magnetiese resonans spektroskopie (^{13}C KMR) het die variasie in ko-monomeer inhoud bevestig van beide die EH en EO polimere. Kristallisasie analise fraksioneering (CRYSTAF), differensiële skandeer kalorimetrie (DSC) en 'n hoë temperatuur hoë verrigting vloeistof chromatografie (HT-HPLC) het die teenwoordigheid van ten minste twee fraksies binne die EH en EO ko-polimeer bevestig wat 'n variasie in hoeveelheid en chemise samestelling getoon het met 'n toename van die ko-monomeer inhoud in die ko-polimeer. CRYSTAF en HT-HPLC data het getoon dat hierdie fraksies in EH en EO ooreenkomstige mikrostrukturele gedrag getoon het. Preparatiewe temperatuur styging elueering fraksioneering (prep-TREF) is gebruik om die polimere te fraksioneer om sodoende kwantitief die poliëtileen fraksies te verky en te analiseer. Verdere analise van die fraksies deur DSC, HT-HPLC, CRYSTAF en ^{13}C KMR het getoon dat die fraksies, bekom van die EH en EO kopolimere met vergelykbare ko-monomeer inhoud, baie dieselfde eienskappe toon. Die analises het ook getoon dat die TREF fraksionering beinvloed word deur die ko-monomeer inhoud van die oorspronklike ko-polimeer.

EH en EO kopolimeer het vergelykbare treksterkte en Young se modulus, indien die komonomeer inhoud minder as 3 mol % is. Klein verskille in treksterkte en Young se modulus is waargeneem vir monsters met 'n komonomeer inhoud van meer as 3 mol %. Hierdie verskille kan toegeskryf word aan die klein verskille in komonomeer inhoud van die monsters asook die vermoë van 1-okteen, in vergelyking met 1-hepteen, om die kristallinitiet te verminder. Die resultate van die projek toon dat 1-hepteen in die plek van 1-okteen gebruik kan word vir die kommersiële vervaardiging van LLDPE.

Acknowledgements

Firstly I would like to thank **God** for life, and for His guidance throughout this study.

My utmost gratitude goes to my supervisor **Prof. Harald Pasch** for the opportunity to study in his group, his guidance, financial support and encouragement throughout the course of this study. The discussions we had were certainly very educative and enlightening.

My most sincere thanks go to the following:

Dr. S. Cheruthazhekatt and **Mr. M.J. Phiri** for their immense help with the analytical instruments used in this study and also for being good friends.

Dr. Dawie Joubert (SASOL) for supplying the Ziegler-Natta LLDPE samples as well carrying out density determinations.

Dr. M. Brand (Maggie) who was very helpful with the synthesis of metallocene LLDPE samples as well as great help with the CRYSTAF instrument.

Dr. Jaco Brand and Mrs Elsa Malherbe for the solution NMR analyses.

Dr. Pritish Sinha for solid state NMR analyses.

Dr. Andy Roediger and Ms. Illana Bergh of Roediger Agencies for allowing me to use their facilities and for the help with the mechanical analyses.

Prof. A.J. van Reenen for the access to the olefins lab where most of the experimental work was carried out.

All members and staff of the Department of Chemistry and Polymer Science, **Mrs Erinda Cooper**, **Mrs Aneli Fourie, Mr Deon Koen, Mr Jim Motshweni** and **Mr Calvin Maart.**

All members of the Pasch's group past and present: **Trevor, Douglas, Mohau, Kerissa, Ashwell, Nadine, Khumo, Lebogang, Zanelle, Guilaume, Nyasha, Pritish, Carlo, Helen and Maggie.**

Mr. Divann Robertson for being helpful with the DSC instrument as well as **Mr. Sifiso Magagula** for being a good friend.

SASOL and **NUST** for funding.

Table of contents

Table of Figures

List of Schemes

List of Tables

List of Symbols

-CH	Methine group
$-CH_2$	Methylene group
$-CH_3$	Methyl group
ΔH_m	Melting enthalpy
ΔH	Enthalpy
MHz	Megahertz
M_w	Weight-average molecular weight
T_c	Crystallisation temperature
T_m	Melting temperature
V_h	Hydrodynamic volume
V_r	Retention volume
θ_m	Magic angle
X_c	Crystallinity

List of Abbreviations

2D-LC	2-dimensional-liquid chromatography
^{13}C	Carbon-13
^{13}C NMR	Carbon-13 nuclear magnetic resonance
ATR	Attenuated total reflectance
ATR-FTIR	Attenuated total reflectance-Fourier transform infrared
BHT	Butylated hydroxytoluene
CEF	Crystallisation elution fractionation
CP-MAS	Cross polarisation magic angle spinning
CRYSTAF	Crystallisation analysis fractionation
DEAC	Diethylaluminum chloride
DMA	Dynamic mechanical analysis
DSC	Differential scanning calorimetry
EH	Ethylene/1-heptene
ELSD	Evaporative light scattering detector
EO	Ethylene/1-octene
FTIR	Fourier Transform infrared spectroscopy
GPC	Gel permeation chromatography
HDPE	High density polyethylene
HPLC	High performance liquid chromatography
HT-2D-LC	High-temperature 2-dimensional liquid chromatography
HT-HPLC	High temperature liquid chromatography
HT-SEC	High-temperature size exclusion chromatography
IR	Infrared
LCB	Long chain branching
LDPE	Low density polyethylene
LLDPE	Linear low density polyethylene
MAO	Methylaluminoxane
m-LLDPE	Metallocene linear low density polyethylene

MM	Molar mass
MMD	Molar mass distribution
MDPE	Medium density polyethylene
NMR	Nuclear magnetic resonance
o-DCB	*ortho*-Dichlorobenzene
PE	Polyethylene
SCB	Short chain branching
SCBD	Short chain branching distribution
SEC	Size exclusion chromatography
SEC-FTIR	Size exclusion chromatography-Fourier-transform infrared
SEM	Scanning electron microscopy
SGIC	Solvent gradient interaction chromatography
TIBA	Tri-isobutyaluminium
TCB	1,2,4-trichlorobenzene
TCE-d2	Deuterated 1,1,2,2-tetrachloroethane
TEA	Triethylaluminium
TREF	Temperature rising elution fractionation
UHMWPE	Ultra-high molecular weight polyethylene
ULMWPE	Ultra-low molecular weight polyethylene
VLDPE	Very-low density polyethylene
ZN	Ziegler-Natta
ZN-LLDPE	Ziegler-Natta linear low density polyethylene

Chapter 1

Introduction

1.1   Background

Polyolefins constitute about 60 % of the global plastics market and continue to grow with an annual increase of approximately 5 − 6 % [1-3]. Polyethylenes and polypropylenes are the major types of polyolefins on the market and their demand continues to grow due their good physical and mechanical properties, non-toxicity, energy efficient production, low cost and easily available raw materials. Polyethylenes contribute about 50 % of all polyolefin global consumption and one of the fastest growing types of polyethylene is linear low density polyethylene (LLDPE). The growth of the LLDPE market has been largely attributed to its superior properties over low density polyethylene (LDPE) [4].

LLDPEs are random copolymers of ethylene and a variety of higher 1-olefins. Commonly used 1-olefins are 1-butene, 1-hexene, 1-octene and 4-methyl-1-pentene [5, 6]. Further odd-numbered comonomers are given in patent literature and these include 1-pentene, 1-heptene and 1-nonene [7, 8]. These 1-olefins introduce short chain branching which is very important to the overall microstructure of LLDPEs. Depending on the 1-olefin used, the length of the short branch or side chain can vary from ethyl through butyl to hexyl in the case of 1-butene, 1-hexene and 1-octene respectively [9]. Short chain branching (SCB) gives LLDPE better mechanical and physical properties as compared to LDPE. The size of the 1-olefin used to induce short chain branching also has a significant importance for the resin produced [9]. It is known that mechanical properties of the LLDPE material improve as the length of the side chain increases [9]. Thus 1-octene gives LLDPE with superior tear resistance and better stretch capabilities [7] as compared to those made from 1-hexene or 1-butene. Dow Chemical's Dowlex, Insite and Engage materials are some examples of commercially available LLDPE materials synthesised using 1-octene as the comonomer. In addition, the type of catalyst used for synthesis plays an important role in the incorporation of the comonomer and overall short chain branch distribution (SCBD). Generally,

metallocene or single site catalysts are known to produce homogeneous resins whilst Ziegler-Natta catalysts produce heterogeneous resins with respect to molar mass and chemical composition distribution.

Due to the high demand in 1-octene for LLDPE purposes, a shortage has been observed on the global monomer market. Fischer-Tropsch derived monomers, in particular 1-heptene, are good alternatives when considering their close similarity to the currently favoured "even numbered" 1-olefins. SASOL produces large quantities of these odd numbered 1-olefins from their Fischer-Tropsch process. Considering their availability as well as comparatively cheaper prices [10], they become interesting alternatives to more conventional monomers. In addition, there are currently no LLDPEs on the market with 1-pentene and 1-heptene as comonomers. SASOL Technology [8] have patented polymerisation procedures involving Fischer-Tropsch derived odd numbered 1-olefins in the manufacture of terpolymers of ethylene and higher 1-olefins. Dow Global Technologies Inc. [7] have also patented the copolymers of ethylene and 1-heptene but such copolymers are still absent from the LLDPE market due to limited access to 1-heptene.

Ethylene/1-heptene (EH) copolymers may have properties that are very similar to those of ethylene/1-octene (EO) copolymers, therefore, replacing 1-octene with 1-heptene as a comonomer in commercial LLDPE may become a favourable option. However, in order to do so, typical EH and EO copolymers must be evaluated and compared to each other regarding molecular structure and structure-property relations. An extensive study on the copolymerisation behaviour of ethylene with 1-butene, 1-pentene, 1-hexene, 1-heptene, 1-octene and 1-nonene was carried out by Joubert [11] as part of his PhD work. In his findings, it was concluded that the type of comonomer plays an important role in the overall physical and mechanical properties of the resins such as density, tensile strength as well as impact strength. However, no details on the molecular heterogeneity of the copolymers were presented. The study also indicates that comparable material properties can be obtained for the monomers if smaller 1-olefins such as 1-pentene are gradually higher in content as compared to 1-octene in the respective copolymers [11]. From their findings, Tincul *et al*. [12-14] suggested that properties of ethylene/1-heptene copolymers may be intermediate to those of ethylene/1-hexene and ethylene/1-octene resins with comparable comonomer contents.

Not much is known about the molecular heterogeneity of LLDPE materials from odd numbered 1-olefins especially in terms of differences in microstructure. Therefore, emphasis is placed on understanding the differences and similarities in microstructure of ethylene/1-heptene and ethylene/1-octene copolymers at a molecular level. The microstructure of LLDPE can be very complex and hence needs a multidimensional analytical approach. With recent advances in analytical techniques it becomes easier to determine the molecular structure of these LLDPEs and correlate them to physical properties thereby answering the ultimate question, "Can 1-heptene be used in the place of 1-octene in the industrial manufacture of LLDPE?" Recent studies [9, 15, 16] have also shown that microstructure i.e. molar mass distribution (MMD) as well as chemical composition distribution (CCD) [17] plays an important role in determining physical and mechanical properties of any polymer resin.

1.2   Aim

The main aim of the project is to investigate the microstructure of ethylene/1-heptene and ethylene/1-octene copolymers using advanced analytical methods and to correlate the obtained information with the physical and mechanical properties of the copolymers. Emphasis is placed on comparing Ziegler-Natta ethylene/1-heptene and ethylene/1-octene copolymers since their comonomers are closely related.

1.3   Objectives

1. To synthesise ethylene/1-heptene and ethylene/1-octene copolymers with different molar masses and different comonomer contents using the following catalyst systems:
    - Ziegler-Natta
    - Metallocene
2. To investigate the molar mass and molar mass distributions as well as the chemical composition distributions using advanced analytical techniques such as high temperature-size exclusion chromatography (HT-SEC), differential scanning calorimetry (DSC), high-temperature high performance liquid chromatography (HT-HPLC), high temperature two-dimensional liquid chromatography (HT-2D-LC) , carbon-13 nuclear magnetic

resonance (^{13}C NMR), Fourier transform infrared spectroscopy (FTIR), and crystallisation analysis fractionation (CRYSTAF).

3. To fractionate the bulk samples using preparative temperature rising elution fractionation (prep-TREF).

4. To analyse the fractions for molar mass and chemical composition distribution using the analytical tools mentioned in Objective 2.

5. To investigate the physical and mechanical properties of the copolymers (density, tensile strength, Young's modulus, melting and crystallisation temperatures as well as crystallinity).

6. To determine the influence of the copolymer microstructure on the physical and mechanical properties of both types of LLDPEs.

1.4   Layout of thesis

Chapter 1

Chapter 1 introduces the problem and identifies the main aim as well as outlines the detailed objectives of the study. A layout of the thesis is also given herein.

Chapter 2

Chapter 2 presents a brief discussion of theoretical and historical backgrounds of polyethylene as well the different catalyst systems used for coordination polymerisation. Types of polyethylene and the conditions used for their manufacture are discussed. Factors affecting molecular properties of LLDPE such as crystallinity and branching are discussed. Attention is also given to the types of analytical techniques used in the fractionation and analysis of the LLDPE materials as they are the core of this study. Advantages and disadvantages of these techniques are also given.

Chapter 3

Experimental procedures used in this study are discussed and explained in Chapter 3. These include synthesis and catalyst preparation, prep-TREF, CRYSTAF, ^{13}C NMR, DSC, FTIR, HT-SEC, HT-HPLC, HT-2D-LC, density and tensile strength determination.

Chapter 4

In Chapter 4, results of the study on the bulk LLDPE samples are discussed and correlated. Molecular properties of different LLDPE samples are discussed and compared to mechanical properties such as tensile strength.

Chapter 5

A detailed discussion on the findings of prep-TREF and fraction analyses is given in Chapter 5. Results of the various fraction analyses techniques are correlated to give a detailed understanding of microstructure and of prep-TREF as a technique itself.

Chapter 6

Conclusions from the findings of the study are drawn in Chapter 6. Recommendations for future work are also given.

1.5   References

1.   Hilken G., *Kunststoffe*, **2005**, 10, 34–40.

2.   Kaminsky W., *Macromol. Chem. Phys.*, **2008**, 209(5), 459–466.

3.   Zhang J., Li B.-G., Fan H., and Zhu S., *J. Polym. Sci., Part A: Polym. Chem.*, **2007**, 45(16), 3562–3569.

4.   Hosoda S., *Polym. J.*, **1988**, 20(5), 383–397.

5.   Zhou X. and Hay J. N., *Eur. Polym. J.*, **1993**, 29(2–3), 291–300.

6.   Hsieh E. T. and Randall J. C., *Macromolecules*, **1982**, 15(5), 1402–1406.

7.   Hagen H. H. and van Der Heijden L. P. P., *Copolymers of ethylene and 1-heptene*, **2004**, United States Patent: US 7312295 B2.

8.   Joubert D. J., Tincul I., and Young D. A., *Polymerization*, **2002**, European Patent: EP 1 231 228 A1.

9.   Gupta P., Wilkes G. L., Sukhadia A. M., Krishnaswamy R. K., Lamborn M. J., Wharry S. M., Tso C. C., DesLauriers P. J., Mansfield T., and Beyer F. L., *Polymer*, **2005**, 46(20), 8819–8837.

10.   Tincul I., Joubert D., and Sanderson R., *Macromol. Symp.*, **2007**, 260(1), 58–64.

11.   Joubert D. J., *Ethylene and propylene copolymers utilizing Fischer-Tropsch α-olefins*, PhD Thesis, Stellenbosch University, **2000.**

12.   Tincul I., Smith J., and van Zyl P., *Macromol. Symp.*, **2003**, 193(1), 13–28.

13.   Joubert D., *Macromol. Symp.*, **2002**, 178(1), 69–80.

14.   Tincul I., Lufuno S., and Rawatlal R., *Macromol. Symp.*, **2004**, 213(1), 357–366.

15.   Li Pi Shan C., Soares J. B. P., and Penlidis A., *Polymer*, **2002**, 43(3), 767–773.

16.   Simanke A. G., Galland G. B., Baumhardt Neto R., Quijada R., and Mauler R. S., *J. Appl. Polym. Sci.*, **1999**, 74(5), 1194–1200.

17.   Piel C., Starck P., Seppälä J. V., and Kaminsky W., *J. Polym. Sci., Part A: Polym. Chem.*, **2006**, 44(5), 1600–1612.

Chapter 2

Historical and theoretical background

2.1   Introduction

Polyolefins have been the dominant materials class on the plastic market. Often it has been predicted that polyolefins would lose market shares to new high performance plastics, but this has never happened thanks to continuous improvements in their performance [1, 2]. A major component of the polyolefins market is polyethylene and it is the most widely used thermoplastic in the world, being fashioned into products ranging from clear food wrap and plastic bags to laundry detergent bottles and automobile fuel tanks [3, 4].

Polyethylenes dominate the current global consumption with an estimated market share of 60 % as of 2010 [5]. Polyethylenes are further subdivided into several classes based on density and molecular structure, which are influenced by polymerisation conditions. Major types of polyethylene (according to sold volumes) are discussed in detail in Section 2.3. Of these classes of polyethylenes, linear low density polyethylene (LLDPE) has over the years continued to grow and take the market share of low density polyethylene (LDPE) due to superior properties such as puncture resistance and better film properties [6, 7]. Details on the differences of these polyethylene resins are given in Section 2.3. The development of current materials which we use in our day to day lives has come a long way.

2.2   Historical background

The earliest report on the synthesis of polyethylene was reported in 1898 by von Pechmann when he observed a white substance that formed when diazomethane was dissolved in ether [8]. Pechmann would later call this composition "polymethylene", making him the first person to name the newly discovered compound. Bamberger and Tschirner [9] later produced and characterised the compound from the same technique as Pechmann. They stated that its structure was $(CH_2)_n$ and it had a melting point of 128 °C.

Industrial development for the synthesis of polyethylene only took place in the early 1930s after a small amount of polyethylene was accidentally produced at British company Imperial Chemical Industries (ICI). ICI established a research program with the goal of investigating the high pressure chemistry of selected organic compounds which also included ethylene [10]. Peacock [10] reports that on 29 March 1933, Eric Fawcett and Reginald Gibson discovered a sub gram quantity of a white waxy polymer of ethylene lining the reaction vessel of a failed experiment in which ethylene and benzaldehyde had been reacted.

In 1953, Karl Ziegler and his group discovered that zirconium and titanium salts produce polyethylene of high molar masses when combined with an aluminium co-catalyst [11-13]. Meanwhile, Giulio Natta found out that isotactic polypropylene (iPP) can be synthesised with certain conditioning and preparations of the catalyst. Both these discoveries led to widespread commercialisation of some key thermoplastics such as LLDPE, high density polyethylene (HDPE) and PP. Both Ziegler and Natta were awarded with the Nobel Prize for chemistry in 1963 for their contributions [11, 14].

Later on, Kaminsky and Sinn discovered several catalyst systems based on metallocene complexes that are highly active in ethylene polymerisation reactions. They also discovered enormous increases in the activity of the metallocene catalysts when methylaluminoxane (MAO) was used as a co-catalyst [15]. These new catalysts offer more control in molecular stereoregulation as well as uniformity in comonomer insertion as compared to Ziegler-Natta catalysts. Comparisons of different catalytic systems that are used to polymerise ethylene are given in Section 2.4.

2.3   Main types of polyethylene

Polyethylenes can be classified in many classes such as ultra-high-molecular-weight polyethylene (UHMWPE) [16], ultra-low-molecular-weight polyethylene (ULMWPE or PE-WAX) [17], high-molecular-weight polyethylene (HMWPE), high-density polyethylene (HDPE) [18], medium-density polyethylene (MDPE) [19], linear low-density polyethylene (LLDPE) [20], low-density polyethylene (LDPE) and very-low-density polyethylene (VLDPE) [21].

However, with regard to sold volumes LDPE, LLDPE and HDPE are the most important [22] and they will form part of the discussion that will follow.

2.3.1   Low density polyethylene (LDPE)

LDPE is manufactured using high pressures with ethylene as the only monomer. Usually pressures ranging between 82 and 286 MPa and temperatures in the range of 132 to 332 °C are used [22]. The density or crystallinity of the resultant resin depends upon the temperature used. Molar mass and molar mass distribution depend upon the pressure used as well the concentration of chain transfer agents (these include 1-olefins such as propylene and 1-butene as well as aliphatic hydrocarbons such as propane and butane). One important feature that characterises the molecular structure of LDPE is long chain branching (LCB). Long chain branching gives LDPE a more complex structure as compared to LLDPE or HDPE. Molar mass increases with decreased temperature or increased pressure and LCB increases with temperature. It is extremely difficult to control the level of long chain branching and batches may vary significantly. A small amount of oxygen or organic peroxide is used as an initiator for the reaction. Molar masses are usually in the range of 10,000 to 50,000 g/mol [23].

Challenges with the manufacture of LDPE include the high capital investment for commercial plant construction, engineering problems that are related to high pressure operation, and high energy expenses in production [24]. Until recently, the production of LDPE has been limited to free radical processes only [25, 26]. The use of catalysts which can form branched polyethylene at low pressures will have enormous advantages as costs will be cut in the equipment used for high pressure reactions and the funds needed for their maintenance.

2.3.2   Linear low density polyethylene (LLDPE)

Linear low density polyethylenes (LLDPEs) are made through the copolymerisation of ethylene and a 1-olefin, for example 1-butene, 1-hexene, 1-octene and 4-methyl-1-pentene [6, 27, 28]. LLDPE is produced using Ziegler-Natta [29], single site [30] or supported chromium catalysts. However, such resins cannot be produced by free radical polymerisation [15]. Several factors affect the end product and these are discussed as follows:

Effect of comonomer; comonomer type and content: The 1-olefin introduces short chain branches (SCB) on the polymer chain backbone. The average distance between these branches along the main chain is approximately 25 – 100 carbon atoms. The methylene sequences between these branches can fold and arrange themselves into lamellae while the branches are excluded into the amorphous regions. In the absence of the comonomer, the crystallisable sequences are longer and therefore form thicker lamellae, resulting in resins with high crystallinities. The type of comonomer that is used in LLDPE synthesis determines the type of branch on the main backbone chain. The ethyl branches formed when 1-butene is used for example, can be partially incorporated into the chain folded regions whereas those of higher 1-olefins cannot [31]. As a result, higher 1-olefin side chains leave the chain folded regions and enter into the amorphous regions where they form tie chains which are responsible for holding the lamella together. It is suggested that the longer side branches lead to a larger fraction of tie molecules in the interlamellar region that causes increase in impact strength [32]. As a result, 1-octene when used as a comonomer will give LLDPE resins with better mechanical properties (e.g. tensile strength) as compared to 1-butene or 1-hexene for example. In this current work, it is expected that ethylene/1-heptene resins show close similarities to ethylene/1-octene resins since their comonomers are closely related.

More comonomer used in LLDPE synthesis contributes to a larger number of side chains being excluded from the chain folded regions. These comonomer units aggregate in the amorphous regions where lack of orderly arrangement contributes to free volume. If the density of the chain folded (crystalline) regions is assumed to remain constant (1 g/cm^3 for 100 % crystalline polyethylene) [33], the resin density will therefore depend on the amount of comonomer used for synthesis. The quantity of comonomer incorporated depends upon the target resin and density decreases as more comonomer is added onto the polyethylene chains [34].

Effect of catalyst: LLDPEs can be produced using Ziegler-Natta, Phillips or metallocene catalysts. Of these catalysts Ziegler-Natta heterogeneous catalysts are widely used, and the resins produced by these catalysts are characterised by considerable heterogeneity in terms of molar mass and chemical composition. This results in heterogeneity in the melting behaviour [27]. Such LLDPEs are considered to be a mixture of fractions of polyethylene with a range of molecular weights and short chain branch content [27]. Heterogeneity leads to challenges in

predicting physical and mechanical properties. However, wider MMDs result in better resin processability. A more detailed discussion on Ziegler-Natta catalysts is given in Section 2.4.1. One of the major contributions of metallocene type catalysts is the preparation of LLDPE resins with uniform molecular structures (i.e. narrow molar mass and chemical composition distributions) [1, 35-37]. A more uniform arrangement of comonomer units allows for better predictability of LLDPE resin properties. Crystallisable methylene sequences of almost uniform length can be obtained as opposed to when Ziegler-Natta type catalysts are used. Metallocene type catalysts are discussed in Section 2.4.2.

Industrial production: The technologies for LLDPE manufacture include gas-phase fluidised-bed polymerisation, polymerisation in solution, polymerisation in a polymer melt under high ethylene pressure, and slurry polymerisation. Most catalysts are fine-tuned for each particular process [22, 38]. A more detailed discussion on the technologies for LLDPE industrial manufacture are given in literature [39-41]. In industry, various conditions are used for polymerisation reactions. Cyclohexane is used as a hydrocarbon solvent (Du Pont) at temperatures between 120 and 220 °C where the formed polymer product is soluble. Reactants (hydrogen, ethylene and comonomer) are fed continuously to a stirred reactor at pressures between 50 and 100 bar. Polymerisation proceeds for 5 to 10 minutes. [42].

General LLDPE properties and advantages: The linearity of the copolymer chains in LLDPE (as opposed to LDPE) provides strength while branching provides toughness [42]. LLDPE has higher tensile strength, puncture resistance, tear properties and elongation than LDPE [43]. Density is typically 0.915 − 0.930 g/cm^3 [15]. General advantages of LLDPE over LDPE are improved chemical resistance, improved performance at low and high temperatures, higher surface gloss, higher strength at a given density, better heat sealing properties and a greater resistance to environmental stress in some applications [42]. Haze or lack of clarity is present in all polyethylenes and is caused by differences in the refractive index of the crystalline and amorphous phases [22] therefore, with more comonomer added, crystalline components are suppressed and other important properties such as clarity, softness, strain recovery and toughness are pronounced [10]. Film impact strength and tear resistance increase with decrease in density [24, 44].

2.3.2.1 Crystallinity of LLDPE

Polyolefins can be classified as being amorphous or semi-crystalline, depending on the polymeric regions present. Linear low density polyethylenes (LLDPEs) fall under semi-crystalline polyolefins. Crystallisation is influenced by the size and shape of substituent groups on a polyolefin backbone [45]. Formation and presence of crystals in polyolefin systems largely influences their physical properties. During crystallisation, chains pack closely together to form an ordered structure. The chains form lamellae, which in turn are organised into spherulites. Spherulites are the dominant feature of bulk crystallisation. In the present study, 1-heptene and 1-octene are expected to impact on the crystallinity of LLDPE in the same way since the branch lengths of their copolymers are almost similar.

While semi-crystalline polyolefins contain crystalline regions, amorphous areas are present as well (as shown in Figure 2.1). Amorphous regions do not take part in the chain crystallisation but are randomly arranged in the inter-spherulitic regions [46]. The 1-olefin comonomer is used to control the crystallinity of the resultant resin and hence other properties such as density and overall mechanical properties of the resins. Therefore by varying the amount of SCB and SCBD a broad range of LLDPEs can be obtained [27].
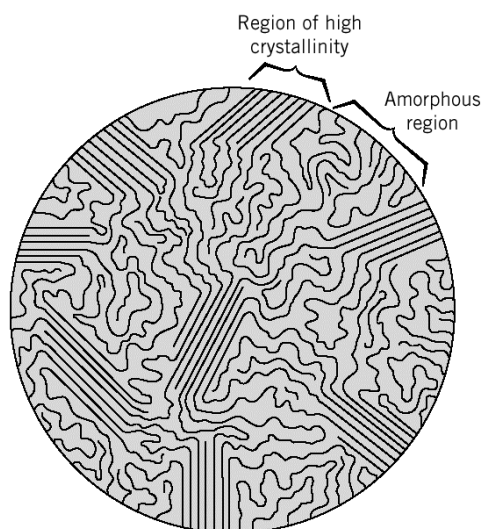
Figure 2.1   Distribution of crystalline and amorphous regions in a polyethylene sample.

Several methods can be used to determine the crystallinity of a polyethylene sample. These techniques include DSC [47], solid state ^{13}C NMR [48], X-ray diffraction [49, 50] and Raman spectroscopy [51, 52]. In the present study, DSC was used as the main technique for determining the crystallinity of polyethylene samples through peak integration and comparison of the peak integrals to the crystallinity of 100 % crystalline polyethylene [47]. Equation 2.1 was used for calculating crystallinity.

$$X\text{c} = \left(\frac{\Delta Hm}{\Delta Hm^{\theta}} \right) \times 100 \text{ %}$$

Equation 2.1 Determination of crystallinity.

$X\text{c} \quad = \quad percentage\ crystallinity$

$\Delta Hm^{\theta} = \quad heat\ of\ fusion\ of\ 100\ \%\ crystalline\ PE\ =\ 293\ \text{J/g}\ [47]$

$\Delta Hm \quad = \quad heat\ of\ fusion\ of\ sample$

2.3.3 High density polyethylene (HDPE)

Commercial production of HDPE was started in 1956 by Phillips Petroleum Co. (United States) and by Hoechst (Europe). HDPE is one of the largest volume commodity plastics produced in the world [24]. HDPE is a linear, nonpolar thermoplastic with up to 80 % crystallinity [22]. Due to its linear structure, molecules tend to align themselves in the direction of flow and this makes the tear strength of the film much lower as compared to LDPE or LLDPE. HDPE can be produced from solution, slurry or gas phase processes as seen with LLDPE (Section 2.3.2) [53]. The main differences between the three major types of polyethylene are summarised in Table 2.1.

Table 2.1   Comparison of the three main types of polyethylene.

HDPE	LDPE	LLDPE
o Coordination polymerisation	o Radical polymerisation	o Coordination polymerisation
o No comonomer used	o No comonomer used	o Comonomer used
o Density $\approx$ 0.942 – 0.965 g/cm^3	o Density $\approx$ 0.910 – 0.925 g/cm^3	o Density $\approx$ 0.910 – 0.925 g/cm^3 [41]
o Little or no branching	o Long and short chain branching	o Short chain branching
o Pressures used are between 5-10 MPa	o Pressures used are between 100-135 MPa	o Pressures used are between 0.1-1 MPa
o Used in water pipes, containers (milk, laundry detergent etc.), electrical wire insulation, trash bags, industrial drums [22]	o Used in films, sealants, adhesives, squeeze bottles, insulators	o Used in plastic bags (where it allows using lower thickness as compared to LDPE), plastic wrap, flexible tubing, toys [22]

2.4   Catalysts used in polyethylene synthesis

Since the accidental discovery of olefin polymerisation, the development of catalysts has been fuelled by the need for more control over the molecular architecture and properties of polyolefins at a molecular level. Various catalysts that have been developed to date offer varying control over molar mass, its distribution and comonomer insertion. Three of the major catalyst types are reviewed in Sections 2.4.1, 2.4.2 and 2.4.3.

2.4.1   Ziegler-Natta catalysts

Catalyst systems used for Ziegler-Natta polymerisations consist of a cocatalyst or activator and the catalyst itself. Commonly used Ziegler-Natta catalysts are TiCl$_3$ and TiCl$_4$ [54]. A brief outline on the development of these catalysts was given in Section 2.2. Active sites of Ziegler-Natta catalysts are formed due to interaction between a transition metal compound and an

organometallic cocatalyst [55]. This is true for metallocene catalysts as well. Common cocatalysts include triethylaluminum (TEA), diethylaluminum chloride (DEAC), and tri-isobutyaluminium (TIBA) [56]. The presence of the many types of active sites in the Ziegler-Natta catalyst systems produces polyolefin resins with broad chemical and molar mass characteristics. Fan *et al.* [57] carried out some work to quantify the number of different active centres through 1-hexene polymerisation with $MgCl_2$-supported Ziegler-Natta catalysts. In their study, they concluded that some active sites which were dormant during 1-hexene homopolymerisation became activated during the ethylene and 1-hexene copolymerisation [57]. Figure 2.2 illustrates the distribution in chemical composition of polyolefin chains produced by different active sites in a Ziegler-Natta catalyst.
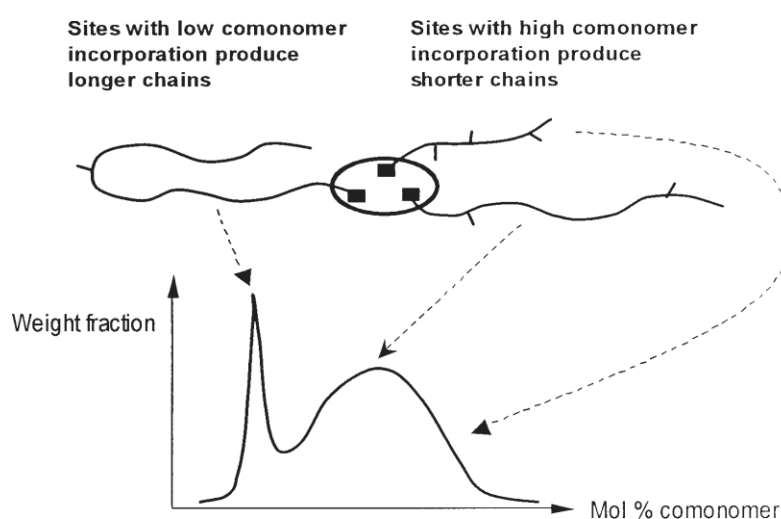
Figure 2.2   Ziegler–Natta copolymers exhibiting broad CCDs. Chains made by different active sites have different microstructural distributions [58].

Crystallisation analysis fractionation (CRYSTAF), temperature rising elution fractionation (TREF), as well as size exclusion chromatography (SEC) were used to investigate the number of active site types present on the catalyst by Da Silva Filho *et al.* [59]. In their results, it was shown that multiple sites on the catalyst are present and can be quantified based on the type of polyethylene chains they produce

Magnesium chloride is mainly used as the catalyst support because of several advantages it possesses [60]. $MgCl_2$ has desirable morphology since it is strong enough to resist particle break

up during handling but still weak enough to disintegrate during polymerisation. In addition, $MgCl_2$ has crystalline forms similar to $TiCl_4$ and it is thought that its lower electronegativity as compared to other metal halides increases polymerisation productivity. Inertness to chemicals used for polymerisation also adds importance to this catalyst support [61]. Figure 2.3 shows how $TiCl_4$ can be chemisorbed onto the $MgCl_2$ structure. This makes some sites more accessible than others. In unsupported catalysts, a large number of potential active sites are hidden inside the $TiCl_4$ crystallite and this lowers the activity of the catalyst. Thus, supported catalysts have higher activity as compared to non-supported catalysts. This is because the active sites are more dispersed and highly accessible for the monomer coordination [1, 60].
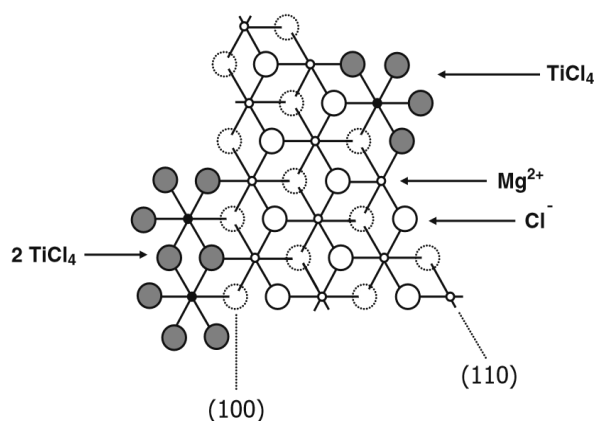
Figure 2.3   Surface structure of $TiCl_4$ on $MgCl_2$ [11].

All Ziegler-Natta type polymerisations take place at a metal-carbon bond and the streoregulation that is predominant at the bond depends mainly on two conditions: (a) whether the centre is part of a crystalline catalyst particle or (b) whether the centre is part of a soluble complex (bimetallic or trimetallic) [62]. Chain propagation occurs much easier than termination, therefore in most industrial polymerisation processes, hydrogen gas is fed into the reactor at known pressures or quantities to regulate chain growth [63]. This is true for both metallocene or Ziegler-Natta catalysed processes. Chain length of the polyolefin also depends on the competition between propagation and termination reactions. Termination reactions are also influenced by high temperature (provides activation energy required for chain termination) as well as the comonomer. Scheme 2.1 gives the mechanism for the Ziegler-Natta catalysis of ethylene.
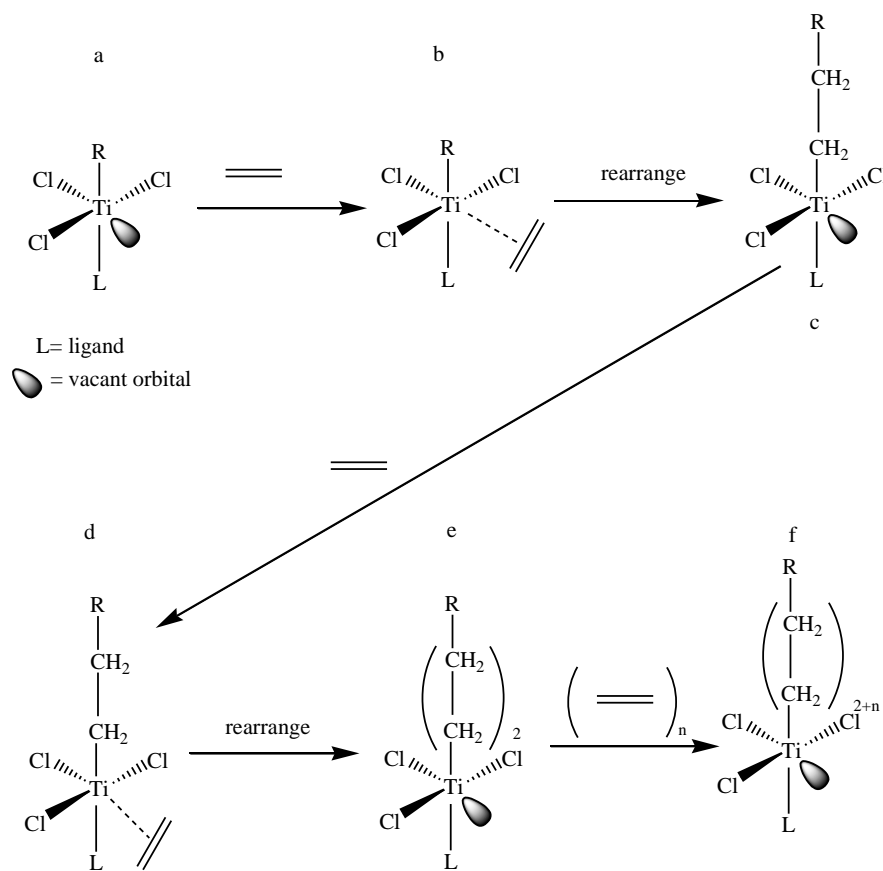
Scheme 2.1   Mechanism for Ziegler-Natta catalysis of ethylene.

2.4.2   Metallocene catalysts

Metallocene catalysts are also referred to as Ziegler-Natta single site catalysts because all their metal cation active sites are assumed to be identical during polymerisation reactions. Therefore, the homogeneity of active sites in metallocene catalysts results in very narrow chemical compositions and molar mass distributions. As stated in Section 2.2, the greatest leap in the development of these catalysts is attributed to the work of Kaminsky and Sinn. Metallocene catalysts are organometallic compounds in which metal centres are sandwiched between aromatic ligands. Ligands that are usually used are dicyclopentadienyl, indenyl or fluorenyl groups [64] and these have a significant influence on molar mass, polymerisation activity [65], comonomer insertion as well as the overall microstructure of the polyolefin produced. The metal centres also greatly affect yields and molar masses of the resins produced (see Table 2.2). Typical examples of metallocene catalysts are shown in Figure 2.4.

Dichloro[rac-ethylenebis(indenyl)]zirconium(IV)   bis(cyclopentadienyl)zirconium(IV)
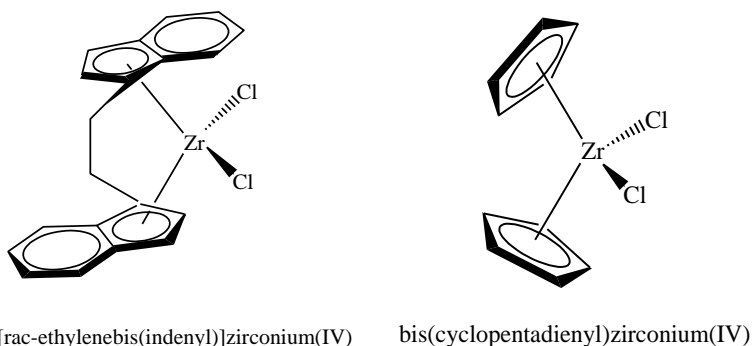
Figure 2.4   Examples of common metallocene (single site) catalysts.

Table 2.2   Different metallocene-aluminoxane systems used for ethylene polymerisation. (330 mL of toluene, 8 bar ethylene pressure and 5 x 10^{-3} mol (AI-O) units). [56]

Metallocene	Cocatalyst	Temperature (°C)	Activity (g PE/g Zr.h.bar)	Mn |(g/mol)
$Cp_2Ti(CH_3)_2$	MAO[a]	20	500	520 000
$Cp_2Ti(CH_3)Cl$	MAO	20	50 000	490 000
Cp_2TiCl_2	MAO	20	90 000	430 000
$Cp_2Zr(CH_3)_2$	MAO	20	9 000	730 000
$Cp_2Zr(CH_3)_2$	MAO	70	70 000	190 000
$Cp_2Zr(CH_3)_2$	MAO	90	3 100 000	106 000
$Cp_2Zr(CH_3)_2$	PAO[b]	70	175 000	500 000
Cp_2ZrCl_2	MAO	90	5 000 000	122 000
$Cp_2Zr(CH_3)_2$	EA[Oc]	60	23 000	500 000
$Cp_2Hf(CH_3)_2$	MAO	70	60 000	441 000
Cp_2HfCl_2	MAO	70	69 000	490 000

[a] methylaluminoxane; [b] isopropylaluminoxane; [c] ethylaluminoxane

The mechanism of metallocene catalysis is as follows:

Activation of metallocene catalyst precursors: Methylaluminoxane (MAO) is used to generate the active site on the catalyst through ligand abstraction. Therefore MAO acts as cocatalyst, forming a complex with the catalyst. Introduction of substituents at certain positions of the two

aromatic ligands modifies the steric, electronic conditions as well as the symmetry of metallocene complexes [64]. A vacant site is produced while the anionic counter ion, formed by ligand abstraction, is weakly coordinated to the metal centre. The monomer is then inserted and rearrangement of the vacant orbital occurs. This paves a way for the growth of the polymer chain through addition of more monomer units.
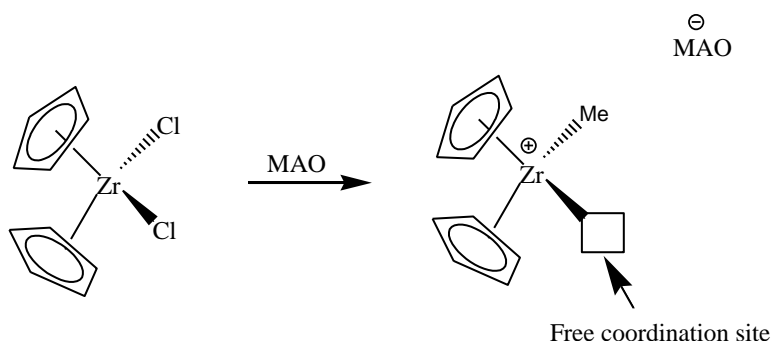
Scheme 2.2   Activation of metallocene catalyst.

Propagation: The propagation step follows the activation step. Subsequent monomer units coordinate to the metal centre and are inserted into the polyethylene chain thereby making the polyethylene chain grow longer. Scheme 2.3 shows how the propagation step proceeds.
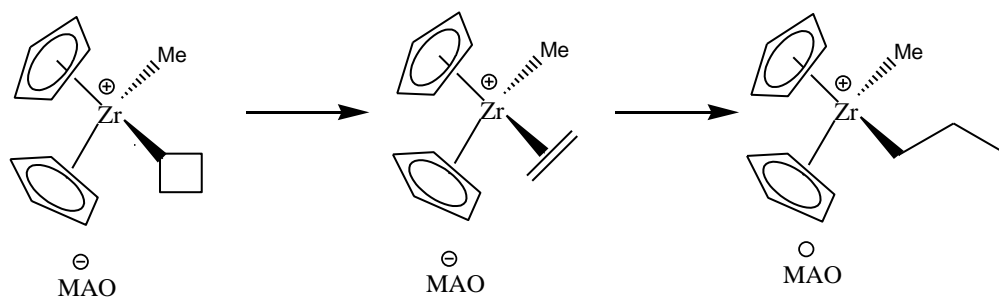
Scheme 2.3   Propagation step of ethylene polymerisation with metallocene catalyst.

Termination: Schemes 2.4 – 2.6 illustrate the three types of termination reactions that are possible with metallocene catalysis. The termination processes in metallocene catalysis are also similar to those in Ziegler-Natta catalysis. The modes of termination can be stated as:

➢ chain transfer through β-elimination with hydride transfer to monomer [66]
➢ chain transfer through β-elimination with hydride transfer to metal [67]

19

➤ chain transfer by hydrogen (hydrogenolysis) [68, 69]
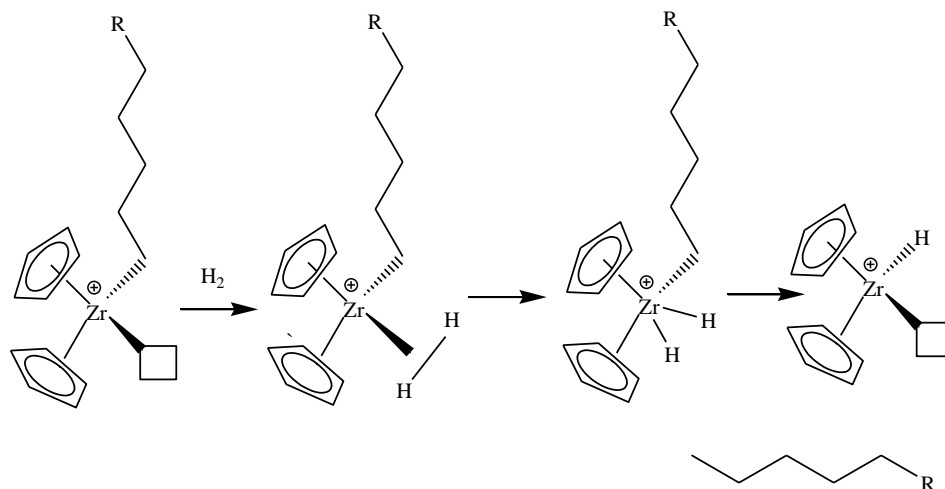
Scheme 2.4   Termination by addition of hydrogen (hydrogenolysis).
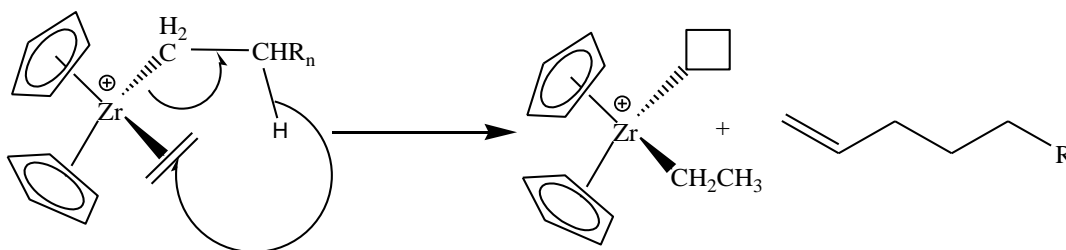
Scheme 2.5   Chain transfer through β-elimination with hydride transfer to monomer.
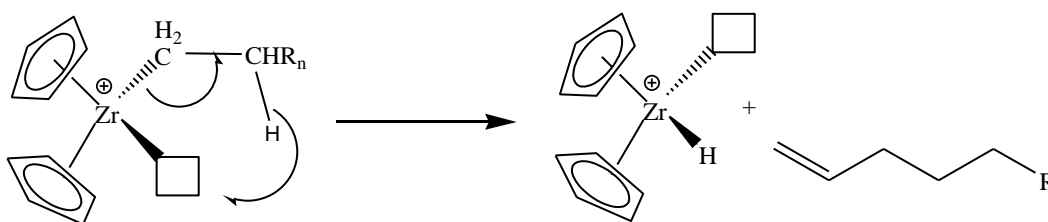
Scheme 2.6   Chain transfer through β-elimination with hydride transfer to metal.

The use of metallocene catalyst systems in industry is limited primarily by their expensive nature. Large quantities of the expensive cocatalyst MAO are required and this has led to the development of MAO-free catalytic systems. Another challenge is the homogenous nature of metallocenes which does not allow their use for gas phase polymerisations [1, 70]. Heterogeneous Ziegler-Natta catalysts are still used widely due the above mentioned reasons.

2.4.3   Phillips catalyst

The Phillips catalyst is a chromium-based catalyst supported on silica. These type of catalysts were discovered by Hogan and Banks in 1951 [71]. Since their discovery, there is still no consensus on issues regarding the oxidation state of the active site, molecular structure of the catalyst and the polymerisation mechanism [72]. While propagation and termination steps for ethylene are well understood, the same cannot be said about the initiation step with the Phillips catalyst. Several studies have suggested the mechanisms for the initiation step [73-75]. Figure 2.5 shows the general structure of a Phillips type catalyst.
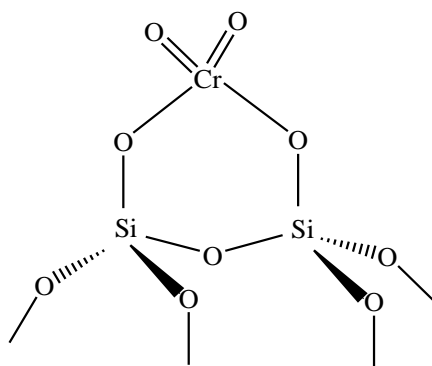
Figure 2.5   General structure of a Phillips catalyst.

Supported Phillips catalysts are used to produce 40-50 % of the worlds' HDPE [76]. These catalysts are also able to copolymerise ethylene with various 1-olefins. Comonomer incorporation is random. In addition, the molecular weight distribution of the polyethylenes produced is significantly larger than that of resins produced by metallocene as well as Ziegler-Natta type catalysts. Reaction temperature is primarily used as the process control tool during polymerisation when Phillips catalysts are used. As reactor temperature increases catalyst activity and polyethylene melt flow index increase. In addition to temperature being a control parameter, ethylene concentration can also be used as a control tool. Temperatures used in conjunction with Philips type catalysis are typically in the range of 65-180 °C [72, 77]. A comparison of Ziegler-Natta, metallocene and Philips catalysts is shown in Table 2.3.

Table 2.3   Comparison of Ziegler-Natta, metallocene and Phillips catalysts.

Ziegler-Natta catalysts	Metallocene (Single-Site) catalysts	Phillips catalysts
o Mainly heterogenised on $MgCl_2$	o Often not supported (SiO_2 can be used)	o Heterogenised on SiO_2
o Alkyl aluminiums used as cocatalyst (e.g. TEA)	o Alkyl aluminium (e.g. MAO) and borates used as cocatalyst	o Activation without cocatalyst
o Multiple type active centres	o Single type active centres	o Multiple type active centres
o Resultant polyolefin has broad molar mass distribution (D>2.0)	o Resultant polyolefin has narrow molar mass distribution (D =2.0)	o Resultant polyolefin has broad molar mass distribution (D>>2.0).
o Heterogeneous comonomer distribution	o Homogenous comonomer distribution	o Heterogeneous comonomer distribution
o Production of HDPE, LLDPE and PP	o Production of HDPE, LLDPE and PP	o Production of HDPE and MDPE
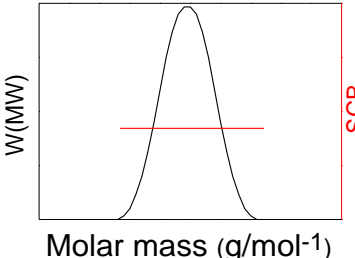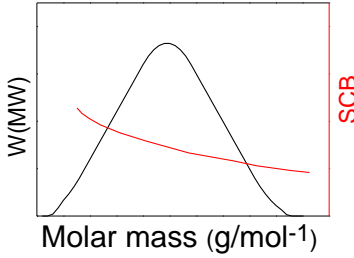
2.5   Characterisation methods

2.6.1   High temperature-size exclusion chromatography (HT-SEC)

Size exclusion chromatography (SEC), also referred to as gel permeation chromatography (GPC), is a technique used to separate and analyse polymer molecules according to their hydrodynamic volume (V_h). SEC separates polymers according to molecular dimensions, regardless of their functionality [78]. Permeation into the pores of the stationary phase depends on the V_h of the macromolecules. Based on the interactions with the pores of the stationary phase the polymer chains are separated according to their V_h, the largest molecules eluting first followed by smaller molecules [78]. Separation of the analyte takes place in a volume smaller than the total column volume. The size of the pores in the column packing should be selected

based on the molar masses of the polymers to be separated. For polymers with broad molar mass distributions, it may be necessary to use several SEC columns in series. A schematic representation of a typical SEC setup is shown in Figure 2.6.
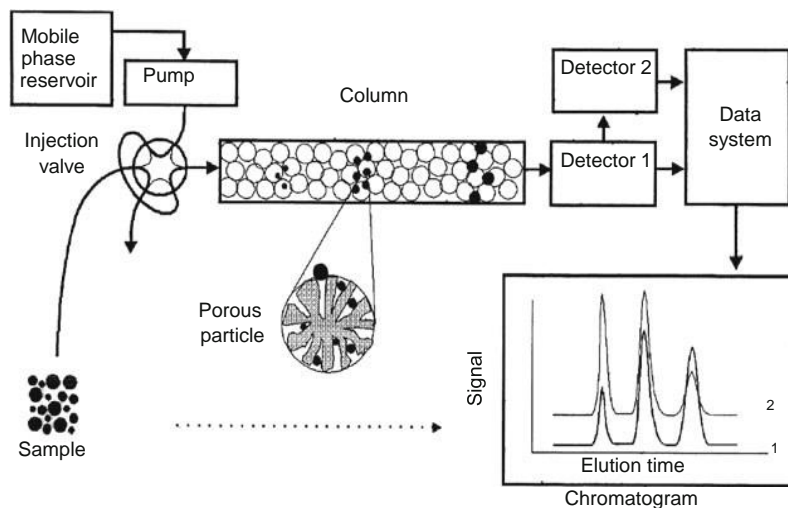
Figure 2.6   Schematic   representation   showing   operation   of   a   size   exclusion chromatograph [78].

Since polyolefins are soluble at temperatures above their melting points, this presents a challenge for column-based chromatography because the complete system from sample injection to the detector must be kept at high temperature to prevent the polyolefin fractions from precipitating out of solution. Temperatures which are therefore used in polyolefin analyses are usually between 110 and 160 °C. Thermodynamically stable high boiling point solvents must therefore be used. Most commonly used solvents for polyolefin analyses are 1,2,4-trichlorobenzene (TCB), *ortho*-dichlorobenzene (*o*-DCB), decalin, methylcyclohexane, α-chloronaphthalene and tetrachloroethylene [79, 80]. Operation at high temperature introduces problems such as sample degradation. Polyolefin chains may degrade during sample preparation or during the SEC separation itself [81, 82]. The most likely outcome of degradation is the reduction of the polyolefin molar masses. To prevent thermo-oxidative degradation, phenolic antioxidants (e.g. butylated hydroxytoluene, BHT) are usually added to the mobile phase in concentrations of 0.2 mg/mL up to 1.5 mg/mL [83, 84].

2.6.2 Carbon-13 nuclear magnetic resonance spectroscopy (^{13}C NMR)

In the present study, solution carbon-13 nuclear magnetic resonance spectroscopy was used to measure the comonomer content (branched carbon content) of ethylene/1-heptene, ethylene/1-octene and ethylene/1-pentene copolymers as well as prep-TREF fractions. Solid state ^{13}C cross polarisation (CP-MAS) experiments were carried out only for qualitative purposes in the analyses of crystalline and amorphous components of EH and EO LLDPE.

The principle of NMR is based on the fact that nuclei of atoms have magnetic properties that can be usefully harnessed to obtain chemical information [85]. NMR is a physical occurrence in which magnetic nuclei in a field absorb and re-emit electromagnetic radiation. Energy of absorption and the intensity of the signal are proportional to the strength of the magnetic field [86, 87]. A spinning charge generates a magnetic field that results in a magnetic moment that is relative to the spin. Sample nuclei can exist in two spin states, namely the excited or higher energy state and the lower energy state. Therefore, irradiation of these nuclei with energy corresponding to the exact spin state energy difference will cause excitation from a lower to a higher energy state. NMR signals are usually reported relative to those of a reference, usually tetramethylsilane (TMS) whose chemical shift is considered to be 0 ppm [88]. In our case, 1,1,2,2-tetrachloroethane (TCE-d2) was used as the internal reference in solution analyses for carbon-13 and it has an observed chemical shift of 74.3 ppm [89]. Chemical shifts for protons are highly predictable since they are primarily determined by simpler shielding effects (electron density), while those of heavier nuclei are more influenced by other factors which include excited states. The structure of the sample can be obtained from the chemical shifts observed.

The solid state technique is based on the principle that the radio frequency pulse sequence starts with cross polarisation. In the case of ^{13}C CP-MAS experiments, protons (^{1}H) are magnetised and their charge transferred to ^{13}C nuclei. This is done to enhance the signal of nuclei with low gyromagnetic ratios to higher ratios. The gyromagnetic ratio is the ratio of a dipole moment to its angular momentum [90]. In order to establish a magnetic transfer, the radio frequency must be applied on two frequency channels and must fulfil the Hartman-Hahn condition [91, 92]. The

magic angle spinning is the sample spinning angle of θ_m which is approximately 54.7° with respect to the direction of the field [93, 94].

The ^{13}C CP-MAS spectra can be deconvoluted into three Lorentzian fits for polyethylene polymers. Position 1 and 3 are signals for carbons in the monoclinic and orthorhombic crystalline environments [95]. Position 2 is the signal of the carbon in the amorphous environment. The total crystallinity is therefore calculated as the sum of the integrals in position 1 and 3. However, in the present study the ^{13}C CP-MAS experiments were only conducted to yield qualitative information. For a more quantitative approach, longer experiment times are required.

Solution ^{13}C NMR has been used extensively for qualitative and quantitative purposes in the analyses of ethylene/1-olefin copolymers [96, 97]. Qualitative uses include polyolefin identification, and comonomer sequencing [97, 98]. Another use is in comonomer content determination through spectral signal integration. Solid state ^{13}C NMR has been used to determine crystalline and amorphous contents of LLDPEs [99, 100] and heterophasic propylene-ethylene copolymers [101]. Botha *et al*. [102] and Assumption *et al*. [103] used the same technique in their studies on characterisation of heterophasic ethylene-propylene copolymers and LLDPE prep-TREF fractions, respectively.

2.6.3   Differential scanning calorimetry (DSC)

This technique was developed by Watson and O'Neill in 1962 and introduced commercially in 1963 at the Pittsburgh Conference on Analytical Chemistry and Applied Spectroscopy [104, 105]. Thermal analysis in DSC is based upon the detection of changes in the enthalpy or heat content of a sample as temperature is changed. The specific heat of a material changes slowly with temperature in a specific physical state, but changes intermittently at a change of state. The supply of thermal energy may also cause chemical processes to occur such as decomposition [106, 107]. These changes are also accompanied by a change in enthalpy. Thus in DSC analyses the cell containing the sample is kept under inert conditions by a flow of nitrogen to minimise the possibility of oxidation processes taking place. Any transition accompanied by the change in specific heat produces a discontinuity in the power signal, so that exothermic or endothermic

enthalpy changes give rise to peaks whose areas when integrated are proportional to the total enthalpy change of the transition. A typical DSC furnace is shown in Figure 2.7.
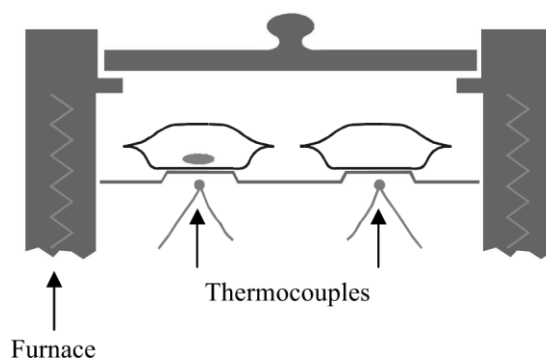
Figure 2.7   **DSC furnace with sample and reference. The sample is shown as the closed pan with a grey pellet to the left while the reference is shown as an empty pan to the right [108].**

DSC has been compared to other characterisation techniques such as CRYSTAF and TREF [109] and it was found that it provides comparable results in determining short chain branching distribution (SCBD). Sarzotti *et al.* [110] compared solution DSC with CRYSTAF and found that DSC exotherms agree well with CRYSTAF profiles. Cooling rates for solution DSC and CRYSTAF were 0.01 °C/min and 0.1 °C/min, respectively. Another variation of DSC referred to as successive self-annealing differential scanning calorimetry (SSA-DSC) has been found to be useful in characterising crystallisable units distribution. Drummond *et al*. [111] found that the technique provides useful information on the branching distribution of LDPE and LLDPE samples, a better result as compared to the standard DSC technique.

2.6.4   Fourier transform infrared spectroscopy (FTIR)

Infrared irradiation was first identified by Sir William Herschel [112] as a distinct region of the energy spectrum. The introduction of Fourier transform infrared spectroscopy in the 1800s and its further development to fast Fourier transform (FFT) in 1964 by Cooley and Tukey [113] contributed to the development of this technique as a quick and reliable one. FTIR is perhaps the most widely used spectroscopic technique for the determination of composition, crystallinity, tacticity as well as conformation of polymeric materials in general [114]. Useful bands are found

in the full range of the mid-infrared spectrum (4000 – 600 cm^{-1}). In addition, various chromatographic methods can be combined with IR spectral acquisition to obtain a wealth of information [89, 115, 116]. It has been also shown by Harvey and Ketley [117] that the type of short chain branching can be identified by FTIR analyses.

Gulmine *et al*. [118] used FTIR to characterise polyethylene and concluded that under optimised conditions it is possible to distinguish LDPE, LLDPE and HDPE when appropriate conditions are met. In their other work this technique was used to characterise aged cross-linked polyethylene [119].

2.6.5   High-temperature high performance liquid chromatography (HT-HPLC)

Analysis of polyolefin materials by high-temperature high performance liquid chromatography (HT-HPLC) was introduced in 2004 [120, 121] through a joint development between Polymer Laboratories, Ltd (Church, Stretton, England) and the group of Pasch and Macko. An instrument capable of operating at high temperatures as well as combining solvents in a gradient method was developed. High temperature HPLC is an important tool for the fast separation of complex polyolefins with regard to their chemical composition. Separations in HPLC are achieved through different mechanisms which include adsorption-desorption and precipitation-redissolution. In gradient HPLC (which was used in this study), precipitation and adsorption processes are frequently combined [122]. Macko and Pasch also discovered that a specific carbon based stationary phase "Hypercarb" enables highly selective separations of polyolefins [122]. Separation on the Hypercarb column depends on interactions of the crystallisable methylene sequences of the polymer with the stationary phase. Therefore, the longer the methylene sequences are, the greater their interactions with the stationary phase and hence their retention volumes (V_r) [123, 124].

One significant advantage of this technique is that it can be used for the analysis of semi-crystalline as well as amorphous polyolefin samples. In comparison to TREF and CRYSTAF, this is a significant advantage as these techniques can only be applied to semi-crystalline copolymers. Pasch *et al*. [125] showed that resin components can be separated according to

chemical composition and identified by this technique. With online coupling of HPLC to high temperature-size exclusion chromatography (HT-SEC) and proton nuclear magnetic resonance spectroscopy (^{1}H-NMR), a wealth of information with regards to the constitutional composition of both new and an established polyolefin resins can be obtained.

2.6.6 High-temperature two-dimensional liquid chromatography (HT-2D-LC)

As with HT-HPLC, HT-2D-LC can now be applied to polyolefin analysis at higher temperatures. It was only in 2010 [121] that the introduction of HT-2D-LC was announced. First results on HT-2D-LC for polyolefins were published by Ginsburg *et al*. [126] and Roy *et al*. [127]. Since then, notable works have been carried out and these include separation and characterisation of impact polypropylene copolymers by Cheruthazhekatt *et al*. [89, 128], who found that complete separation of each component according to chemical composition and molar mass can be achieved through HT-2D-LC. A typical 2D-LC instrument set up is shown in Figure 2.8.
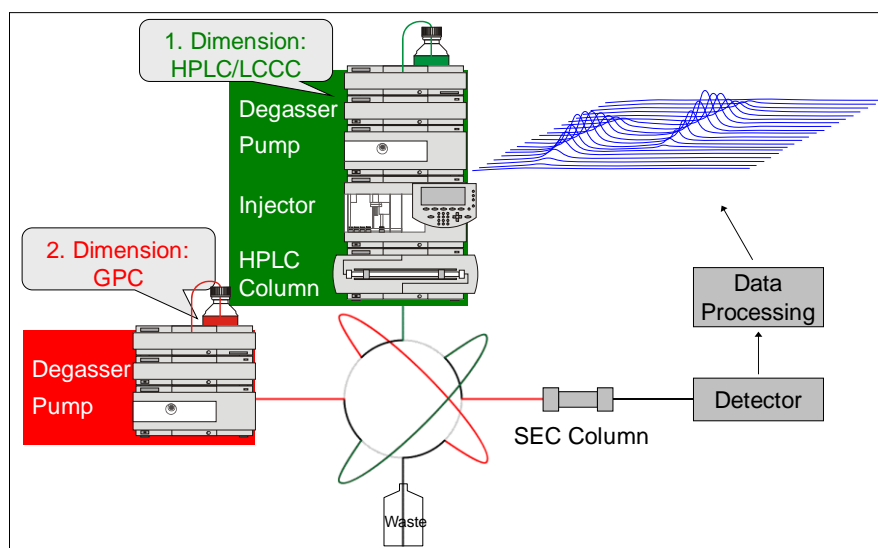
Figure 2.8   Diagram of a 2D instrument [78].

2.6.7 Separation by crystallisability

In order to obtain more information on the microstructure of semi-crystalline polyolefins, several techniques have been developed to fractionate the resins according to their crystallisabilities.

Two main such techniques which have established themselves as indispensable tools are temperature rising elution fractionation (TREF) and crystallisation analysis fractionation (CRYSTAF). Crystallisation elution fractionation (CEF), a newly developed technique [129-132] is also discussed in literature.

2.6.7.1   Temperature rising elution fractionation (TREF)

TREF is one of the most widely used techniques for fractionating semi-crystalline polyolefins. TREF only fractionates semi-crystalline polyolefins and is sensitive to differences in chain crystallinity or solubility. Soares [133] defines TREF as sensitive to and based on the relationship between molecular structure, chain crystallinity and dissolution temperature. Although this technique is one of the oldest in analysis of polyolefins, it is still one of the most important. As far as development of this technique goes, the earliest work done with regard to separation of polyethylene fractions according to composition was reported by Desreux and Spiegels in 1950 [134]. Kenzo Shirayama and co-workers were the first to name the technique "TREF" when they reported how the short chain branches of polyethylene are distributed over the various molar masses [135]. However, in the 1970s Leslie Wild and co-workers developed what is known as analytical TREF [136], which slightly varies from preparative TREF [137].

Short chain branching distribution (SCBD) as well as molar mass distribution (MMD) has a marked influence on the polyethylene properties. Determination of these distributions can lead to a more complete understanding of the behaviour of LLDPE in the end-use applications and TREF is an important tool used to understand SCB and SCBD [138]. In TREF the polyolefin sample is first dissolved in a good solvent like xylene at a high temperature, which is above its melting point. This solution is then immediately introduced into a column filled with an inert support substance such as glass beads or sea sand and sometimes silica gel [139]. The temperature is then decreased at a programmed slow and constant cooling rate for example, $1 - 2$ °C per hour. As quoted by Soares [133], Wild *et al.* suggests a cooling rate of not above 2 °C/hr to avoid co-crystallisation and molar mass influences during the precipitation or cooling step. This allows polyolefin chains to crystallise onto the inert support in orderly fashion from higher to lower crystallinities. The cooling rate, which is controlled by a continuously stirred oil bath, is one of the key factors for the efficient separation of different fractions as the crystallisation step

mainly determines the quality of the fractionation. In the second and last step pure solvent is pumped through the column and the temperature is increased in a slow programmed manner [137]. This step is commonly referred to as the "elution" step. Figure 2.9 shows the separation mechanism.
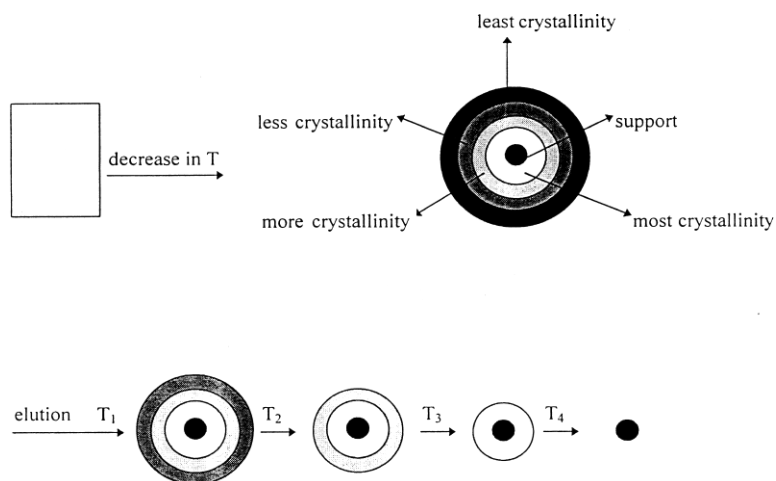
Figure 2.9   TREF separation mechanism [138].

Preparative TREF (prep-TREF): In prep-TREF, a larger sample size is fractionated so that fractions can be obtained for further analyses. Prep-TREF is time consuming, labour intensive (filtering, drying and analysing fractions) and consumes significant amounts of solvent (up to 6 litres of xylene per sample) as compared to analytical TREF and CRYSTAF. Soares [133] compared the two TREF techniques and some of the key differences are shown in Table 2.4. Figure 2.10 shows a schematic diagram of a prep-TREF experiment setup.
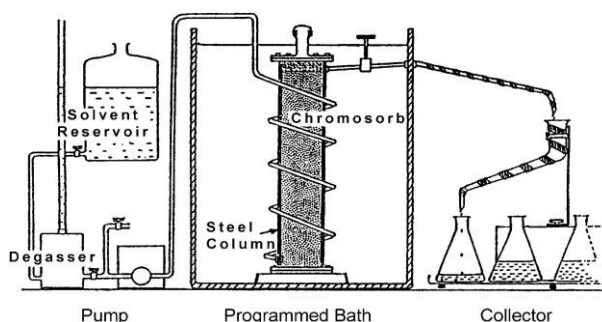
Figure 2.10   Schematic diagram of a preparative TREF experiment setup. [139]

Analytical TREF: As stated by Wild *et al*. [139] the major bottleneck associated with the prep-TREF system is the large number of fractions that need to be processed. He also states that the efficiency of the separation would be probably less than ideal owing to the large size of the column system. Therefore, analytical TREF was developed in which both column and sample sizes are reduced considerably. In addition, the concentration of the eluting solution is monitored by an in-line detector. Analytical TREF is generally automated. A comparison between analytical and preparative TREF is given in Table 2.4.

Table 2.4   Comparison between the two types of TREF [133].

Preparative TREF	Analytical TREF
o Fractions are collected at pre-determined temperature intervals	o Continuous operation
o Information about molecular structure is obtained off-line by additional analytical techniques (^{13}C NMR, DSC, SEC, FTIR, HPLC)	o Information about molecular structure is obtained on line by means of a calibration curve
o Requires larger amounts and larger sample sizes	o Requires smaller columns and smaller sample sizes
o Time-consuming but generates detailed information about polyolefin microstructure	o Faster than preparative TREF but generates less information about polyolefin microstructure

2.6.7.2   Crystallisation analysis fraction (CRYSTAF)

Crystallisation analysis fractionation was developed by Benjamin Monrabal in 1991 [140]. It was developed as an alternative to TREF with the main aim of minimising sample analysis time. The main difference between the two methods of analysis is that while the crystallisation step is very important in both techniques, data collection in TREF is done only during the elution step and in CRYSTAF during the crystallisation step [141]..This method of analysis consists of two major steps. Firstly, the polyolefin is dissolved at a low concentration of approximately 1 mg/mL. Usually this is done by dissolving 20 – 30 mg of a polyolefin sample in 30 – 35 mL of TCB

solvent. Such low concentrations are ideal in order to minimise the effects of co-crystallisation [139].

After dissolution, constant cooling is carried out in small regular steps to allow the polymer fractions to crystallise, starting with those that have high crystallisabilities (i.e. zero or very few branches). This results in a decrease in solution concentration and as the solution temperature is decreased further, polymer chains that have more branching will also precipitate. Figure 2.11 shows the relationship between crystallisation temperature and branch content for a typical LLDPE resin synthesised by a Ziegler-Natta catalyst.
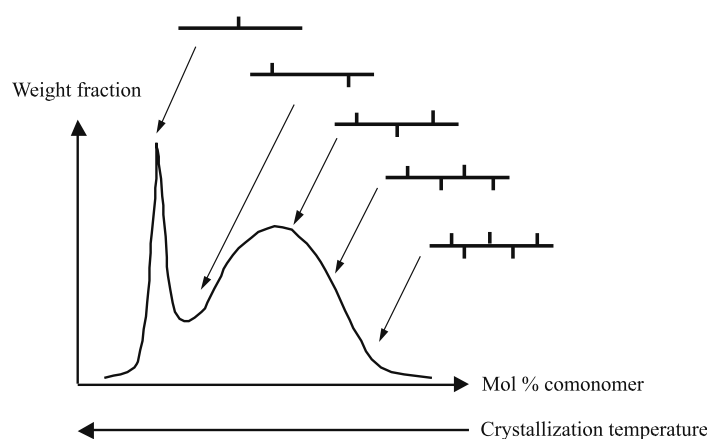
Figure 2.11   Chemical composition heterogeneity of Ziegler-Natta catalysed LLDPE. [58]

CRYSTAF has also been compared to other characterisation techniques, for example, Gabriel *et al*. [109] compared the technique to TREF and DSC profiles. They found that the results of the three techniques are qualitatively comparable with respect to the distribution of comonomer and the branching degree. They however recommended the use of a combination of all three methods especially for polyolefins with a high degree of undercooling such as polypropylene.

Anantawaraskul *et al*. [141] compared results obtained from TREF and CRYSTAF at same cooling rates by studying polyolefin blends with known multimodal CCDs. TREF was found to provide better resolution of the multimodal polyolefin blends than CRYSTAF. However, CRYSTAF is favoured because of its shorter analysis times and its resolution for CCD separation can be improved by slower cooling rates (CRYSTAF will still give shorter analysis time even at slower cooling rates). Several factors may affect the fractionation process in

CRYSTAF and these include chain microstructure (i.e. molar mass, comonomer content and comonomer type), operating conditions and cocrystallisation. These factors are discussed in detail in literature [30, 141-145]. Cocrystallisation is the main limitation in CRYSTAF analyses. Figure 2.12 shows typical cumulative and differential CRYSTAF curves obtained after data processing.
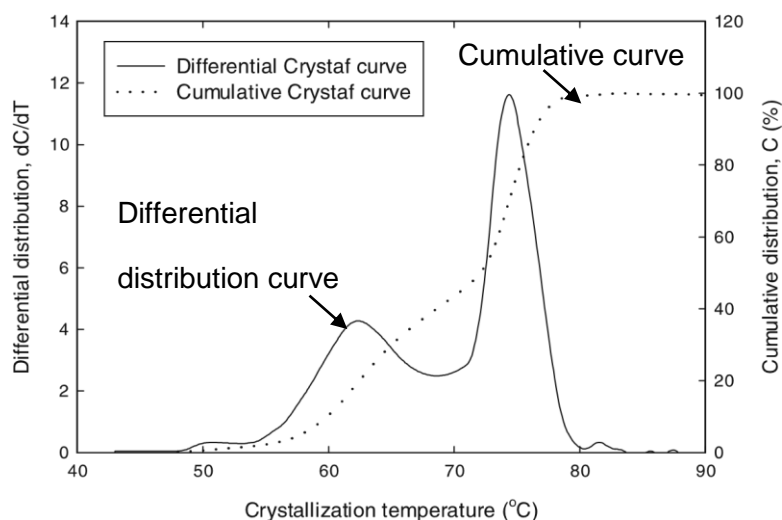
Figure 2.12   Cumulative and differential CRYSTAF profiles. [146]

2.6   Mechanical analyses

Peacock [10] defines mechanical properties of a polyethylene specimen as those attributes that involve the physical rearrangement of its component molecules or distortion of initial morphology in response to an applied force. It is also known that the macroscopic scale properties such as tensile strength and Young's modulus are dependent on microstructure [25, 27, 37, 138, 147-149]. Therefore, much emphasis has been placed in understanding of microstructural properties. In addition to microstructure, which is primarily influenced by catalyst type, polymerisation conditions and the type of short chain branching (SCB) may also play a major role in governing the mechanical properties. Our main interest is in differences in microstructural properties of ethylene/1-heptene and ethylene/1-octene copolymers.

2.6.1   Tensile strength

Stress-strain or tensile test is one of the most used mechanical tests for polymers [150, 151]. Typically, the testing involves taking a sample with a fixed cross-section area, and then pulling it with a tonometer, gradually increasing force until the sample breaks. It is known that results vary for different polymers and can also vary for the same sample of polymer. Variation is primarily due to the diverse structures found in different polymers. Repeat measurements are made (typically between 3 and 10) in order to determine a quantity such as yield stress and the mean of the measurements is then quoted as the value of the quantity under investigation [152].

Speed of testing is defined as the relative rate of motion of the grips or test fixtures. Different rates are used for different sample types, varying typically from 1 to 500 mm/min. Dumbbell-shaped (dog-bone) or straight-sided specimens are usually used under defined conditions of pre-treatment, temperature, humidity and deformation rate [151, 153]. Figure 2.13 shows a typical stress-strain graph. Almost all polymers that are not cross-linked will neck during tensile testing.
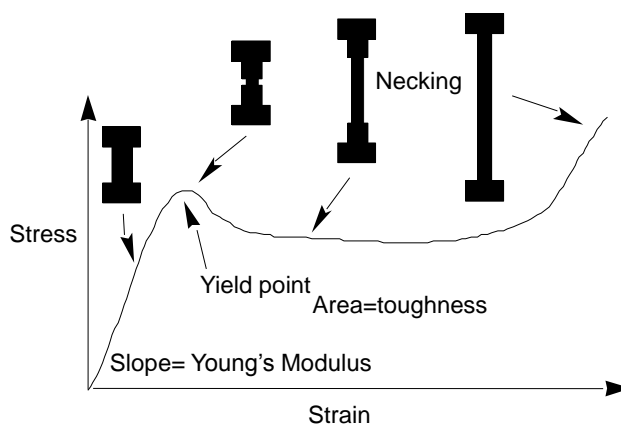
Figure 2.13   Typical stress-strain curve of a semi-crystalline polymeric material.

2.6.2   Young's modulus

Young's modulus is also known as tensile modulus or elastic modulus. It can be defined as the ratio of the stress (force per unit area) along an axis to the strain (ratio of deformation over initial length) along that axis in the range of stress in which Hooke's law applies. Young's modulus or the modulus of elasticity is a measure of stiffness of a material [154]. When a polyethylene

sample is subjected to an external stress, there is an initial deformation prior to yield (as shown in Figure 2.13) that is homogenous and is largely recoverable when the external stress is removed. Its value is normally derived from the initial slope of the stress strain curve. For LLDPEs, stiffness decreases with increase in the comonomer content [7]. Therefore, polyethylene homopolymer is stiffer than LLDPE. Young's modulus can also be represented as shown in equation 2.2.

$$E \equiv \frac{tensile\ stress}{extensional\ strain} = \frac{\sigma}{\varepsilon} = \frac{\frac{F}{A_\circ}}{\frac{\Delta L}{L_\circ}} = \frac{FL_\circ}{A_\circ \Delta L}$$

Equation 2.2 Young's Modulus

Where:

E = $Young's\ modulus$

F = $Force\ exerted\ on\ an\ object$

$A_\circ$ = $original\ cross-sectional\ area\ through\ which\ the\ force\ is\ applied$

ΔL = $amount\ by\ which\ the\ length\ changes$

$L_\circ$ = $original\ length\ of\ the\ object$

Gupta *et al*. [27] found that mechanical properties of 1-octene based LLDPE are enhanced relative to those based on 1-hexene and 1-butene. However, at a higher speed of tensile testing 1-octene samples and 1-hexene samples performed equally. It would be interesting to compare mechanical properties of closely related comonomers such as 1-octene and 1-heptene.

2.7   References

1.   Albizzati E. and Galimberti M., *Catal. Today*, **1998**, 41(1), 159–168.

2.   Jorgensen J. K., Larsen A., and Helland I., *e-Polymers*, **2010**, 10(1), 1596–1612.

3.   Hagen H. H. and van Der Heijden L. P. P., *Copolymers of ethylene and 1-heptene*, **2004**, United States Patent: US 7312295 B2.

4.   Simanke A. G., De Lemos C., and Pires M., *Polym. Test.*, **2013**, 32(2), 279–290.

5.   Kaminsky W., *Macromol. Chem. Phys.*, **2008**, 209(5), 459–466.

6.   Adisson E., Ribeiro M., Deffieux A., and Fontanille M., *Polymer*, **1992**, 33(20), 4337–4342.

7.   Piel C., Starck P., Seppälä J. V., and Kaminsky W., *J. Polym. Sci., Part A: Polym. Chem.*, **2006**, 44(5), 1600–1612.

8.   Von Pechmann H. and Frobenius L., *Ges.*, **1898**, 31, 2643.

9.   Bamberger E. and Tschirner F., *Ber. Dtsch. Chem. Ges.*, **1900**, 33(1), 955–959.

10.   Peacock A., *Handbook of Polyethylene: Structures: Properties, and Applications,* CRC Press, New York, **2000,** 1–24.

11.   Kaminsky W. and Böhm L., *Polyolefins: 50 Years After Ziegler and Natta,* Springer, **2013,** 60–79.

12.   Ziegler K., *Angew. Chem.*, **1952**, 64, 323–329.

13.   Ziegler K. and Gellert H.-G., *Polymerization of ethylene*, **1955**, United States Patent: US 2699457 A.

14.   Natta G. and Corradini P., *II Nuovo Cimento (1955-1965)*, **1960**, 15, 40–51.

15.   Malpass D. B., *Introduction to Industrial Polyethylene: Properties, Catalysts, and Processes,* John Wiley & Sons, New Jersey, **2010,** 15–96.

16.   Kelly J. M., *J. Chromatogr. A*, **2002**, 42(3), 355–371.

17.   Kawai F., Watanabe M., Shibata M., Yokoyama S., Sudate Y., and Hayashi S., *Polym. Degrad. Stab.*, **2004**, 86(1), 105–114.

18.   Beach D. L. and Kissin Y., *Wiley-Interscience, Encyclopedia of Polymer Science and Engineering.*, **1986**, 6, 454–490.

19.   Donatelli A., *J. Appl. Polym. Sci.*, **1979**, 23(10), 3071–3076.

20.   James D. E., *Wiley-Interscience Encyclopedia of Polymer Science and Engineering.*, **1986**, 6, 429–454.

21.   Benham E. A. and McDaniel M. P., *Linear, very low density polyethylene polymerization process and products thereof*, **1993**, United States Patent: 5,274,056.

22. Kissin Y. V., Pebsworth L. W., Kissin Y. V., Kissin Y. V., Lieberman R. B., Kissin Y. V., Lappin G. R., Nemec L. H., Sauer J. D., and Wagner J. D., *Olefin Polymers*, in *Van Nostrand's Encyclopedia of Chemistry*, John Wiley & Sons, Inc., **2005,** 1–53.

23. Doak K. W., *Ethylene polymers,* John Wiley & Sons, New York, **1986,** 383.

24. Kissin Y. V., Pebsworth L. W., Kissin Y. V., Kissin Y. V., Lieberman R. B., Kissin Y. V., Lappin G. R., Nemec L. H., Sauer J. D., and Wagner J. D., *Olefin Polymers*, in *Van Nostrand's Encyclopedia of Chemistry*, John Wiley & Sons, Inc., **2005,** 1–38.

25. Bubeck R. A., *Mater. Sci. Eng., R*, **2002**, 39(1), 1–28.

26. Read D. and McLeish T., *Macromolecules*, **2001**, 34(6), 1928–1945.

27. Gupta P., Wilkes G. L., Sukhadia A. M., Krishnaswamy R. K., Lamborn M. J., Wharry S. M., Tso C. C., DesLauriers P. J., Mansfield T., and Beyer F. L., *Polymer*, **2005**, 46(20), 8819–8837.

28. Hosoda S., *Polym. J.*, **1988**, 20(5), 383–397.

29. Teng H.-X., Shi Y., Jin X.-G., and Cheng S. Z. D., *Chin. J. Polym. Sci.*, **2002**, 20(4), 347–352.

30. Sarzotti D. M., Soares J. B., and Penlidis A., *J. Polym. Sci., Part B: Polym. Phys.*, **2002**, 40(23), 2595–2611.

31. Yam K. L., *The Wiley Encyclopedia of Packaging Technology,* John Wiley & Sons, New York, **2010,** 983–987.

32. Liu T. M. and Baker W. E., *Polym. Eng. Sci.*, **1992**, 32, 944–955.

33. Bunn C. W., *Trans. Faraday Soc.*, **1939**, 35, 482–491.

34. Malpass D. B., *Handbook to Industrial Polyethylene,* John Wiley & Sons, New Jersey, **2012,** 59–133.

35. Galland G. B., Da Silva L. F., and Nicolini A., *J. Polym. Sci., Part A: Polym. Chem.*, **2005**, 43(20), 4744–4753.

36. Galland G. B., Seferin M., Mauler R. S., and Dos Santos J. H. Z., *Polym. Int.*, **1999**, 48(8), 660–664.

37. Simanke A. G., Galland G. B., Freitas L., da Jornada J. A. H., Quijada R., and Mauler R. S., *Polymer*, **1999**, 40(20), 5489–5495.

38. Soares J. B. P. and McKenna T. F. L., *Polyolefin Reaction Engineering,* Wiley, Germany, **2013,** 54–107.

39.   Soares J. B. P. and Simon L. C., *Coordination Polymerization*, in *Handbook of Polymer Reaction Engineering*, Wiley, Weinheim,**2005,** 365–430.

40.   Soares J. B. P., McKenna T., and Cheng C. P., *Coordination Polymerization,* Blackwell Publishing, Oxford, **2007,** 29–117.

41.   Vasile C., Pascu M., and Limited R. T., *Practical Guide to Polyethylene,* iSmithers Rapra Publishing, Shrewsbury, **2005,** 21–30.

42.   Robertson G. L., *Food Packaging: Principles and Practice,* Taylor & Francis, United States, **2013,** 12–31.

43.   Hashemi S. and Williams J., *Polymer*, **1986**, 27(3), 384–392.

44.   Joubert D. J., *Ethylene and propylene copolymers utilizing Fischer-Tropsch α-olefins*, PhD Thesis, Stellenbosch University, **2000.**

45.   Mandelkern L., *Crystallization of polymers,* McGraw-Hill New York, **1964,** 291–337.

46.   Baer E., *Engineering Design for Plastics,* Reinhold Publishing Corporation, New York, **1964,** 143–198.

47.   Mirabella F. M. and Bafna A., *J. Polym. Sci., Part B: Polym. Phys.*, **2002**, 40(15), 1637–1643.

48.   Hansen E. W., Kristiansen P. E., and Pedersen B., *J. Phys. Chem. B*, **1998**, 102(28), 5444–5450.

49.   Krimm S. and Tobolsky A. V., *J. Polym. Sci.*, **1951**, 7(1), 57–76.

50.   Aggarwal S. and Tilley G., *J. Polym. Sci., Part A: Polym. Chem.*, **1955**, 18(87), 17–26.

51.   Strobl G. and Hagedorn W., *J. Polym. Sci., Part B: Polym. Phys.*, **1978**, 16(7), 1181–1193.

52.   Rull F., Prieto A., Casado J., Sobron F., and Edwards H., *J. Raman Spectrosc.*, **1993**, 24(8), 545–550.

53.   Choi K.-Y. and Ray W. H., *J. Macromol. Sci., Rev.*, **1985**, 25(1), 57–97.

54.   Shamiri A., Chakrabarti M. H., Jahan S., Hussain M. A., Kaminsky W., Aravind P. V., and Yehye W. A., *Materials*, **2014**, 7(7), 5069–5108.

55.   Zakharov V. A., Bukatov G. D., and Yermakov Y. I., *On the mechanism of olefin polymerization by Ziegler-Natta catalysts*, in *Industrial Developments*, Springer, **1983,** 61–100.

56.   Kaminsky W., *Catal. Today*, **1994**, 20(2), 257–271.

57. Fan Z., Zhang L., Xia S., and Fu Z., *J. Mol. Catal. A: Chem.*, **2011**, 351, 93–99.

58. Soares J. B. P. and Anantawaraskul S., *J. Polym. Sci., Part B: Polym. Phys.*, **2005**, 43(13), 1557–1570.

59. Da Silva Filho A. A., Soares J. B. P., and Galland G. B., *Macromol. Chem. Phys.*, **2000**, 201(12), 1226–1234.

60. Xie T., McAuley K. B., Hsu J. C., and Bacon D. W., *Ind. Eng. Chem. Res.*, **1994**, 33(3), 449–479.

61. Barbé P. C., Cecchin G., and Noristi L., *The catalytic system Ti-complex/MgCl$_2$*, in *Catalytical and Radical Polymerization*, Springer Berlin Heidelberg, Berlin,**1986,** 1–81.

62. Boor J., *Ind. Eng. Chem. Res.*, **1970**, 9(4), 437–456.

63. Petitjean L., Pattou D., and Ruiz-López M., *Tetrahedron*, **2001**, 57(14), 2769–2774.

64. Alt H. G. and Köppl A., *Chem. Rev.*, **2000**, 100(4), 1205–1221.

65. Möhring P. C. and Coville N. J., *J. Mol. Catal. A: Chem.*, **1995**, 96(3), 181–195.

66. Kaminsky W., *J. Polym. Sci., Part A: Polym. Chem.*, **2004**, 42(16), 3911–3921.

67. Hey T. W. and Wass D. F., *Organometallics*, **2010**, 29(16), 3676–3678.

68. Hajela S. and Bercaw J. E., *Organometallics*, **1994**, 13(4), 1147–1154.

69. Chadwick J. C., Heere J. J., and Sudmeijer O., *Macromol. Chem. Phys.*, **2000**, 201(14), 1846–1852.

70. Harrison D., Coulter I. M., Wang S., Nistala S., Kuntz B. A., Pigeon M., Tian J., and Collins S., *Journal of Molecular Catalysis A: Chemical*, **1998**, 128(1–3), 65–77.

71. Kissin Y., *The Beginner's Course: General Description of Transition Metal Catalysts and Catalytic Polymerization Reactions*, in *Studies in Surface Science and Catalysis*, Elsevier, **2007,** 1–34.

72. Weckhuysen B. M. and Schoonheydt R. A., *Catal. Today*, **1999**, 51(2), 215–221.

73. Groeneveld C., Wittgen P., Swinnen H., Wernsen A., and Schuit G., *J. Catal.*, **1983**, 83(2), 346–361.

74. Jozwiak W., Dalla Lana I., and Fiedorow R., *J. Catal.*, **1990**, 121(1), 183–195.

75. McGuinness D. S., Davies N. W., Horne J., and Ivanov I., *Organometallics*, **2010**, 29(22), 6111–6116.

76. McDaniel M. P., *Advances in Catalysis*, **2010**, 53, 123–606.

77.   Salamone J. C., *Polymeric Materials Encyclopedia,* CRC Press, **1996,** 8091–8093.

78.   Pasch H. and Trathnigg B., *Multidimensional HPLC of Polymers,* Springer, Berlin, **2013,** 1–56.

79.   Rao B., Balke S. T., Mourey T. H., and Schunk T. C., *J. Chromatogr. A*, **1996**, 755(1), 27–35.

80.   Ibhadon A., *J. Appl. Polym. Sci.*, **1991**, 42(7), 1887–1890.

81.   Parth M., Aust N., and Lederer K., *Int. J. Polym. Anal. Charact.*, **2003**, 8(3), 175–186.

82.   Mes E., De Jonge H., Klein T., Welz R., and Gillespie D., *J. Chromatogr. A*, **2007**, 1154(1), 319–330.

83.   Pasti L., Melucci D., Contado C., Dondi F., and Mingozzi I., *J. Sep. Sci.*, **2002**, 25(10-11), 691–702.

84.   Sun T., Brant P., Chance R. R., and Graessley W. W., *Macromolecules*, **2001**, 34(19), 6812–6820.

85.   Stothers J. B., *Q. Rev. Chem. Soc.*, **1965**, 19(2), 144–167.

86.   Levy G. C., Lichter R. L., and Nelson G. L., *Carbon-13 Nuclear Magnetic Resonance Spectroscopy,* Krieger Publishing Company, **1992,** 4–7.

87.   Stothers J., *Q. Rev. Chem. Soc.*, **1965**, 19(2), 144–167.

88.   Hayashi S. and Hayamizu K., *Bull. Chem. Soc. Jpn.*, **1991**, 64, 685–687.

89.   Cheruthazhekatt S., Harding G. W., and Pasch H., *J. Chromatogr. A*, **2013**, 1286, 69–82.

90.   Yamazaki T., Muhandiram R., and Kay L. E., *J. Am. Chem. Soc.*, **1994**, 116(18), 8266–8278.

91.   Hediger S., Meier B., Kurur N. D., Bodenhausen G., and Ernst R., *Chemical physics letters*, **1994**, 223(4), 283–288.

92.   Hediger S., Meier B., and Ernst R., *Chemical physics letters*, **1995**, 240(5), 449–456.

93.   Schaefer J. and Stejskal E., *J. Am. Chem. Soc.*, **1976**, 98(4), 1031–1032.

94.   Stejskal E., Schaefer J., and Waugh J., *J. Magn. Reson.*, **1977**, 28(1), 105–112.

95.   Jarrett W. L., Mathias L. J., and Porter R. S., *Macromolecules*, **1990**, 23(24), 5164–5166.

96.   Randall J. C., *J. Polym. Sci., Part B: Polym. Phys.*, **1973**, 11(2), 275–287.

97.   Hsieh E. T. and Randall J. C., *Macromolecules*, **1982**, 15(5), 1402–1406.

98.   Hsieh E. T. and Randall J. C., *Macromolecules*, **1982**, 15(2), 353–360.

99.   Kitamaru R., Horii F., and Murayama K., *Macromolecules*, **1986**, 19(3), 636–643.

100.   Wang M., Bernard G. M., Wasylishen R. E., and Choi P., *Macromolecules*, **2007**, 40(18), 6594–6599.

101.   Botha L. and van Reenen A., *Eur. Polym. J.*, **2013**, 49(8), 2202–2213.

102.   Botha L., Sinha P., Joubert S., Duveskog H., and van Reenen A., *Eur. Polym. J.*, **2014**, 59, 94–104.

103.   Assumption H., Vermeulen J., Jarrett W. L., Mathias L. J., and van Reenen A., *Polymer*, **2006**, 47(1), 67–74.

104.   Watson E. S., O'Neill M. J., Justin J., and Brenner N., *Anal. Chem.*, **1964**, 36(7), 1233–1238.

105.   Menczel J. D., Judovits L., Prime R. B., Bair H. E., Reading M., and Swier S., *Differential scanning calorimetry (DSC),* **2009**.

106.   Elvira M., Tiemblo P., and Gomez-Elvira J., *Polym. Degrad. Stab.*, **2004**, 83(3), 509–518.

107.   Camacho W. and Karlsson S., *Polym. Degrad. Stab.*, **2002**, 78(2), 385–391.

108.   Schick C., *Calorimetry*, in *Polymer Science: A Comprehensive Reference, 10 Volume Set*. 2012. p 793–823.

109.   Gabriel C. and Lilge D., *Polymer*, **2001**, 42(1), 297–303.

110.   Sarzotti D. M., Soares J. B. P., Simon L. C., and Britto L. J. D., *Polymer*, **2004**, 45(14), 4787–4799.

111.   Drummond K. M., Hopewell J. L., and Shanks R. A., *J. Appl. Polym. Sci.*, **2000**, 78(5), 1009–1016.

112.   Herschel W., *Philos. Trans. R. Soc. London*, **1800**, 284–292.

113.   Cooley J. W. and Tukey J. W., *Math. Comput.*, **1965**, 19(90), 297–301.

114.   Koenig J. L., *Spectroscopy of Polymers,* Elsevier, New York, **1999,** 35–147.

115.   Cheruthazhekatt S. and Pasch H., *Anal. Bioanal.Chem.*, **2013**, 405(26), 8607–8614.

116.   De Goede E., Mallon P., and Pasch H., *Macromol. Mater. Eng.*, **2010**, 295(4), 366–373.

117.   Harvey M. C. and Ketley A. D., *J. Appl. Polym. Sci.*, **1961**, 5(15), 247–250.

118.   Gulmine J. V., Janissek P. R., Heise H. M., and Akcelrud L., *Polym. Test.*, **2002**, 21(5), 557–563.

119.   Gulmine J. V. and Akcelrud L., *Polym. Test.*, **2006**, 25(7), 932–942.

120.   Heinz L.-C. and Pasch H., *Polymer*, **2005**, 46(26), 12040–12045.

121.   Pasch H., Malik M. I., and Macko T., *Adv. Polym. Sci.*, **2013**, 251, 77–140.

122.   Macko T. and Pasch H., *Macromolecules*, **2009**, 42(16), 6063–6067.

123.   Macko T., Brüll R., Alamo R. G., Stadler F. J., and Losio S., *Anal. Bioanal.Chem.*, **2011**, 399(4), 1547–1556.

124.   Macko T., Brüll R., Alamo R. G., Thomann Y., and Grumel V., *Polymer*, **2009**, 50(23), 5443–5448.

125.   Pasch H., Albrecht A., Bruell R., Macko T., and Hiller W., *Macromol. Symp.*, **2009**, 282(1), 71–80.

126.   Ginzburg A., Macko T., Dolle V., and Brüll R., *J. Chromatogr. A*, **2010**, 1217(44), 6867–6874.

127.   Roy A., Miller M. D., Meunier D. M., Willem Degroot A., Winniford W. L., Van Damme F. A., Pell R. J., and Lyons J. W., *Macromolecules*, **2010**, 43(8), 3710–3720.

128.   Cheruthazhekatt S., Pijpers T. F. J., Harding G. W., Mathot V. B. F., and Pasch H., *Macromolecules*, **2012**, 45(4), 2025–2034.

129.   Monrabal B., Sancho-Tello J., Mayo N., and Romero L., *Macromol. Symp.*, **2007**, 257(1), 71–79.

130.   Cheruthazhekatt S., Mayo N., Monrabal B., and Pasch H., *Macromol. Chem. Phys.*, **2013**, 214(19), 2165–2171.

131.   Monrabal B. and Romero L., *Macromol. Chem. Phys.*, **2014**, 215(18), 1818–1828.

132.   Suriya K., Anantawaraskul S., and Soares J. B. P., *J. Polym. Sci., Part B: Polym. Phys.*, **2011**, 49(9), 678–684.

133.   Soares J. B. P. and Hamielec A. E., *Polymer*, **1995**, 36(8), 1639–1654.

134.   Desreux V. and Spiegels M., *Bull. Soc. Chim. Belg*, **1950**, 59, 476.

135.   Shirayama K., Okada T., and Kita S. I., *J. Polym. Sci., Part A: Polym. Chem.*, **1965**, 3(3), 907–916.

136.   Wild L. and Glöckner G., *Temperature rising elution fractionation*, in *Separation Techniques Thermodynamics Liquid Crystal Polymers*, Springer, **1991,** 1–47.

137. Pasch H., Malik M. I., and Macko T., *Recent advances in high-temperature fractionation of polyolefins*, in *Polymer Composites–Polyolefin Fractionation–Polymeric Peptidomimetics–Collagens*, Springer, **2013,** 77–140.

138. Xu J. and Feng L., *Eur. Polym. J.*, **2000**, 36(5), 867–878.

139. Wild L., Ryle T., Knobeloch D., and Peat I., *J. Polym. Sci., Part B: Polym. Phys.*, **1982**, 20(3), 441–455.

140. Monrabal B., *J. Appl. Polym. Sci.*, **1994**, 52(4), 491–499.

141. Anantawaraskul S., Soares J. B. P., and Wood-Adams P. M., *J. Polym. Sci., Part B: Polym. Phys.*, **2003**, 41(14), 1762–1778.

142. Nieto J., Oswald T., Blanco F., Soares J. B. P., and Monrabal B., *J. Polym. Sci., Part B: Polym. Phys.*, **2001**, 39(14), 1616–1628.

143. Brüll R., Pasch H., Raubenheimer H. G., Sanderson R., van Reenen A. J., and Wahner U. M., *Macromol. Chem. Phys.*, **2001**, 202(8), 1281–1288.

144. Graef S. M., Brüll R., Pasch H., and Wahner U. M., *e-Polymers*, **2003**, 3(1), 51–59.

145. Anantawaraskul S., Soares J. B., and Wood-Adams P. M., *Macromol. Chem. Phys.*, **2004**, 205(6), 771–777.

146. Anantawaraskul S., Soares J. B. P., and Wood-Adams P. M., *Fractionation of Semicrystalline Polymers by Crystallization Analysis Fractionationand Temperature Rising Elution Fractionation*, in *Polymer Analysis Polymer Theory*, Springer, **2005,** 1–54.

147. Li Pi Shan C., Soares J. B. P., and Penlidis A., *Polymer*, **2002**, 43(3), 767–773.

148. Simanke A. G., Galland G. B., Baumhardt Neto R., Quijada R., and Mauler R. S., *J. Appl. Polym. Sci.*, **1999**, 74(5), 1194–1200.

149. Kim Y.-M. and Park J.-K., *J. Appl. Polym. Sci.*, **1996**, 61(13), 2315–2324.

150. Daniels C. A., *Polymers: Structure and Properties,* Taylor & Francis, **1989,** 42–51.

151. Mark J. E., *Physical Properties of Polymers Handbook,* Springer, **2007,** 430–441.

152. Swallowe G. M., *Mechanical Properties and Testing of Polymers: An A-Z Reference,* Springer, **1999,** 242–247.

153. Stuart B. H., *Polymer Analysis,* John Wiley & Sons, Sydney, **2008,** 209–235.

154. Askeland D. and Fulay P., *The Science & Engineering of Materials,* Cengage Learning, United States, **2005,** 198–207.

Chapter 3

Experimental Procedures

3.1   Materials

Ziegler-Natta linear low density polyethylene (ZN-LLDPE)

Eleven samples which included five ethylene/1-heptene (EH), five ethylene/1-octene (EO) linear low density polyethylene copolymers and one polyethylene homopolymer were kindly synthesised and supplied by SASOL.

Catalysts and monomers

The zirconium compound catalyst *rac*-Et[Ind]$_2$ZrCl$_2$ and the co-catalyst methylaluminoxane (MAO, 10 w/v % in toluene) were obtained from Sigma-Aldrich. Ethylene gas (99.9 %) was obtained from AFROX. The 1-olefins: 1-pentene (97 %), 1-heptene (97 %) and 1-octene (98 %) were obtained from ACROS ORGANICS, Sigma-Aldrich and SAFC respectively and were used as received.

Solvents

Xylene (Sigma-Aldrich, 99 %) was used as received for all prep-TREF elution steps. 1,1,2,2-tetrachloroethane (Merck, 99.5 %) was used as an internal reference as well as a solvent for all solution ^{13}C NMR preparations. 1,2,4-trichlorobenzene (TCB) Chromasolv® (Sigma-Aldrich, $\geq$ 99 %) was used as the mobile phase in HT-HPLC while TCB Reagent plus® (Sigma-Aldrich $\geq$ 99 %) was used as the mobile phase in high temperature-size exclusion chromatography (HT-SEC). 1-decanol (Aldrich, 99 %) was used as the primary mobile phase in HT-HPLC. Toluene was purchased from Sigma-Aldrich was dried by refluxing over sodium/benzophenone and distilled under inert atmosphere.

Stabilisers

Stabilisers were used during prep-TREF as well as in analysis of polyethylene copolymers in HT-SEC. Irganox 1010 (Ciba Speciality chemicals) was used at 2 w/w % during the dissolution of the prep-TREF samples to prevent oxidative degradation during the course of fractionation. 0.0125 w/v % butylated hydroxytoluene (BHT $\geq$ 99.0 %, Sigma-Aldrich) was added to the TCB mobile phase in HT-SEC.

3.2   Synthesis of metallocene LLDPE

3.2.1   Catalyst preparation

rac-Et[Ind]$_2$ZrCl$_2$ (0.05 g ,1.17 $\times$ 10^{-4} moles) of the catalyst was weighed and dissolved in dry toluene (20 mL). The catalyst solution was stirred for six hours before use. 1 mL (5.87 $\times$ 10^{-6} moles) of the solution was taken and diluted with 10 mL dry toluene before adding 3 mL (0.0052 moles) MAO. All catalyst preparations were done using a glove box and/or standard Schlenk techniques.

3.2.2   Polymerisation of metallocene LLDPE

Homo- and co-polymerisations were carried out in a 200 mL semi-batch stainless steel reactor equipped with a glass insert and a magnetic stirrer. A typical polymerisation procedure was carried out as follows:

The reactor was heated to 100 °C and cooled under nitrogen to ambient temperature in order to drive off any moisture present before adding dry toluene (100 mL). The reactor was then put in an oil bath and the temperature maintained at 75 °C for 20 minutes. MAO (2 mL, 0.0034 moles) was added as a scavenger to remove any moisture or oxygen still left in the solvent. The comonomer was then added followed by ethylene which was maintained at a constant feed pressure of 800 kPa. The monomer and comonomer were allowed to mix at 75 °C for 10 minutes. After that, the activated catalyst was introduced into the reactor to start the reaction. The stirring was maintained at 1400 rpm for all polymerisations. The polymerisation was

allowed to proceed for 2 hours after which the reaction was stopped by adding a mixture of methanol containing 10 % v/v HCl.

3.3   Analytical techniques

3.3.1   High temperature-size exclusion chromatography (HT-SEC)

The molar mass (MM) and molar mass dispersity of the LLDPE samples were determined on a PL-GPC 220 High Temperature Chromatograph (Polymer Laboratories, Church Stretton, UK) equipped with a differential refractive index (RI) detector. The LLDPE samples (1.5 – 2 mg) were dissolved in 2 mL of TCB for 2 – 3 hours together with 0.025 % BHT which acted as a stabiliser to prevent sample decomposition/degradation. TCB with 0.0125 % BHT was used as the mobile phase at a flow rate of 1 mL/min. Three 300 × 7.5 mm PLgel Olexis columns (Polymer Laboratories, Church Stretton, UK) were used together with a 50 × 7.5 mm PLgel Olexis guard column and 200 μL of each sample was injected. All experiments in HT-SEC were carried out at 150 °C. The instrument was calibrated using narrowly distributed polystyrene standards (Polymer Laboratories, Church Stretton, UK).

3.3.2   Fourier-Transform infrared spectroscopy (FTIR)

Attenuated total reflectance (ATR) measurements of the bulk LLDPEs and their prep-TREF fractions were recorded on a Thermo Nicolet iS10 spectrometer. Solid samples were used in all the analyses with no prior modifications. Spectra recorded from 4 000 to 650 cm^{-1} were obtained from a collection of 64 scans at a resolution of 4 cm^{-1} with automatic background subtraction. Thermo Scientific OMNIC software (version 8.1) was used for data collection and processing.

3.3.3   Differential scanning calorimetry (DSC)

A TA Instruments Q100 calorimeter calibrated with indium metal standard was used for all melting and crystallisation determinations. Calibration was carried out according to standard procedures. All measurements were carried out under the same conditions of heating and cooling at a rate of 10 °C/min for a temperature range of 10 to 200 °C .The samples were subjected to three cycles with the first cycle (first heating) used to erase the thermal history of the sample.

After each cycle, the temperature was kept constant for 2 minutes. The second and third cycle (first cooling and second heating, respectively) were used for quantitative and qualitative purposes. Measurements were conducted in a nitrogen atmosphere at a purge gas flow rate of 50 mL/min. 4 – 5 mg of each sample were used for analysis and aluminium pans and flat lids were used as sample containers. An empty aluminium pan and lid were used as a reference.

3.3.4 High temperature high-performance liquid chromatography (HT-HPLC)

Chromatographic experiments were performed using a solvent gradient interaction chromatograph (SGIC) constructed by Polymer Char (Valencia, Spain). The instrument has an autosampler (which is a separate unit connected to the injector with a heated transfer line), two separate ovens, switching valves and two pumps which are equipped with vacuum degassers (Agilent, Waldbronn, Germany). For solvent gradient elution in HPLC, a high-pressure binary gradient pump (Agilent, Waldbronn, Germany) was utilised. The evaporative light scattering detector (ELSD, model PL-ELS 1000, Polymer Laboratories, Church Stretton, England) was used with the following parameters: gas flow rate of 1.5 SLM, 160 °C nebuliser temperature and an evaporative temperature of 270 °C. A Hypercarb column (Hypercarb®, Thermo Scientific, Dreieich, Germany) with 100×4.6 mm internal diameter packed with porous graphite particles which have a particle diameter of 5 μm (making a surface area of 120 m^2/g) and pore size of 250 Å was used for all HT-HPLC experiments. The column was placed in an oven and the temperature maintained at 160 °C. The flow rate of the mobile phase during analysis was 0.5 mL/min. To achieve separation, a linear gradient was applied from 100 % 1-decanol to 100 % TCB within 10 minutes after sample injection. These conditions were held for 20 minutes before re-establishing 1-decanol to 100 %. Figure 3.1 shows the gradient profile of the mobile phase composition used in the experiments. For all HT-HPLC analyses a concentration of 1 – 1.2 mg/mL was used (approximately 4 mg in 4 mL of 1-decanol) with 20 μL of each sample being injected.
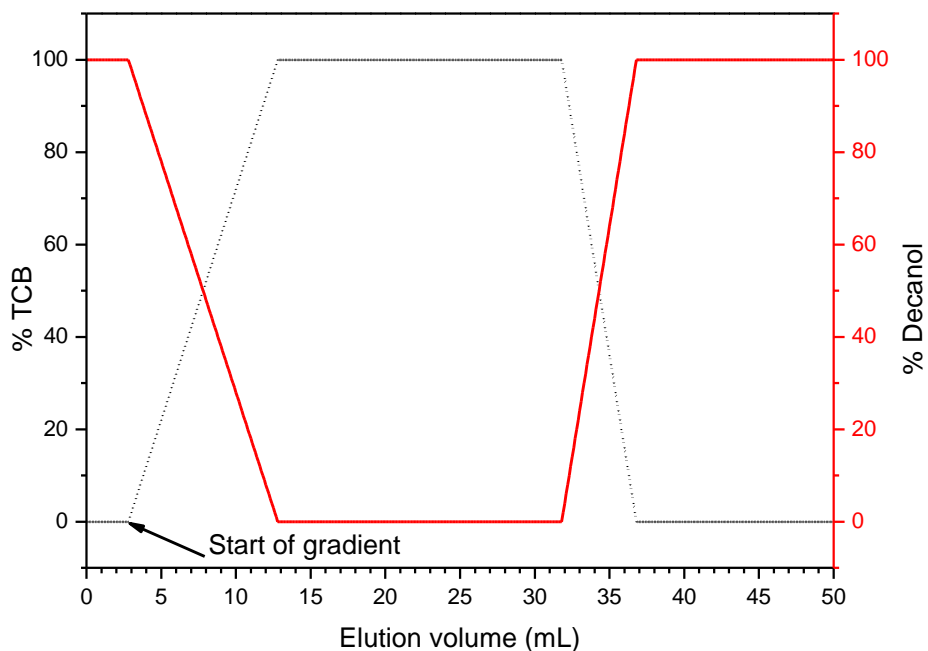
Figure 3.1   Solvent gradient profile used in HT-HPLC analyses.

3.3.5   High temperature two-dimensional liquid chromatography (HT-2D-LC)

Bulk LLDPEs were analysed using HT-2D-LC. HT-HPLC and HT-SEC were coupled with the aid of an electronically controlled eight-port valve system (VICI Valco instruments, Houston, Texas) equipped with two 100 μL sample loops. Injection into the first dimension (HT-HPLC) was carried out using a 110 μL sample loop and the flow rate was 0.05 mL/min with the same gradient as explained in Section 3.3.4 and illustrated in Figure 3.2. A flow rate of 2.75 mL/min was used in the second dimension (HT-SEC) and TCB was used as the mobile phase. In the second dimension, a PL Rapide H (Polymer Laboratories, Church Stretton, U.K.) 100×10 mm internal diameter column with a 6 μm particle diameter was used at 160 °C. The column was kept in an oven at this temperature during the analysis. An evaporative light scattering detector (ELSD) was used for detection.
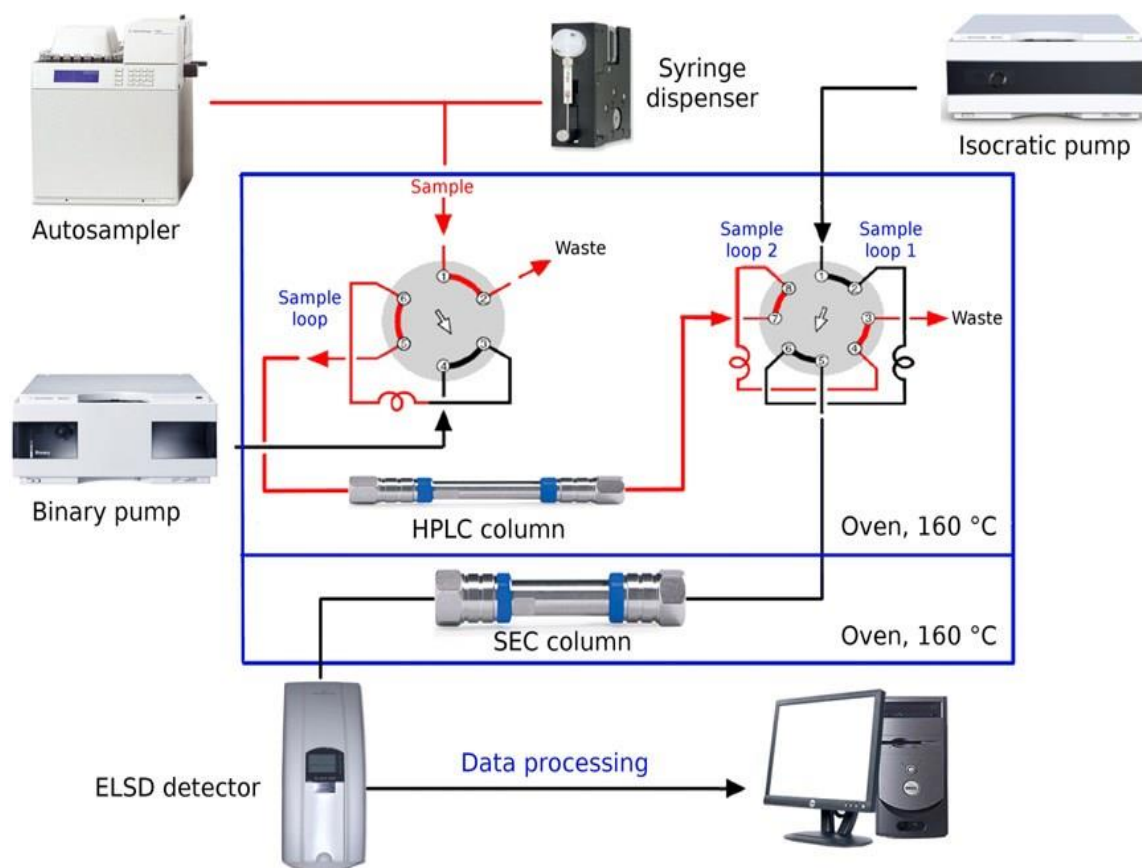
Figure 3.2   High temperature two-dimensional liquid chromatography [1].

3.3.6   Carbon-13 nuclear magnetic resonance spectroscopy (^{13}C NMR)

Bulk LLDPE and prep-TREF fractions were analysed using solution ^{13}C NMR to determine their structure as well as the comonomer content. Approximately 60 mg of each sample was dissolved in 1.5 mL of deuterated 1,1,2,2-tetrachloroethane (TCE-d2) solvent to make a homogeneous solution which was later analysed on a 600 MHz Varian Unity Inova NMR spectrometer, at a resonance frequency of 150 MHz for carbon. TCE-d2 was also used as an internal reference. Analysis was done at 120 °C.

The peaks associated with branching carbons as well as backbone carbons were integrated and the integrals of the peaks were used to determine the comonomer content in mole % using equation 3.1

$$Comonomer\ content\ [C]mole\ \% = \frac{2 \times \sum Br}{\sum backbone\ carbons} \times 100\ \%$$

Equation 3.1 Calculation of comonomer content in mol %.

Where:

$[C] =\ comonomer\ content$

$Br\ =\ branching\ carbon\ atoms$

Solid state ^{13}C cross polarisation (CP) NMR experiments were used for qualitative purposes. The details on the experimental procedure are given in literature [2, 3].

3.3.7 Crystallisation analysis fractionation (CRYSTAF)

A model 200 Polymer Char S.A (Valencia Spain) CRYSTAF instrument was used for all crystallisation analysis fractionation experiments on bulk LLDPE samples as well as their prep-TREF fractions. Approximately 20 mg of each sample were dissolved in 35 mL of TCB in five stainless steel reactors simultaneously at 160 °C. Dissolution was carried out for 90 to 150 minutes depending on sample type with constant stirring. The temperature was then brought down to 100 °C and stabilised for 1 hour before the solution was slowly cooled to 30 °C at the rate of 0.1 °C/min to minimise the effects of co-crystallisation [4] During the crystallisation stage, the solution concentration was measured as a function of temperature and the results recorded.

3.3.8 Preparative-temperature rising elution fractionation (Prep-TREF)

Preparative TREF was carried out using an instrument built in-house. 3.0 g of sample were dissolved in 300 mL of xylene at 130 °C to make a solution with a concentration of approximately 1 wt %). 2.0 % w/w Ingranox 1010 (Ciba Speciality Chemicals, Switzerland) was used as a stabiliser to prevent sample decomposition at high temperatures. The reactor was then quickly transferred to a temperature-controlled oil bath and filled with sea sand which acted as the crystallisation support. To prevent immediate crystallisation of the sample, the support and

cooling oil bath were preheated to 130 °C. To facilitate the controlled crystallisation of the mixture, the oil bath was cooled at a controlled rate of 1 °C/hour. After cooling was completed (from 130 °C to 20 °C), the crystallised polymer and support were loaded into a stainless steel column which was then placed into a modified gas chromatography oven for elution (as shown in Figure 3.5).
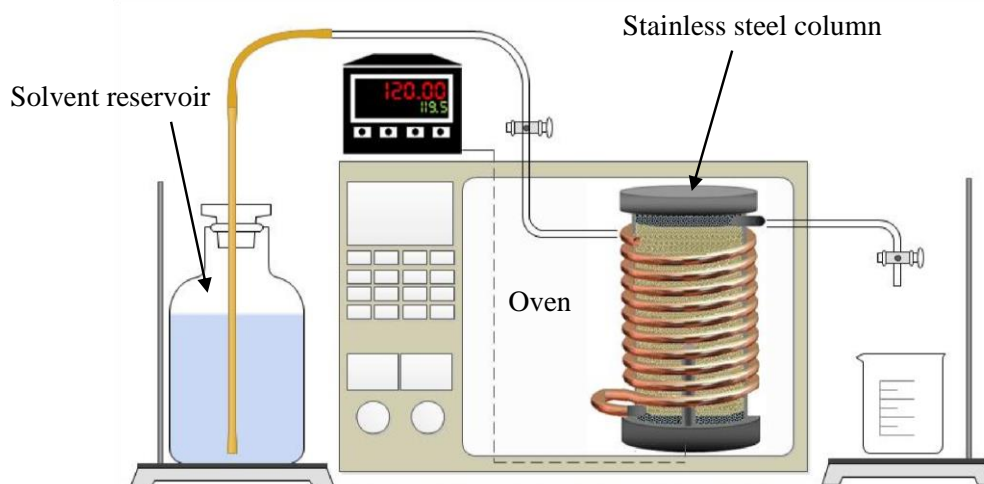
Figure 3.3   An illustration of the setup during the elution step in prep-TREF. [5]

Xylene was preheated and introduced to the column at set intervals to elute the polyethylene fractions as temperature was raised. The fractions were then isolated by precipitating in acetone. In order to remove all the solvent all the fractions were vacuum dried for at least 8 hours.

3.4   Mechanical analyses

3.4.1   Moulding of test specimens

Samples for tensile testing were made using a Thermo Scientific Haake Mini Jet II injection moulding apparatus. The melt temperature was between 200 °C and 250 °C with the mould temperature being kept at 60 °C for all samples. The injection force was modified according to the melt flow index of the samples. After injection, the mould was opened and the sample was rapidly cooled.

3.4.2 Tensile strength determination

Tensile properties of the injection-moulded test samples were determined according to ASTM D 638 M standards. All the samples were 5.2 mm thick, 1.6 mm wide and had a 42 mm gauge length. All tests were carried out after more than 24 hours of moulding on a Lloyd Instruments LRX tensile testing apparatus. Modulus and tensile properties were measured at an extension rate of 50 mm/min.

3.4.3 Density

3.4.3.1 Column filling and calibration:

Two beakers were filled with distilled water and iso-propanol respectively, to the same level with the combined volumes roughly equal to 90 % of the column's volume. The beakers were then placed at the same level, the one containing propanol on a scissor jack and the other with water on a stirrer with stirring bar running. An illustration of the experimental setup is shown in Figure 3.6. The beakers were connected in series with a U-tube fitted with a valve at the top and filled with propanol to allow it to be siphoned into the beaker containing water when the flow to the column is started. From the beaker containing the water, a second U-tube, also fitted with a valve, with the leg going into the density column slightly longer than the one in the beaker, is installed in such a way that the liquid will run into the column along the column's wall to minimise mixing of the liquid in the column. The temperature of the column was controlled by a cooling bath of which the liquid circulates through the column's jacket. This temperature was set at 25 °C. Both valves were then opened and the liquid ran into the column. As the level in the beaker containing water dropped, propanol was siphoned into the water, mixing the two liquids, thereby continuously changing the water/propanol ratio.
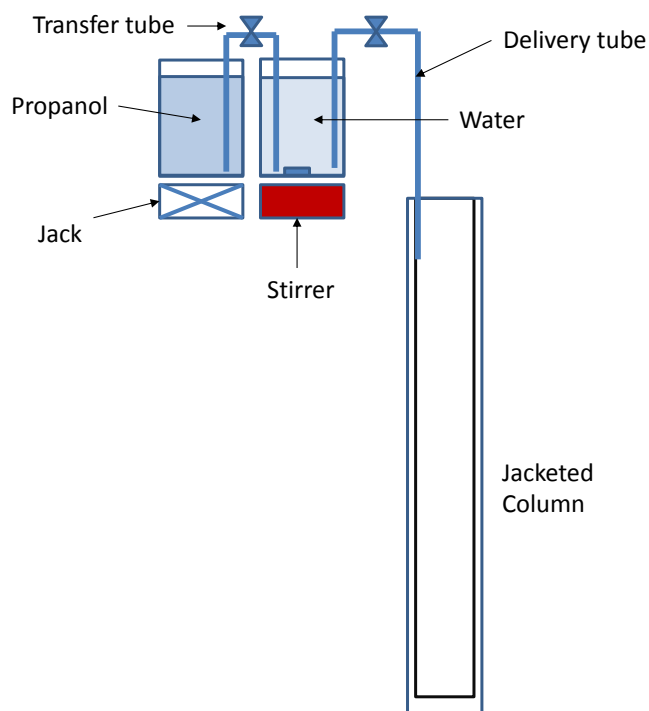
Figure 3.4   Column set up for density determination.

When the column was full (beakers should both be nearly empty), 5 glass spheres of known density where dropped into the column and the column left to stabilise for 48 hours.

Once equilibrium was reached, the height of each ball was measured by means of a tape measure attached to the side of the column and these heights plotted against the densities of the spheres. A linear relationship between height and density was observed. The function describing this relationship was then used to determine the density of samples within the density range established by the glass spheres.

3.4.3.2   Sample conditioning and density measurement:

A polymer sample pellet was placed in a DSC pan and the temperature increased to about 30 °C above its melting temperature and kept isothermally for at least 5 minutes, after which the temperature was decreased at a rate of 10 °C to the temperature of the column. It was ensured that the sample did not contain any voids. The sample was then wetted with a small amount of iso-propanol and dropped into the column. When the sample reached its equilibrium height, its

height was recorded and its density determined from the function obtained from the glass spheres. Before recording the sample height, it was made sure that no bubbles were clinging to the sample surface.

3.5   References

1.   Ginzburg A., Macko T., Dolle V., and Brüll R., *J. Chromatogr. A*, **2010**, 1217(44), 6867–6874.

2.   Botha L., Sinha P., Joubert S., Duveskog H., and van Reenen A., *Eur. Polym. J.*, **2014**, 59, 94–104.

3.   Assumption H., Vermeulen J., Jarrett W. L., Mathias L. J., and van Reenen A., *Polymer*, **2006**, 47(1), 67–74.

4.   Pasch H., Brüll R., Wahner U., and Monrabal B., *Macromol. Mater. Eng.*, **2000**, 279, 46–51.

5.   Swart M., *The Effect of Controlled Degradation with an Organic Peroxide on the Molecular Characteristics and Properties of Heterophasic Propylene-Ethylene Copolymers (HECO)*, PhD Thesis, Stellenbosch University, **2013.**

Chapter 4

Ziegler-Natta linear low density polyethylene (ZN-LLDPE) bulk sample analyses

4.1   Introduction

Microstructures of Ziegler-Natta (ZN) synthesised ethylene/1-heptene (EH) and ethylene/1-octene (EO) linear low density polyethylenes (LLDPEs) copolymers may be closely related given the close similarity of the comonomers used in their production. In this chapter, the molecular properties of the two types of LLDPE are discussed from the results obtained from the experimental procedures described in Chapter 3. Comparisons with low molar mass ZN-LLDPE copolymers and metallocene linear low density polyethylene (m-LLDPE) will also be made where appropriate. The main focus of the present discussion is the comparison between EH and EO copolymers of similar molar masses and comonomer contents.

4.2   Molar mass (MM) and molar mass distribution (MMD)

Molar mass is known to influence physical properties of polyethylene resins in general. Therefore, in our study it was important to compare resins of almost similar molar masses. Figure 4.1 shows the molar mass distributions of the two sets of EH and EO LLDPE samples. It can be seen from the diagrams that the MMD curves are unimodal, and the increase in comonomer content does not affect the modality. Luruli *et al*. [1] found that the molar mass distributions of ethylene/1-pentene copolymers broaden towards lower molar masses as the comonomer content is increased. Bimodality in the molar mass distributions could also be observed at higher comonomer contents (6.9 mol % in their case).
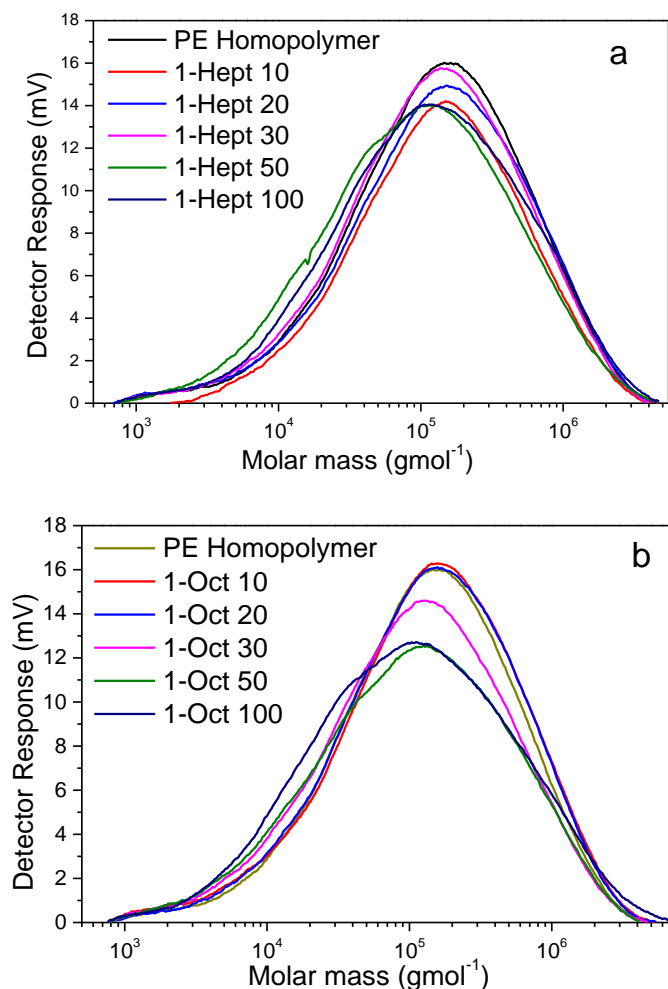
Figure 4.1   Molar mass distributions of (a) EH and (b) EO copolymers.

An increase in the comonomer content of both types of LLDPE does not significantly change their molar mass distributions. Under the same conditions of polymerisation, molar masses of EH and EO resins do not show any trend as more comonomer is used for synthesis. The same was observed with the dispersities of the resins. A summary of the ZN-LLDPE molar masses and dispersities are given in Table 4.1. High dispersities (>2) are known to be typical of heterogeneous catalysts due to their multi-type active site nature [2]. Differences in the reactivities of comonomers are also known to cause differences in MMDs since a more reactive comonomer will be incorporated at a faster rate into the polyethylene chain [3]. Higher reactivity of the comonomer also leads to a more exothermic reaction which provides activation energy for chain termination. In our case, the differences in reactivity between 1-heptene and 1-octene are assumed to be small since the two comonomers are closely related.

Table 4.1 **A summary of ZN-LLDPE properties.**

Sample Name	[C] [a] mol %	[C] [a] weight %	M_w [d] (kg/mol^{-1})	Đ [b]	T_m [c] (°C)	T_c [c] (°C)	X_c [c,d] (%)
1-Hept 10	0.44	1.52	267	8.1	129.1	115.6	48.6
1-Hept 20	0.80	2.75	303	9.1	128.1	115.7	45.2
1-Hept 30	1.60	5.39	278	7.7	126.6	114.4	35.5
1-Hept 50	4.30	13.59	235	8.1	124.1	111.9	17.6
1-Hept 100	5.80	17.73	294	9.0	123.2	111.4	11.4
1-Oct 10	0.35	1.39	309	8.6	130.9	116.7	52.4
1-Oct 20	0.84	3.28	303	7.7	128.9	116.4	46.2
1-Oct 30	1.50	5.74	258	8.3	126.3	114.2	39.2
1-Oct 50	5.10	17.70	270	9.5	124.3	112.1	19.4
1-Oct 100	6.40	21.48	296	10.4	123.9	112.5	11.5
PE[e]	0	0	284	7.3	133.8	119.2	69.0

[a] As calculated from solution ^{13}C NMR spectra [b] As determined by HT-SEC [c] Determined by DSC

[d] $X_c = (\Delta H_m / \Delta H_m^{\Theta} \times 100 \%)$, $\Delta H_m^{\Theta} = 293$ J/g [4]

[e] Polyethylene homopolymer

4.3 Chemical composition analyses of bulk LLDPE

Chemical composition (CC) plays a very important role in the physical and mechanical properties of LLDPEs. It is also known that no one method can give all the required information in order to fully understand the complex nature of polyolefins. Therefore, several methods of characterisation were used in order to elucidate the chemical composition of the LLDPE resins in the present study. The findings from these analyses are discussed in the sections that follow.

4.3.1 NMR analyses

Solution ^{13}C NMR is one of the most reliable tools for measuring the average comonomer content of polyolefin resins. The technique also provides useful information on the differences in

the type of comonomer used in the LLDPE resins. Figures 4.2 and 4.3 which show solution NMR spectra of EH and EO LLDPE respectively, demonstrate the differences in their spectra. Peak signal assignments were based on Randall [5] and others [1, 6, 7]. Despite there being close similarities in the spectra, the signals corresponding to the second carbon in the branch from the main chain, (4 in EH copolymers and 5 in EO copolymers) are different. In EH copolymers, the signal exists separately at a chemical shift of 27.21 ppm (see Figure 4.2) while in EO copolymers the signal merges with that of the second carbon (β carbon) in the backbone chain. This becomes a distinguishing feature between the two types of copolymers.
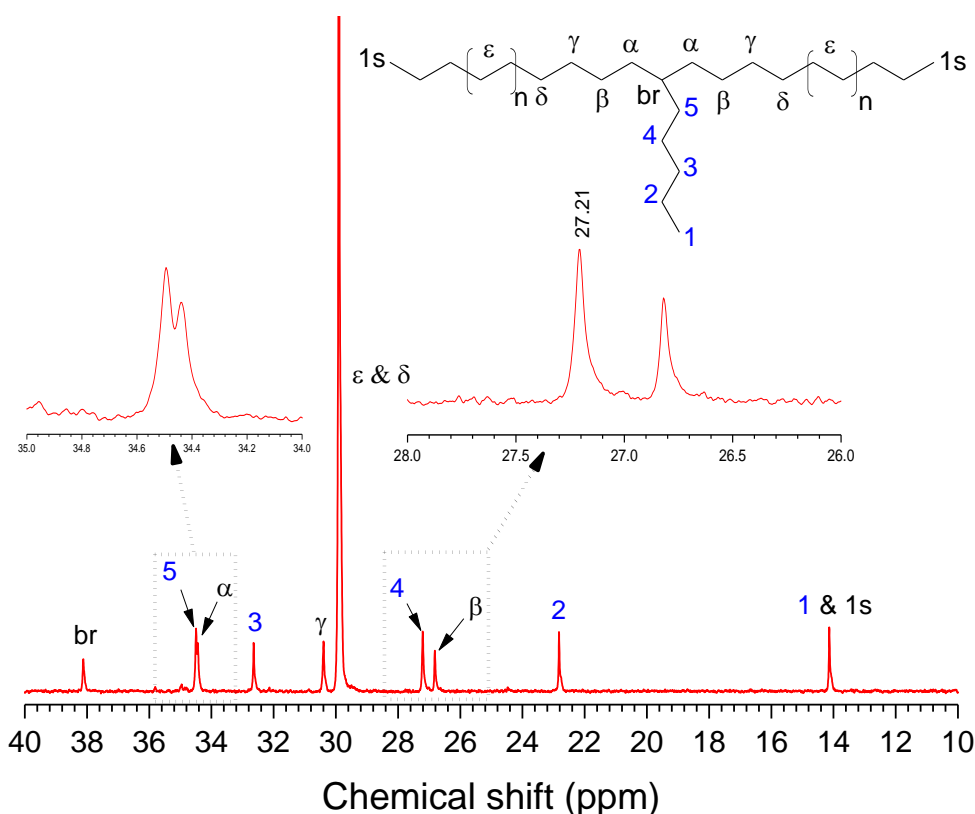
Figure 4.2   **Solution ^{13}C NMR spectrum of 1-Hept 50.**

It is known that as the side chain in the ethylene/1-olefin copolymer becomes longer (from six carbons onwards), the β carbon signal merges with that of the second carbon from the branch.

58
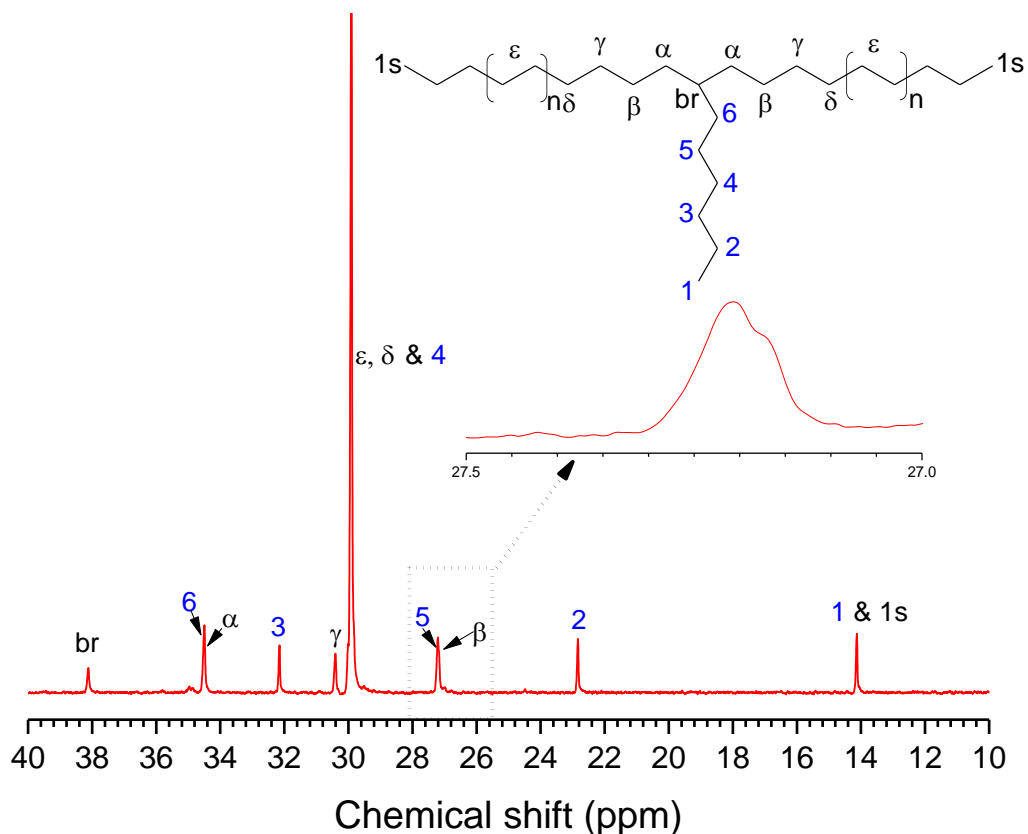
Figure 4.3   Solution ^{13}C NMR spectrum of 1-Oct 100.

The comonomer content was calculated from the NMR spectra, using Equation 3.1 stated in Chapter 3. It was calculated as the ratio of the intensity of the branched carbon (br) signal to the intensities of the total backbone carbon signals. Normalised spectral signal intensities increased with increase in the comonomer content. Details on the average comonomer contents of the ZN-LLDPE resins are shown in Table 4.1. Normalised spectra of both sets of samples are shown in Figure B.1, Appendix B. The average chemical composition varied from 0.44 to 5.80 mol % in EH copolymers while in EO copolymers it was between 0.35 and 6.40 mol %. Having information on average comonomer content allows for comparison between the two sets of copolymers.

4.3.2   FTIR analyses

Figure 4.4 shows the FTIR spectra of the two sets of EH and EO LLDPEs.
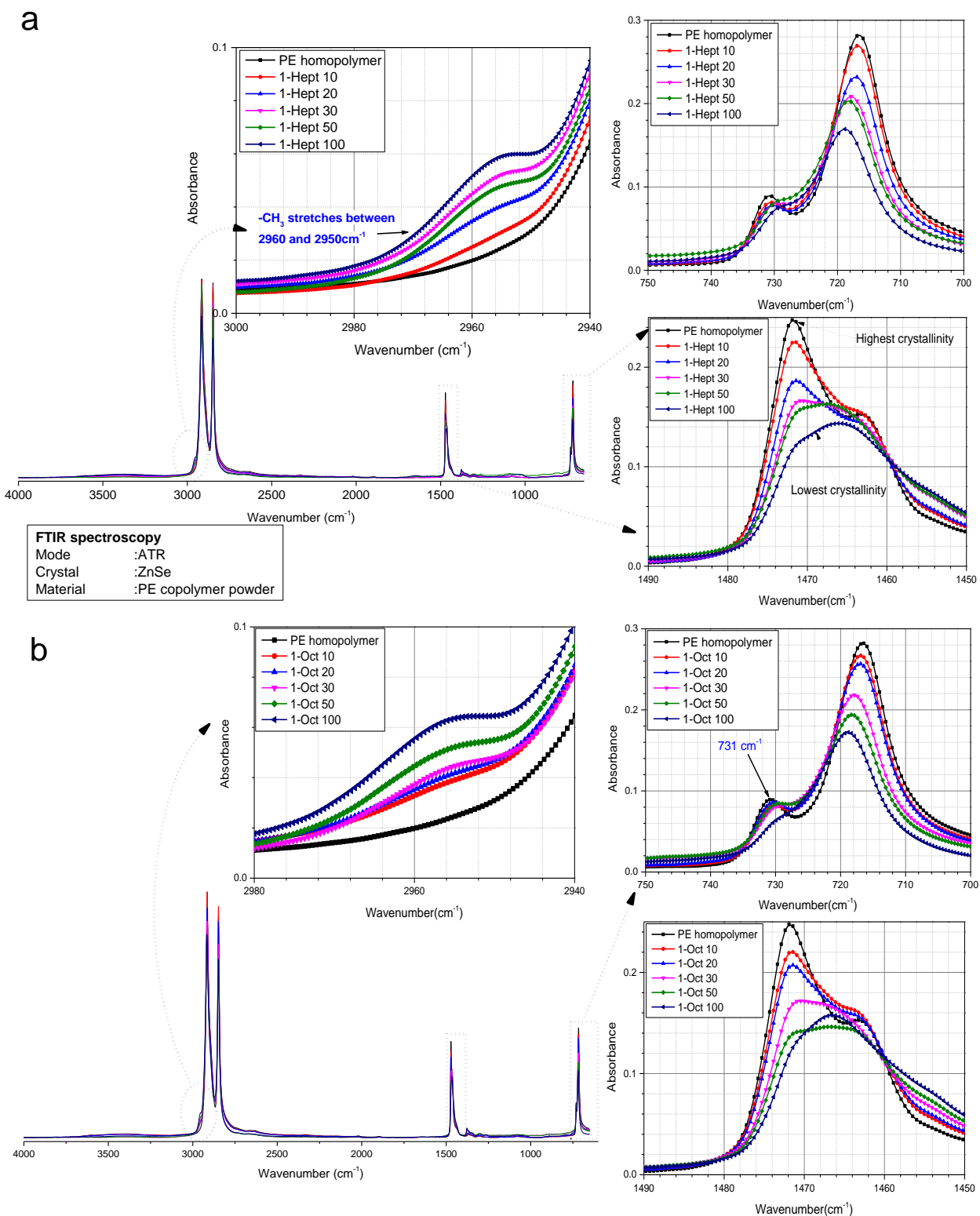
Figure 4.4   FTIR spectra for (a) EH and (b) EO ZN-LLDPE copolymers.

One quick way of analysing the chemical structure and crystallinity of polyolefin resins is through Fourier Transform infrared spectroscopy (FTIR). The compositional analysis of ethylene copolymers by FTIR is well established in literature [8-11]. Considering the FTIR spectra of both sets of LLDPEs, several important observations can be made. For both sets of samples -CH_3 stretches at 2960 cm^{-1} (see Figure 4.4) increase as the comonomer content increases.

Secondly, a peak showing -CH_2 bending deformations in the spectral region of 1480 – 1463 cm^{-1} reveals the change in crystallinity of the samples [12]. It is known that as the crystallinity of the LLDPEs increases, the peak splits. It can be seen from Figures 4.4a and b that as the comonomer content increases, the peak split decreases. Lastly, the absorption peak at 731 – 720 cm^{-1} [11] due to the deformation vibration in (-CH_2)$_n$ where (n≥4) [13, 14], decreases with increase in the comonomer content. The ratio of the peak absorbances at 731 and 720 cm^{-1} is frequently used for calculating percentage crystallinity of the samples although this was not done in the present study. Harvey and Ketley [15] showed that different types of side chains can be identified with small differences in the spectral absorbances between 735 and 722 cm^{-1}. However, such characterisation was not carried out in this work.

4.3.3   DSC analyses

DSC analyses of the bulk LLDPE resins were carried out using the technique described in Chapter 3. Figure 4.5 shows DSC crystallisation curves obtained during the first cooling cycle. The first heating cycle was used to erase the thermal history of the polyethylene resins and was not used for any quantitative or qualitative work. Firstly, it can be observed that the crystallisation temperatures (T_c) decrease as the comonomer content increases. T_c decreases from 119.2 °C for the polyethylene homopolymer to 111.4 and 112.5 °C for 1-Hept 100 and 1-Oct 100 respectively. This trend is expected as more comonomer is incorporated into the polymer chains, shortening the crystallisable methylene sequences. This in turn lowers the crystallinity of the resins and hence the energy required to weaken the intermolecular forces which hold the polymer chains together in spherulites. Several studies have also reported this observation with LLDPE resins [1, 16, 17]. One clear manifestation of the decrease in crystallinity with increasing comonomer content is the decrease in the crystallisation peak area. At roughly similar comonomer contents, the effect of the comonomer (1-heptene or 1-octene) on crystallinity is

comparable for both sets of samples. Crystallinities of both sets of LLDPE resins were calculated from the DSC melting curves and the values are shown in Table 4.1.
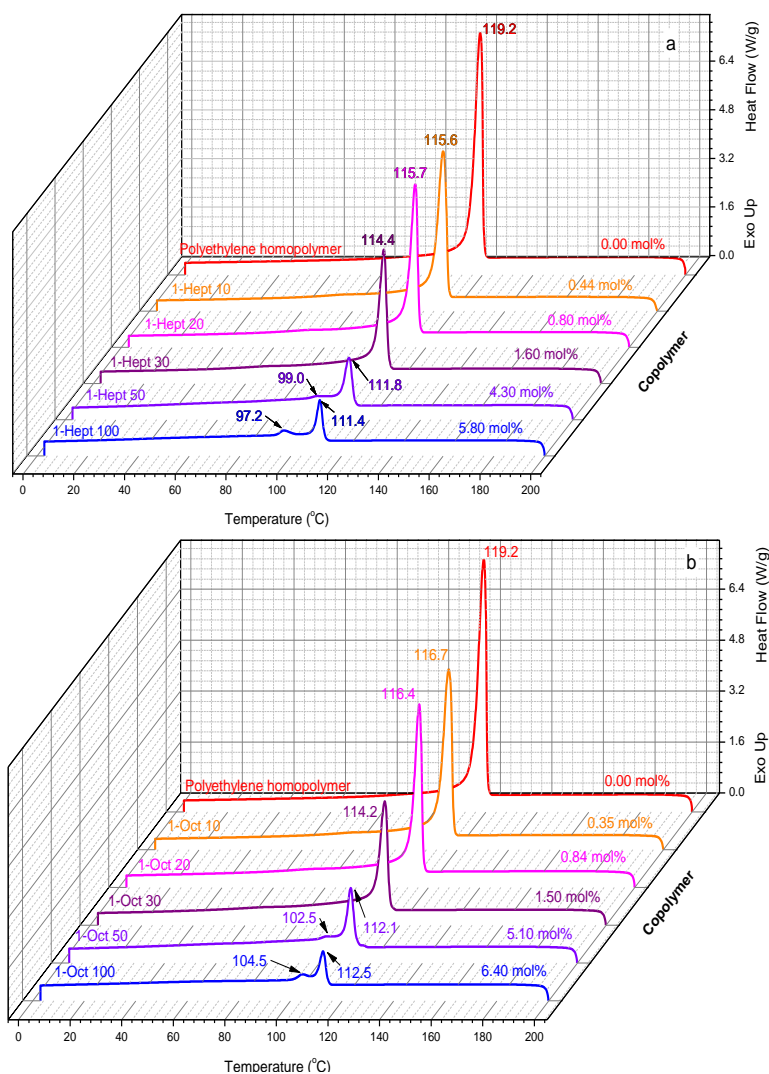
Figure 4.5   DSC first crystallisation exotherms for (a) EH and (b) EO ZN-LLDPE.

At higher comonomer contents, the LLDPE resins from both sets of samples show a second lower melting peak. The peak is attributed to the presence of a second fraction which has higher comonomer content (the copolymer). Ziegler-Natta catalysts possess multiple type active sites [18-20] and the accessibility to some of them by the comonomer is limited by both its size and the location of the site on the catalyst support. As a result some active sites will produce polyethylene, which can be seen as the sharp crystallisation peak in all resin exotherms. Other actives sites produce copolymer fractions with different levels of comonomer incorporation. In

our case, the difference in the comonomer type is expected to play a less important role since the difference between 1-heptene and 1-octene is only one methylene group. Therefore, as far as the catalyst's selectiveness towards the comonomer is concerned, we expect the difference to be negligible.

In order to obtain more information on the various fractions present in the higher comonomer content resins, their crystallisation peaks were deconvoluted using Lorentzian and Gaussian fits. Figures 4.6a-d show the deconvoluted DSC crystallisation exotherms. At least three chemically distinct fractions were seen from the deconvoluted peaks.
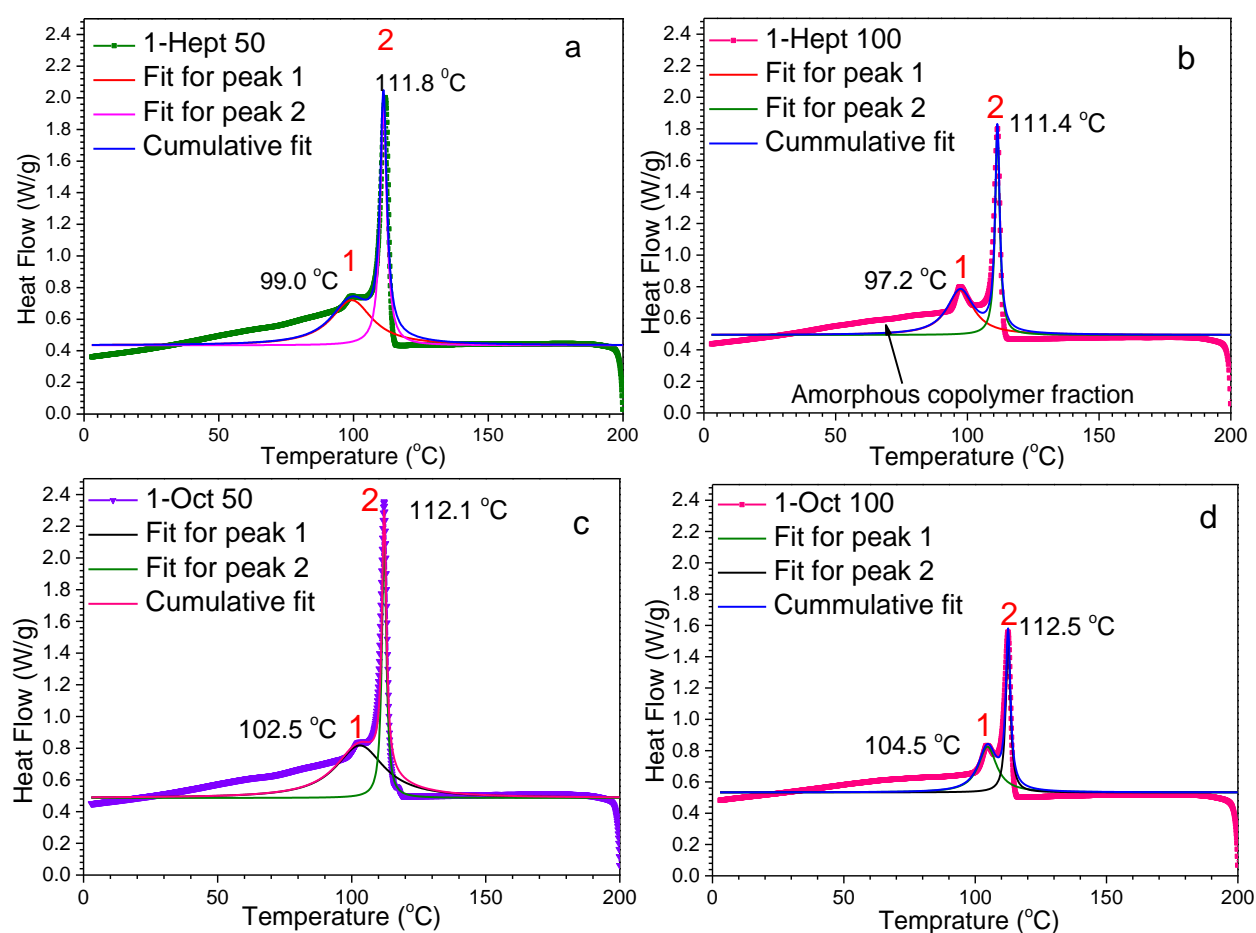
Figure 4.6   Deconvoluted DSC crystallisation exotherms of 1-Hept 50 (a), 1-Hept 100 (b), 1-Oct 50 (c) and 1-Oct 100 (d).

Figure 4.6a shows two peaks; one has a lower T_c of 99.0 °C and the second has a T_c of 111.8 °C. Material not included within the deconvoluted peaks is assumed to consist of amorphous and

possibly material with very low crystallinity. It can be noted from Figures 4.6b and d that the lower melting peak (peak 1), is more pronounced in the higher comonomer content resins. DSC provides the first insight into the heterogeneity of the copolymer resins and interestingly, 1-heptene and 1-octene appear to have similar influences on these changes at roughly similar comonomer contents.

Figures 4.7a and b show the second melting endotherms of both sets of LLDPEs. As was previously seen with crystallisation curves (Figure 4.5), peak areas of the melting endotherms also decrease with increase in the comonomer content of the LLDPE resins. This is also attributed to a decrease in the crystallinity. DSC crystallisation exotherms gave more information on the presence of the different fractions within the copolymer resins. Melting peaks were, however, less sensitive to the presence of chemically different fractions.
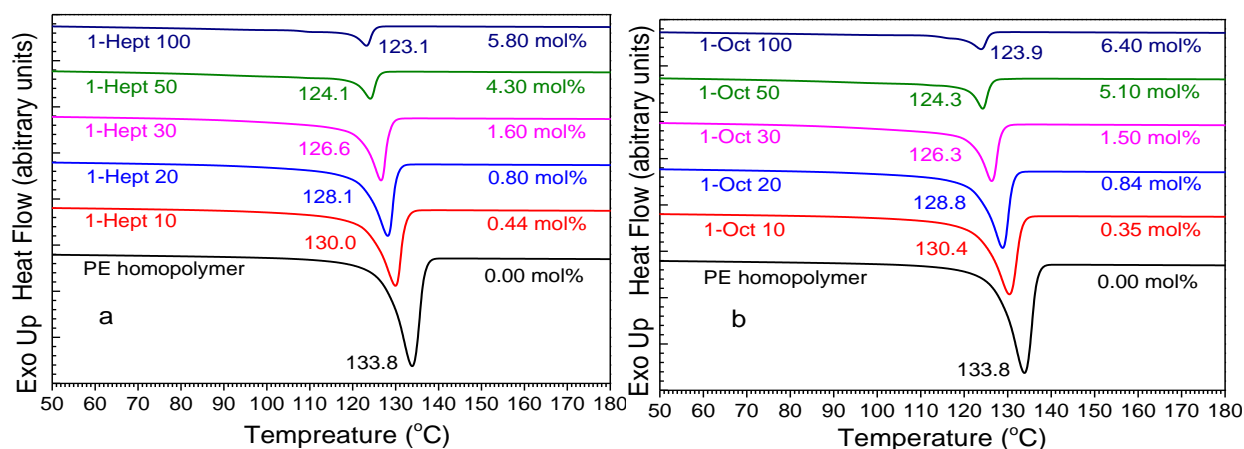
Figure 4.7   DSC second melting endotherms for EH (a) and EO (b) ZN-LLDPE copolymers.

Melting (T_m) and crystallisation (T_c) temperatures of the two sets of resins were compared in order monitor the effect of 1-heptene and 1-octene as comonomers on the LLDPE resins. Figure 4.8a compares the T_m of both sets of samples while Figure 4.8b compares their T_c. At roughly similar comonomer contents, the T_m of both sets of LLDPEs are comparable. This is an indication of 1-heptene's ability to mimic 1-octene in the LLDPE resins. However, the T_c of 1-Oct 100 is higher as compared to the low comonomer resins.
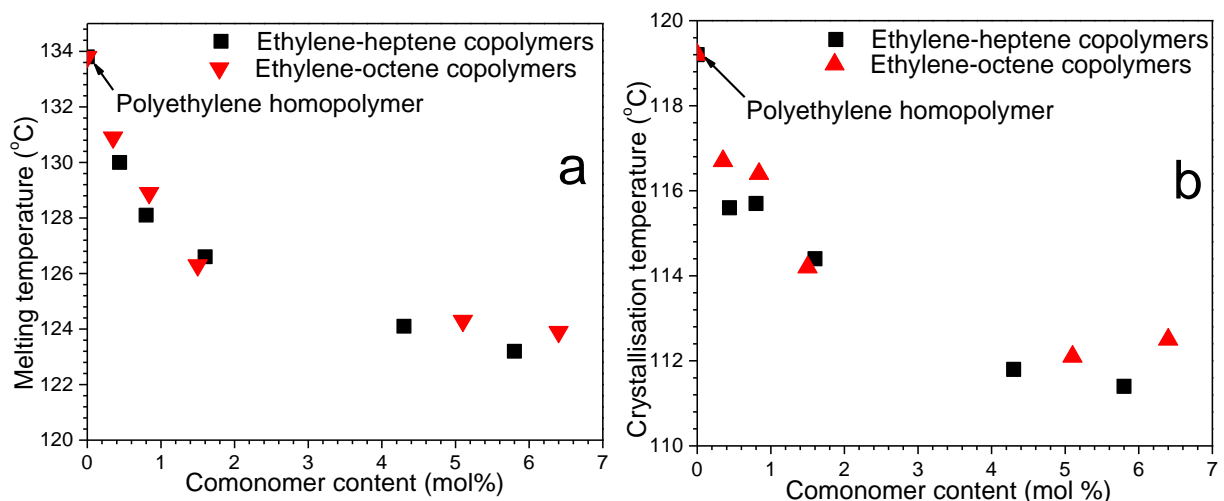
Figure 4.8　　**Effect of comonomer content on second melting (a) and first crystallisation temperatures (b) of ZN-LLDPE resins.**

Gabriel *et al*. [21] studied LLDPE copolymers of ethylene/1-hexene and they found that DSC curves of ZN-LLDPE are comparable to those obtained from TREF and CRYSTAF. This implies that the heterogeneity observed in DSC can also be easily recognised in the solution-based techniques mentioned. CRYSTAF analyses were carried out as a way of determining chemical composition distribution within the resins.

4.3.4　　CRYSTAF analyses

Figures 4.9a and b show the differential distribution CRYSTAF curves for EH and EO ZN-LLDPE respectively. Figures 4.9c and d show the cumulative distribution curves of the respective samples. Firstly, as the comonomer content increases, the crystalline fraction which is seen as a peak between 83 and 86 °C decreases in area and a subsequent increase in the soluble fraction (30 °C and below) is observed. It is interesting to note that even if the crystalline peaks for both sets of LLDPEs decrease, their peak crystallisation temperatures only show slight shifts towards lower temperatures as the comonomer content is increased. The fractions maintain high crystallinity while peak broadening and the slight shift in peak melting temperatures indicate slight comonomer incorporation. From Figure 4.9c and d it can be seen that there is a significant amount of material present between 30 and 80 °C. The fraction in this region is regarded as semi-crystalline. Therefore, from CRYSTAF findings we can conclude that the LLDPE resins used in

the present study, regardless of the type of comonomer, contain three main fractions. The first is a soluble fraction (copolymer) which increases in quantity with increase in the comonomer content. The second fraction is semi-crystalline (as seen from the cumulative curves) and it shows no recognisable trend with the change in the comonomer content of the bulk resins. Lastly, a highly crystalline fraction which is present in all resins is also observed.
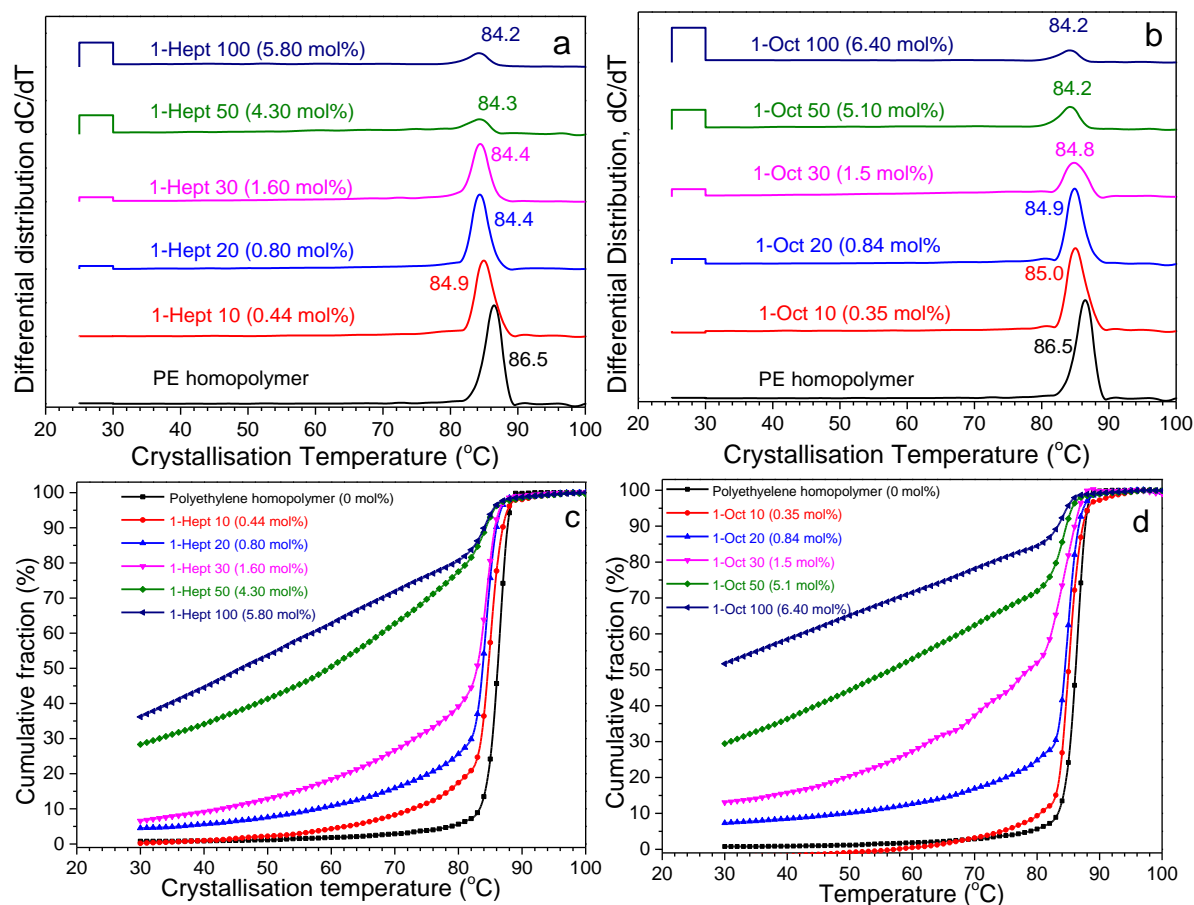
Figure 4.9   Differential and cumulative CRYSTAF curves for EH (a and c) and EO (b and d) ZN LLDPE in comparison to PE homopolymer.

The quantities of the soluble and crystalline fractions present in both sets of resins were plotted against their bulk LLDPE comonomer contents. Figure 4.10 shows the variation of both CRYSTAF soluble and crystalline fractions as a function of bulk LLDPE comonomer content. It is clear that the crystalline fractions, as previously indicated, decrease with the increase in bulk LLDPE comonomer content. The soluble fraction, as shown in Figure 4.10, increases with increase in the comonomer content.
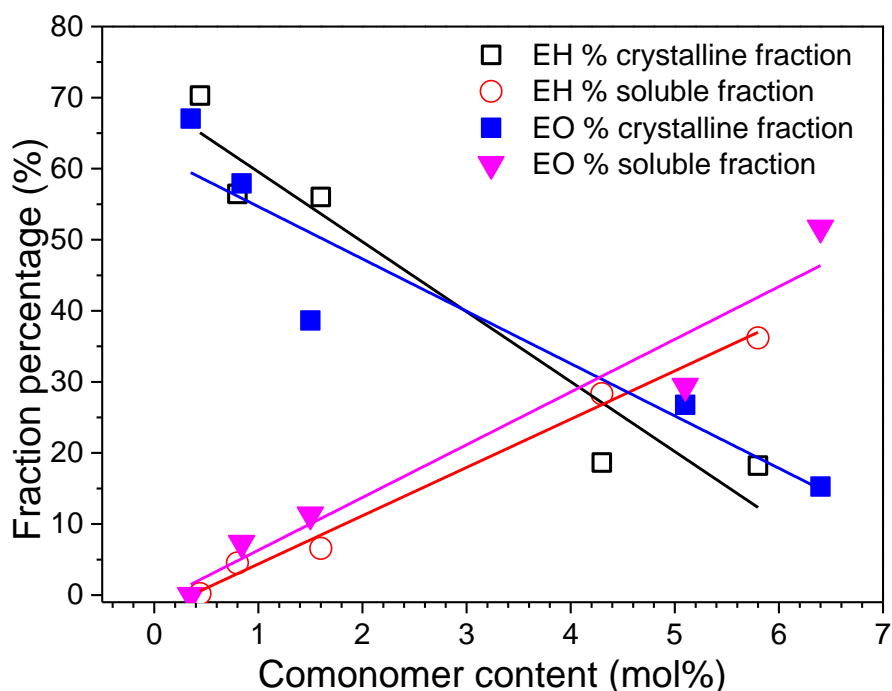
Figure 4.10   Plot of CRYSTAF crystalline and soluble fraction percentages as a function of comonomer content.

Figures 4.11a and b show comparisons of two LLDPEs with roughly similar comonomer contents. It can be seen from the comparisons that there is little difference in CCD of the two types of resins at low comonomer contents. At higher comonomer contents, differences in the soluble fractions can be seen. The EO copolymer has significantly more of the soluble fraction as compared to the EH copolymer. This however, can be attributed to the higher comonomer content of the EO copolymer. 1-octene may also be a better comonomer than 1-heptene at inducing the formation of amorphous/soluble material in the LLDPE resins.

Unlike the CRYSTAF curves presented in previous studies [22-24], the CRYSTAF curves of the resins under study show little variation in peak crystallisation temperature. Instead, there is polyethylene present that decreases on the expense of fractions crystallising between 30 and 80 °C.
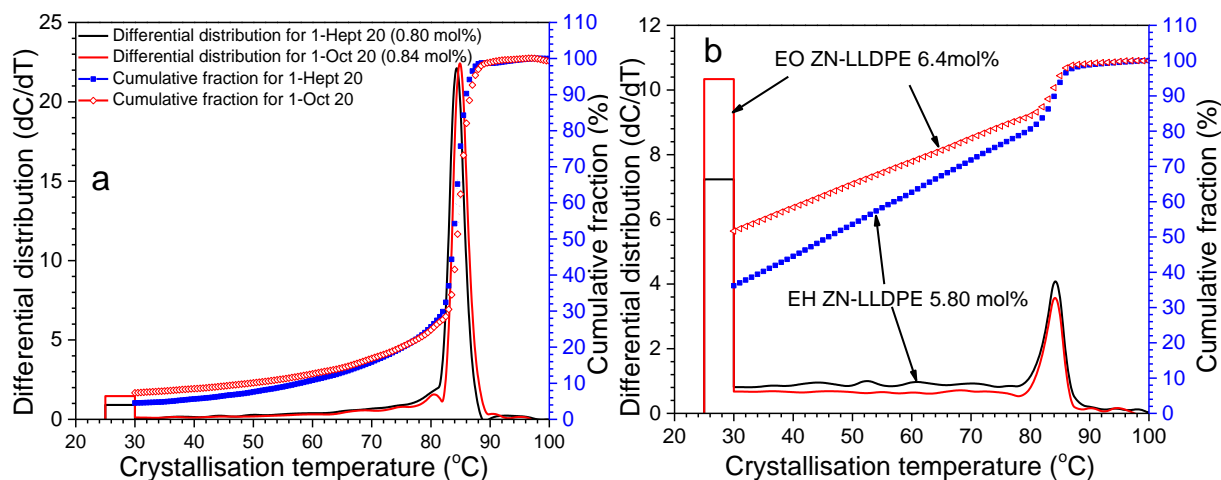
Figure 4.11   CRYSTAF differential and cumulative curve overlays comparing the CCDs of ZN-LLDPE. Low comonomer resins (a) and higher comonomer resins (b) are compared.

For comparison, m-LLDPE CRYSTAF curves are shown in Figure 4.12. Interestingly, the CRYSTAF curves seem to follow the same CCD distribution pattern as that seen with ZN-LLDPE resins i.e. with increase in comonomer content, crystalline material decreases while soluble fractions increase. However, cumulative CRYSTAF curves for m-LLDPE resins (Figures 4.12b, d and f) appear to be different from those of ZN-LLDPE (Figures 4.9c and d). A sharp decrease in the cumulative fraction curve is observed between 78 and 84 °C. Furthermore, the change in cumulative fraction between 30 and 60 °C is small even at higher comonomer contents as compared to that of ZN-LLDPE. This implies that the semi-crystalline fraction is lower in amount in m-LLDPE as compared to ZN-LLDPE.

As seen with ZN-LLDPE copolymers, a slight shift in peak crystallisation temperatures of the crystalline fraction is observed as the comonomer content is increased. It is expected that the behaviour of the two types of catalysts has an impact on the CRYSTAF profiles. However, the widely accepted behaviour of metallocene catalysts on comonomer incorporation does not adequately match the results. Metallocene catalysts are believed to have single type active sites which produce polyethylene resins with narrow CCD [25, 26]. Not much difference can be observed between m-LLDPE and ZN-LLDPE especially with the changes in soluble and crystalline fractions. Details on the yields obtained from the synthesis of m-LLDPE are shown in Tables F.1-F.3 in Appendix F.
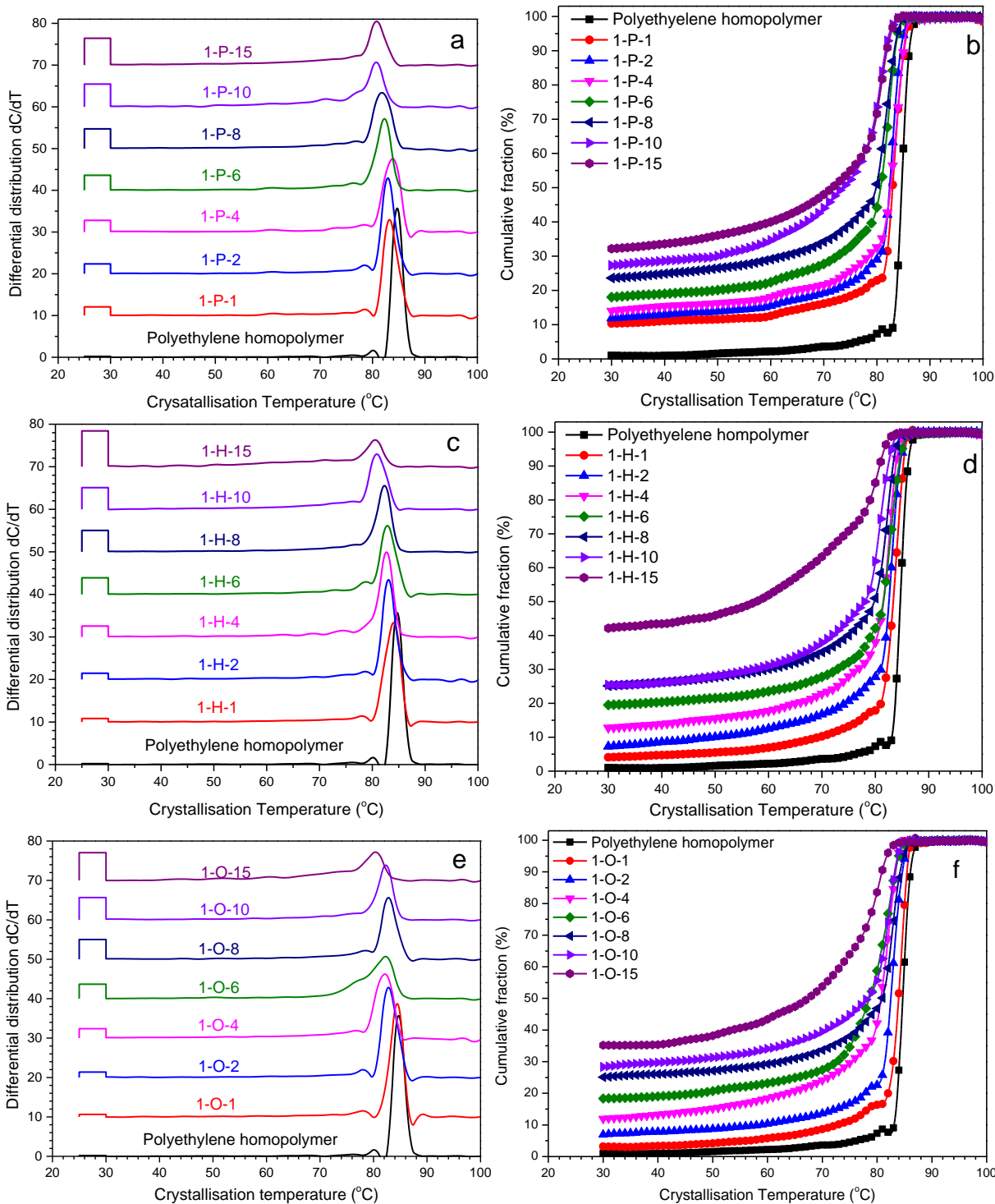
Figure 4.12   Metallocene LLDPE differential and cumulative CRYSTAF curves. Ethylene/1-pentene copolymers are shown in (a) and (b), ethylene/1-heptene copolymers in (c) and (d), ethylene/1-octene in (e) and (f).

TREF and DSC results reported elsewhere [27, 28] showed that the CCD of metallocene LLDPE samples were not as homogenous as expected. Kim and Soares [29] studied the effect of different catalyst support treatments in the 1-hexene/ethylene copolymerisation with supported metallocene catalysts. In their work they found that metallocene catalysts do produce narrow molar mass resins. However, CCD analyses of the resins made by different catalysts suggested that even metallocene catalysts tend to show two or more types of active sites. This was attributed to the presence of a support, which alters some of the catalyst active sites. In our case, the metallocene catalyst was not supported. A possible explanation for this observation, therefore, would be composition drifting due different amounts of the comonomer being present at the start of each polymerisation reaction. The presence of more comonomer favours its rapid incorporation into the copolymer chains. Zhang *et al.* [30] also explained the observed chemical composition heterogeneity of ethylene/1-hexene LLDPEs made with more comonomer as being due to composition drifting. Xu [31] suggests that either active sites in metallocene catalysts may not be homogenous or fluctuation in the local polymerisation environment may also result in compositional heterogeneity of the copolymers.

Crystallisabilities of polymer chains are related directly to methylene sequence lengths within the polymer chains [32, 33]. The longer the methylene sequences, the higher the crystallisabilities of the copolymer chains. The mechanism of separation in high temperature-high performance liquid chromatography (HT-HPLC) is based upon adsorptive interactions of the polymer chains with the Hypercarb stationary phase [34-36]. These interactions are dependent on the length of methylene sequences as with crystallisation in CRYSTAF. Therefore, the longer these sequences are, the greater the interactions with the stationary phase. Retention volumes (V_r) of the copolymer chains (EH or EO) with such characteristics are higher in comparison to those with shorter sequences. It becomes interesting to compare CCD information obtained from CRYSTAF with that obtained from a chromatographic separation such as HT-HPLC.

4.3.5 HT-HPLC analyses

Figures 4.13a and b show HT-HPLC chromatograms for EH and EO ZN-LLDPE respectively. As stated in the above paragraph, HT-HPLC can separate copolymer chains according to methylene sequence length. What is evident in the chromatograms shown in Figure 4.13 is the

existence of two predominant chemically distinct fractions. The first component has a low V_r and its peak increases in size as the bulk LLDPE comonomer content increases. There is also an observable shift in peak V_r towards lower elution volumes as the comonomer content increases, which signifies a chemical change in the fraction. Lower retention volumes are attributed to copolymer chains with shorter methylene sequences and lower molar masses. The trend is true for both sets of copolymers. The peaks are also symmetrical, and the distribution of copolymer chains within the peaks could be due to a molar mass effect or differences in methylene sequences or both.
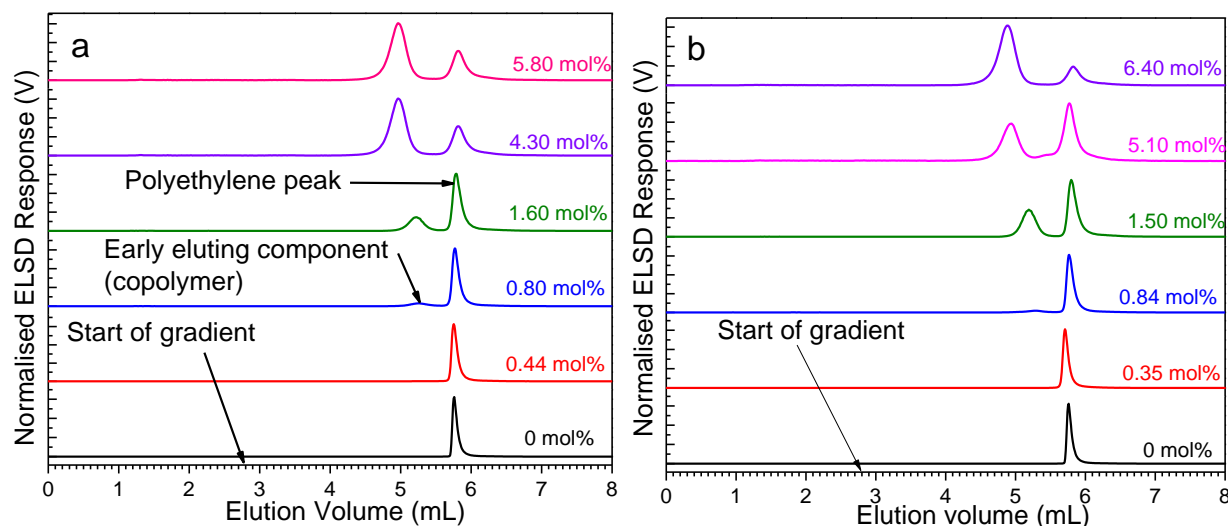
Figure 4.13   Chromatograms showing elution volumes of EH ZN-LLDPE (a) and EO ZN-LLDPE (b) copolymers as detected by an ESLD detector.

A second peak with the same V_r as that of the polyethylene homopolymer (peak maximum ≈ 5.8 mL) is also observed for all copolymers. The peak decreases in size with increase in the comonomer content of the LLDPEs. However, V_r does not change with increase in the comonomer content. The second peak is expected to have almost similar chemical composition as polyethylene homopolymer, though peak broadening at higher comonomer contents suggests a slight change in microstructure. Possibly, at higher comonomer contents, the polyethylene chains may have a few branches due to slight comonomer incorporation.

When HT-HPLC results are compared to DSC and CRYSTAF results, similarities can be drawn from the change in chemical composition of the two sets of ZN-LLDPE resins. Firstly, DSC

findings (Section 4.3.3) indicate a decrease in crystallinity of the LLDPE resins as the comonomer content is increased. HT-HPLC results show a decrease in the component with longer methylene sequences (polyethylene fraction) with increase in the comonomer content. The solubility of some of the copolymer fractions in CRYSTAF and the absence of DSC crystallisation peaks for the same component suggests a lack of methylene sequences of crystallisable length. However, HT-HPLC shows that all of copolymer fractions elute after the start of the gradient, which means the copolymer chains have methylene sequences that are long enough to interact with the stationary phase. Figure 4.14 compares the findings from DSC, CRYSTAF and HT-HPLC.
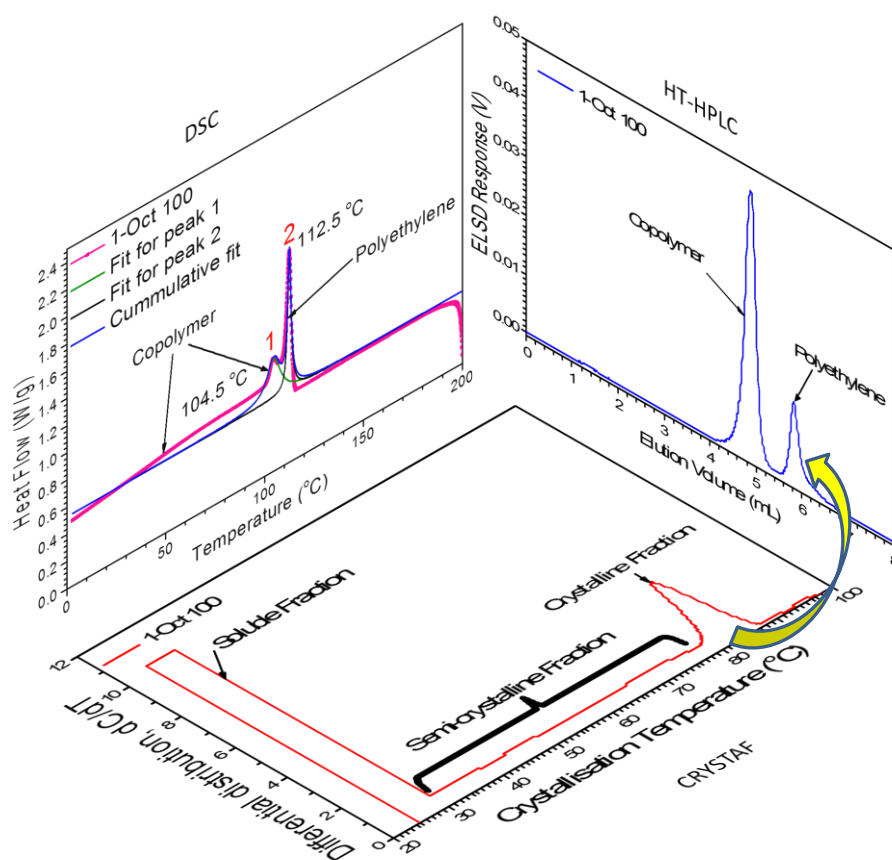
Figure 4.14   A comparison of DSC, CRYSTAF and HT-HPLC plots of 1-Oct 100 (6.4 mol %).

Figure 4.15 compares the HT-HPLC chromatograms of EH and EO LLDPE copolymers with roughly similar comonomer contents.
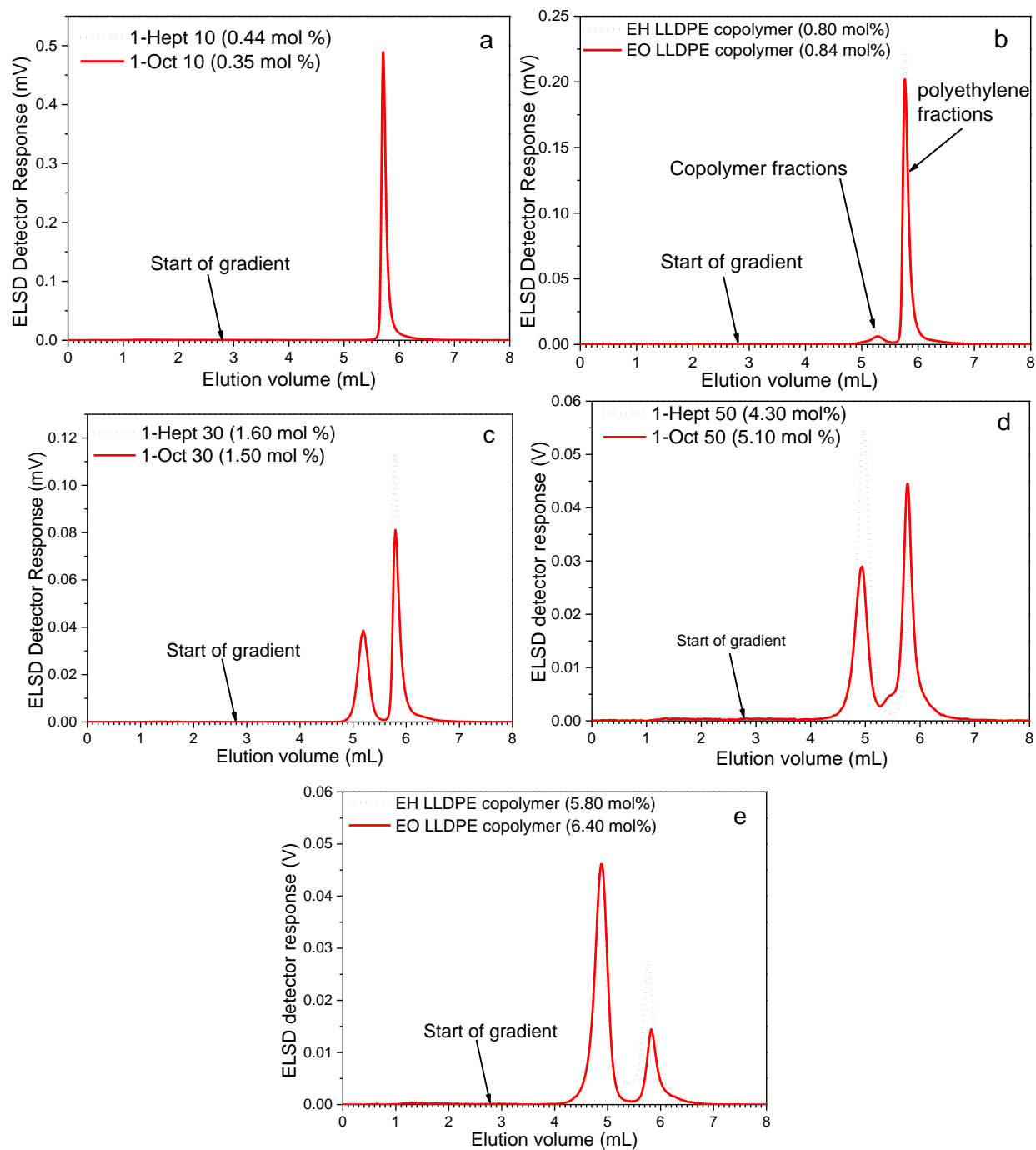
Figure 4.15   Overlays of chromatograms of EH and EO copolymers with comparable comonomer contents.

While it is difficult to observe the presence of chemically different constituents at low comonomer contents in DSC, the presence of different fractions is clearly brought out by HT-HPLC. The copolymer fraction is observed at as low as 0.80 mol % in EH copolymers and 0.84

mol % in EO copolymers and the differences between the chromatograms are rather marginal. When higher comonomer content resins (Figure 4.14e) are compared it can be seen that there is a small difference between the two chromatograms. An increase in the comonomer content decreases V_r of the copolymer peak. EH and EO copolymer peaks show the same V_r at similar comonomer contents. Therefore the difference in the comonomer (1-heptene or 1-octene) does not affect HT-HPLC retention volumes.

The crystalline component peaks in CRYSTAF, as well as the last eluting peaks in HT-HPLC were integrated and their areas plotted against the bulk LLDPE comonomer contents. Figure 4.16 shows the variation of the peak areas as a function of comonomer content. HT-HPLC peaks areas of EH copolymers (red open circles) are comparable to those of EO copolymers (solid red triangles). The comparison of the peak areas is particularly interesting as the ability of 1-heptene as a comonomer to lower the crystallinity can be compared to that of 1-octene.
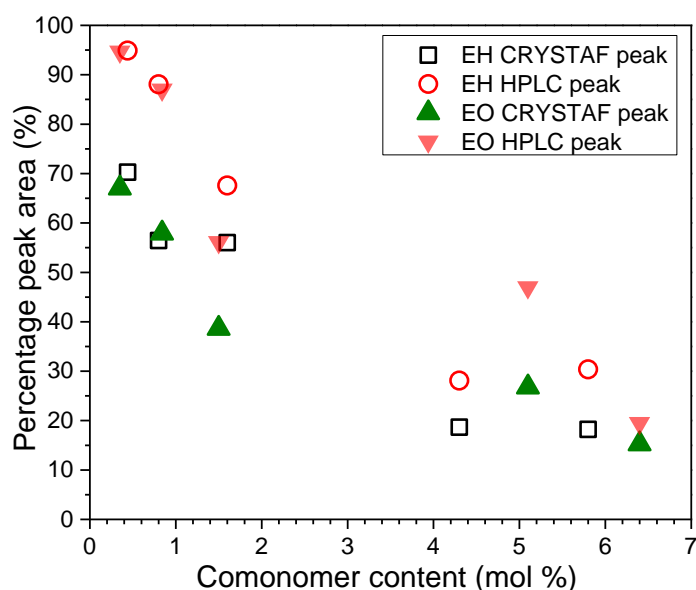
Figure 4.16   **Plot showing comparison of CRYSTAF crystallisation peak areas and the HT-HPLC polyethylene peak areas of EH and EO copolymers. The peak areas were obtained after integrating the homopolymer peaks in CRYSTAF and in HT-HPLC.**

4.3.6   HT-2D-HPLC analyses

Macko *et al*. [37] showed in their recent work that although chemical composition is the primary parameter that governs separation, molar mass also plays a role. In order to obtain more information on the variation of chemical composition with molar mass, 2D experiments were carried out on the ZN-LLDPE samples. Figure 4.17 shows the 2D-chromatograms of 1-Oct 10 (0.35 mol %) and 1-Oct 100 (6.4 mol %). Despite the poor resolution due to poor detector response, two regions of interest can be seen.
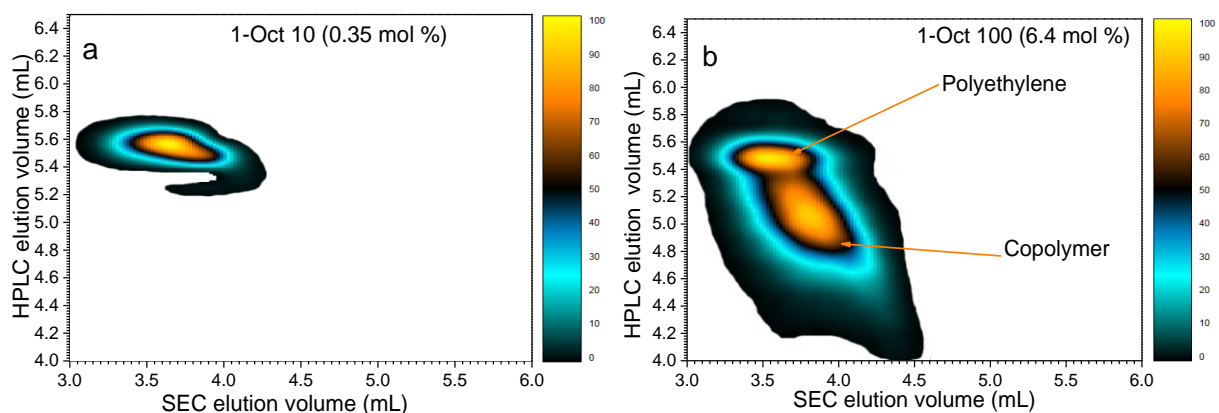
Figure 4.17   2D chromatograms of 1-Oct 10 (a) with a comonomer content of 0.35 mol % and 1-Oct 100 (b) with a comonomer content of 6.4 mol %.

The first component which elutes earlier in the HT-HPLC dimension is the copolymer. Due to weaker interactions of the copolymer chains with the Hypercarb column, their retention volumes (V_r) are correspondingly lower. The fraction is heterogeneous as seen by the area occupied in comparison to the late eluting polyethylene fraction. Molar mass also plays a role in HT-HPLC separation as previously mentioned in Section 4.3.5. The polyethylene fraction (as seen from Figure 4.17b) has higher molar mass as compared to the copolymer. This is in complete agreement with previously known information regarding comonomer distribution according to molar mass within an LLDPE resin that copolymer chains with the highest comonomer content have the lowest molar masses.

4.4   Physical properties and mechanical analyses

4.4.1   Density

Figures 4.18a and b show the variation of the ZN-LLDPE densities with increase in comonomer content. It is clear from the diagrams that there is a linear dependency of density on the comonomer content for both sets of samples. Figure 4.18b shows the dependency of density on the comonomer content in weight %. The effectiveness of 1-heptene in lowering density is almost identical to that of 1-octene. Hong *et al.* [17] found the same correlation to weight % and mol % to be true when they compared 1-decene based LLDPE to 1-octene and 1-hexene based LLDPEs. Since the density of crystalline regions remains constant (1 g/cm^3 for polyethylene crystal as calculated in [38]), the change in density can be attributed to change in the content of the amorphous fraction (since comonomer units are located in the amorphous regions).
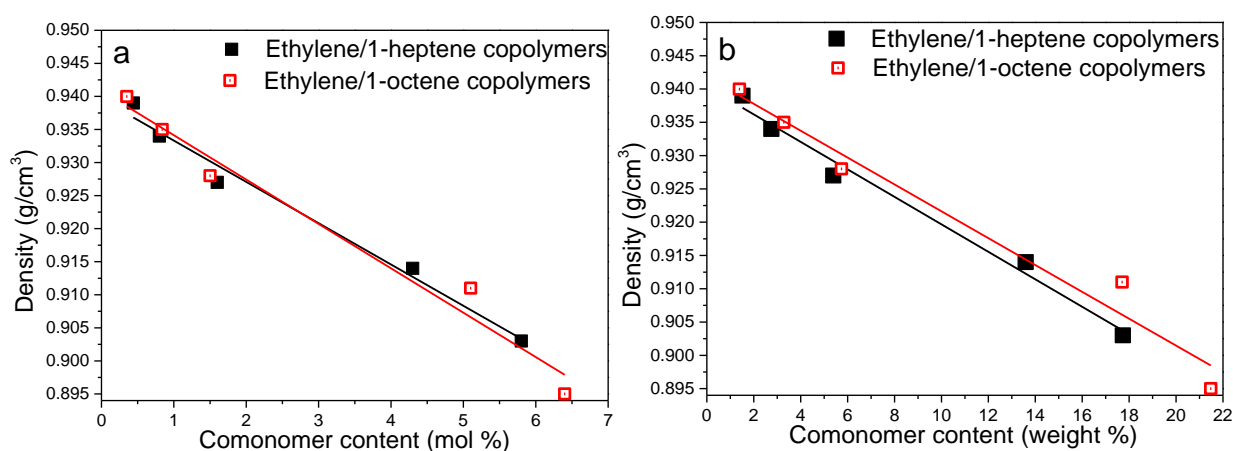
Figure 4.18   Effect of comonomer content on the density of EH and EO ZN-LLDPE in (a) mol % and (b) weight %.

This is particularly interesting as it was seen in Section 4.3.4 and 4.3.5 (CRYSTAF and HT-HPLC respectively) that the crystalline fractions within the resins decrease linearly with the increase in comonomer content (see Figure 4.10). Therefore, the decrease in density follows the same trend as the decrease in the crystalline (polyethylene homopolymer) fractions.

4.4.2   Crystallinity

The increase in short chain branching (SCB) is known to cause a decrease in the crystallinity of LLDPE resins [17, 39-44]. As seen earlier from DSC analyses (Figures 4.8a and b, Section 4.3.3), both T_m and T_c decrease with increase in the comonomer content. This is attributed to a decrease in crystallinity of the resins as the short chain branching increases. However, detailed information on the quantities of crystalline and amorphous fractions cannot be readily and reliably obtained from DSC curves. DSC measures the heats of crystallisation and melting in the polymer melt where effects of entanglement, secondary crystallisation and cocrystallisation play a more important role than in solution based techniques such as CRYSTAF and TREF. In addition, amorphous material does not show any recognisable peaks which make the quantification of such material a challenge.

Figure 4.19 shows the effect of comonomer content on crystallinity. Crystallinities of the LLDPE samples were calculated from enthalpies derived from DSC melting curves. Mirabella and Bafna [4] compared crystallinities obtained from DSC and X-ray diffraction (XRD) and concluded that the crystallinity values obtained by simple division of the observed heat of fusion ΔH_m by a constant ΔH_m^{θ} is sufficiently accurate.
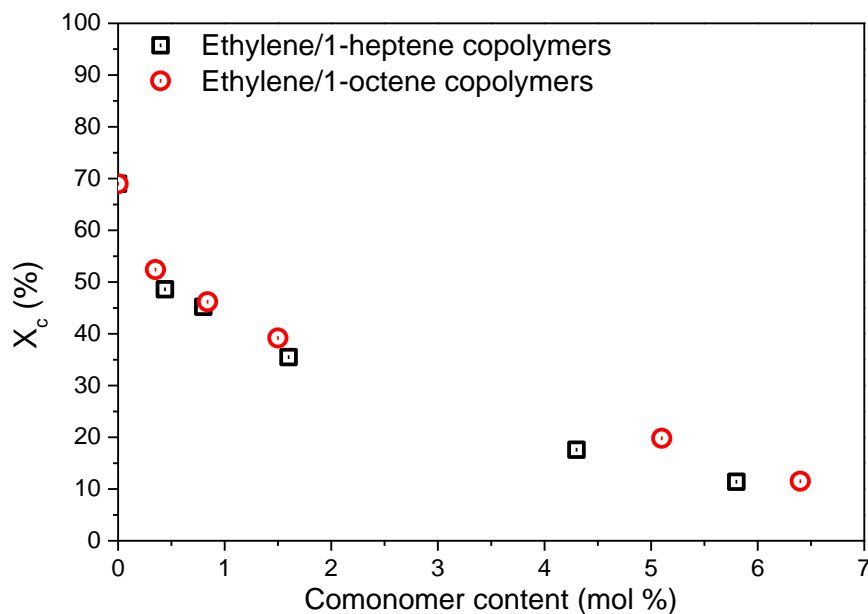
Figure 4.19   Effect of comonomer content on crystallinity.

It can be seen that the differences in crystallinity of the two types of resins (EH and EO) are small. Even a small amount of comonomer (less than 0.5 mol %) has a significant effect on the crystallinity of the copolymer. Unlike density, the decrease in crystallinity follows an exponential decay trend. Hong *et al*. [17] also found the same trend in their work which has been previously mentioned (Section 4.4.1). They also found that crystallinity, as being detectable by standard DSC, disappears in copolymers with > 10 mol % 1-olefin units. The same can be expected with EH and EO copolymers.

A more suitable approach of observing crystalline and non-crystalline components in LLDPE resins is through solid state ^{13}C NMR. The technique is used to investigate the molecular motion and phase structure of solid polymers [45]. Figures 4.20a and b show the findings from ^{13}C CP-MAS NMR experiments. The CP-MAS experiment favours methylene groups in rigid environments because magnetisation transfer is more effective in these regions [46]. An increase in the crystalline peak is attributed to an increase in crystallinity [46]. Studies on polyethylene samples have shown that instead of the two phase model (that polyethylene samples consist only of crystalline and non-crystalline components), crystalline-amorphous interfacial components are also present in addition to the rubbery amorphous phase [45, 47]. These crystalline-amorphous interfacial components can be similar to the semi-crystalline fractions observed in the CRYSTAF profiles. In order to quantify the three components from ^{13}C CP-MAS spectra, a quantitative experiment followed by the deconvolution of the peaks has to be carried out. The CP-MAS experiments were however not quantitative, as such experiments take longer times to complete per sample and were used only as a complementary tool in understanding the effect of comonomer content on the crystalline and non-crystalline components. From Figures 4.20a and b, the crystalline component has an observed peak at 32.18 ppm. A value of 32.89 ppm is reported in literature [48] and the differences can be attributed to different experimental instruments and conditions. However, it can be evidently seen from the ^{13}C CP-MAS spectra that the crystallinity of the LLDPE resins regardless of the comonomer type, decreases with increase in comonomer content.
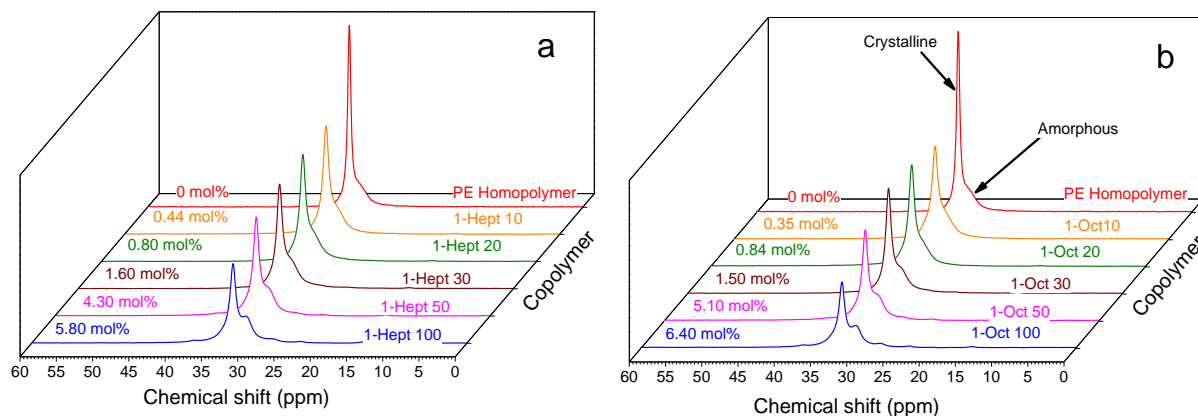
Figure 4.20 ^{13}**C CP MAS spectra of ZN-LLDPE EH (a) and EO (b) copolymers.**

It is interesting to compare the findings from DSC crystallisation exotherms with ^{13}C CP-MAS spectra as they are comparable in their change in peak areas as well as development of a second peak. ^{13}C CP-MAS experiments show a decrease in the crystalline peak which was also observed in DSC. The peaks which develop in DSC are, however, different from those seen from solid state experiments. In DSC, the lower melting peak has crystallisable methylene sequences which show that it is semi-crystalline in nature. ^{13}C CP-MAS spectra show a second peak which corresponds to the amorphous fraction in the LLDPE resins. The amorphous fractions cannot be observed in DSC as they do not show crystallisation or melting peaks. ^{13}C CP-MAS can, therefore, be a better tool in quantifying crystalline, semi-crystalline and amorphous fraction as compared to DSC. Having obtained information from molecular characterisation analyses, it can be easier to explain changes in mechanical properties.

4.4.3   Tensile strength and Young's modulus

Figure 4.21a compares the tensile strengths of EH and EO resins as their comonomer contents are increased. As expected, tensile strengths of both sets of samples decrease with increase in the comonomer content. The same observation was made when Young's modulus was compared for both sets of samples.
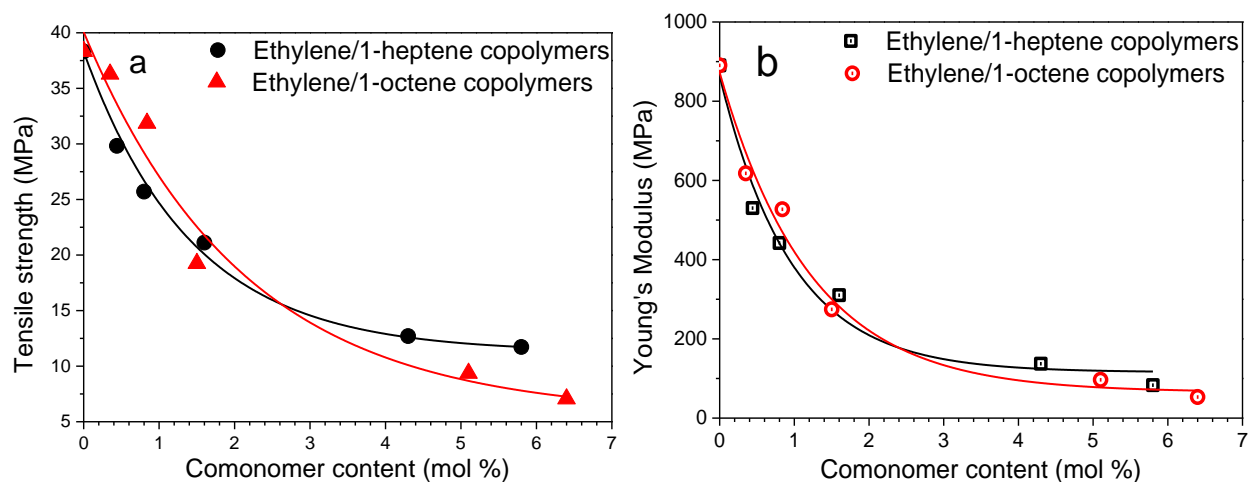
Figure 4.21   Variation of tensile strength (a) and Young's modulus (b) of EH and EO ZN-LLDPE copolymers with increase in comonomer content.

Low molar mass ZN-LLDPE (Figure E.3a and b, Appendix E) showed similar trends in tensile strength and modulus. Several studies [17, 49-51] found the same effect of comonomer content on tensile strength and modulus. A summary of the values of tensile strength and Young's modulus for EO and EH LLDPE are given in Table E.1 in Appendix E.

It is known that tensile strength and modulus of elasticity are dependent on the crystallinity of the polyolefin resin [52] as the different components (amorphous, semi-crystalline and crystalline) all play a part in the final mechanical properties. However, as far as resistance to yielding is concerned, the quantity of crystalline material plays a major role. Under a tensile load, slippage of chain folded layers of polymer chains and their reorientation occurs. The tensile strength at yield depends on the ability of the lamellae to resist the straightening out and reorientation. Therefore, the changes in the crystalline and amorphous contents will have an effect on the tensile strength at the yield point.

When the two types of resins are compared, it can be seen that their tensile strengths at low comonomer contents are almost the same. Differences only become noticeable at higher comonomer contents (> 3 mol %). On taking a closer look at CRYSTAF and prep-TREF findings, differences in the amorphous/soluble fraction (care needs to be taken when referring to the soluble fraction as being completely amorphous, in our case it is not) of the higher comonomer content resins could be seen. Figure 4.11b (Section 4.3.4) shows clear differences in

the soluble fractions from CRYSTAF profiles of the EH and EO resins. However, the crystalline fractions, as seen from the diagram are comparable. In order to get more detailed information on the quantities of the higher comonomer content resins, we compared the prep-TREF weight percentages of two of the copolymers with the highest comonomer content from each set. Figure 4.22 shows the comparison of prep-TREF fractions of 1-Oct 50, 1-Hept 50, 1-Oct 100 and 1-Hept 100 with 5.10, 4.30, 6.40 and 5.80 mol % comonomer content respectively. This comparison was included only for comparative purposes to explain observed differences in tensile strength. Prep-TREF findings are discussed in detail in Chapter 5.
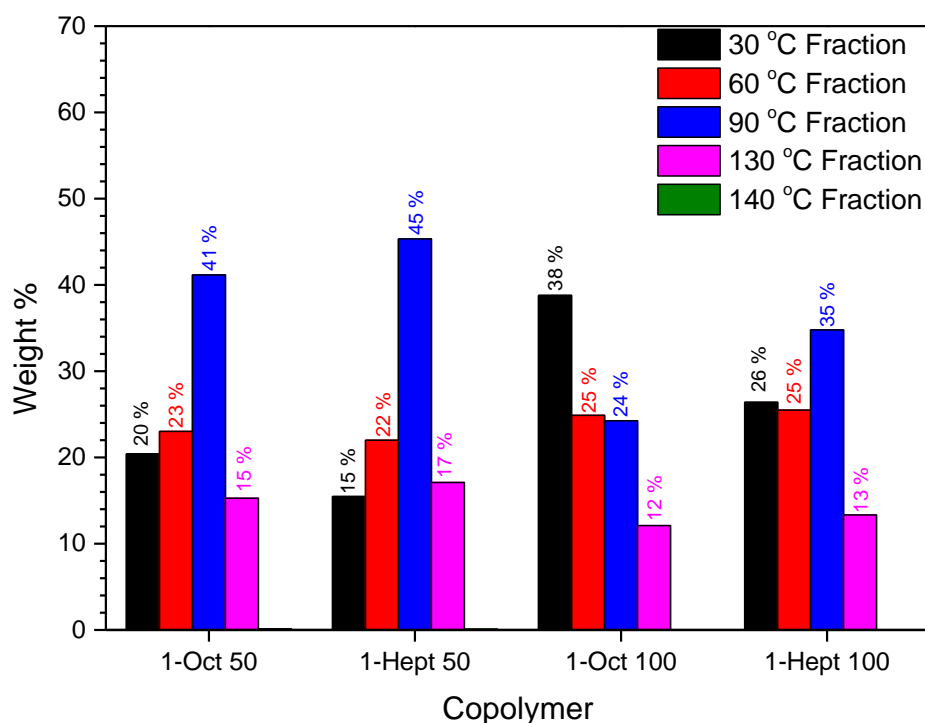
Figure 4.22   Comparison of prep-TREF fractions of 1-Oct 50, 1-Hept 50, 1-Oct 100 and 1-Hept 100. The resins have 5.10, 4.30, 6.40 and 5.80 mol % comonomer content respectively.

It can be seen from the diagram that in both instances EO copolymers have more soluble fraction as compared to EH resins. The difference in the soluble fractions of 1-Oct 50 and 1-Hept 50 is approximately 5 % while that between 1-Oct 100 and 1-Hept 100 is approximately 12 %. Differences can also be seen in the 90 °C fractions which are higher in EH copolymers. These differences in material distribution are critical in explaining the observed differences in tensile

strength. The presence of more soluble material (in CRYSTAF and prep-TREF) indicates an increase in amorphous content. Therefore the crystalline material is dispersed more in the amorphous matrix of EO copolymers as compared to those of EH copolymers. The differences in the tensile strength are therefore more appropriately explained as being due to the ability of 1-octene in producing resins that have more amorphous material as compared to resins produced with 1-heptene as a comonomer. These differences can however be adjusted by properly altering comonomer feed or polymerisation conditions and catalyst amounts.

There exists a direct relationship between tensile strength and modulus of elasticity. Figure 4.23 illustrates this relationship for both sets of EH and EO ZN-LLDPE samples. As expected, an increase in the tensile strength is also reflected by an increase in the modulus. Differences in the relationships were observed for both sets of copolymers.
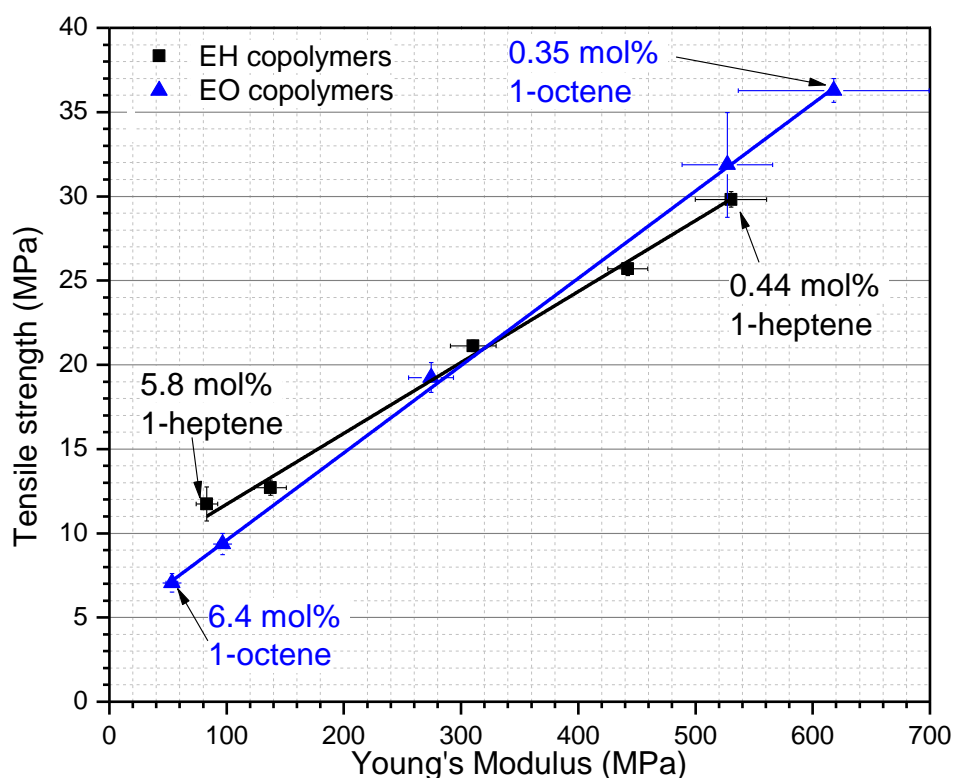
Figure 4.23   Relationship between tensile strength and Young's modulus for EH and EO ZN-LLDPE copolymers.

The steeper slope for EO copolymers can be attributed to the slightly higher ability of 1-octene in lowering crystallinity as compared to 1-heptene. Therefore, at lower comonomer contents, EO copolymers show higher tensile strength as well as a higher modulus of elasticity. More so, at higher comonomer contents EO copolymers show a slightly higher efficiency in lowering crystallinity as shown by the lower tensile strength and lower modulus of elasticity.

This finding correlates well with density comparisons (Figure 4.18 in Section 4.4.1). When the variations of densities of both sets of copolymers with comonomer content are compared, it is found out that 1-octene is slightly better at lowering density as compared to 1-heptene.

4.5   Conclusions

Ethylene/1-heptene and ethylene/1-octene linear low density resins of variable comonomer contents were successfully prepared using Ziegler-Natta and metallocene catalysts. The present study focused on comparing Ziegler-Natta EH and EO copolymers. For a better comparison, synthesis was carried out in a manner that produced resins EH and EO with comparable molar masses.

HT-SEC confirmed the close similarities in molar masses as well as the dispersities of the LLDPE resins. Molar mass distributions of the copolymers were unimodal, and addition of more comonomer to the resins did not have any effect on the modality of the distributions. Solution ^{13}C NMR showed increasing resin comonomer content as more comonomer was used for synthesis. At similar synthesis conditions, the EH and EO resins produced had almost similar comonomer contents. FTIR was used as complementary tool and an increase in $-CH_3$ stretches at 2960 cm^{-1} confirmed an increase in the comonomer content of both sets of copolymers. A decrease in crystallinity was also confirmed through the $-CH_2$ bending deformations at spectral ranges of 1480 – 1463 cm^{-1}.

DSC revealed a decrease in T_m and T_c with increasing comonomer content, which were comparable in both sets of copolymers. X_c was calculated from ΔH_m values obtained from DSC melting endotherms. The decrease in X_c for both sets of copolymers was comparable even at higher comonomer contents. DSC also revealed an increase in chemical composition heterogeneity of both sets of copolymers as comonomer content was increased. Deconvolution of

the DSC crystallisation exotherms of the higher comonomer content resins showed presence of three chemically distinct fractions.

EH and EO copolymers showed similar trends in CRYSTAF analyses. For both sets of copolymers, a decrease in the crystalline fractions and subsequent increase in the soluble fractions was observed. CRYSTAF also showed the presence of three main fractions namely the soluble, semi-crystalline and crystalline fractions. However, EO CRYSTAF profiles showed increased soluble fractions in comparison to EH copolymers when higher comonomer content resins were compared, an indication of more amorphous copolymer being present in 1-octene based resins. This was attributed to slightly higher comonomer contents of EO resins, as well as 1-octene's slightly better ability in disrupting uniform arrangement of polyethylene sequences in the lamellae.

HT-HPLC analyses showed the presence of two chemically distinct fractions. The first fraction was seen as lower eluting peak while the second had a retention volume (V_r) similar to that of the polyethylene homopolymer. HT-2D-LC also revealed that the first elution peak (copolymer) had lower molar mass as compared to the polyethylene peak. The copolymer peak increased with increase in comonomer content and this was attributed to more copolymer chains being present as compared to the homopolymer. HT-HPLC also confirmed DSC and CRYSTAF results which showed a decrease in the highly crystalline fractions (polyethylene fraction) for both sets of samples. The decrease in the crystalline fraction was comparable for EH and EO copolymers.

Tensile strength and Young's modulus were highly comparable at comonomer contents of < 3 mol %. Small differences observed at higher comonomer contents were attributed to the higher amount of amorphous material present in EO copolymers.

References

1. Luruli N., Grumel V., Brüll R., Du Toit A., Pasch H., van Reenen A. J., and Raubenheimer H. G., *J. Polym. Sci., Part A: Polym. Chem.*, **2004**, 42(20), 5121–5133.

2. Balbontin G., Camurati I., Dall'Occo T., and Zeigler R. C., *J. Mol. Catal. A: Chem.*, **1995**, 98(3), 123–133.

3.   Herbert I. R., *Statistical analysis of copolymer sequence distribution*, in *NMR spectroscopy of polymers*, Springer, **1993,** 50–79.

4.   Mirabella F. M. and Bafna A., *J. Polym. Sci., Part B: Polym. Phys.*, **2002**, 40(15), 1637–1643.

5.   Randall J. C., *J. Polym. Sci., Part B: Polym. Phys.*, **1973**, 11(2), 275–287.

6.   Galland G. B., de Souza R. F., Mauler R. S., and Nunes F. F., *Macromolecules*, **1999**, 32(5), 1620–1625.

7.   De Pooter M., Smith P., Dohrer K., Bennett K., Meadows M., Smith C., Schouwenaars H., and Geerards R., *J. Appl. Polym. Sci.*, **1991**, 42(2), 399–408.

8.   Blitz J. P. and McFaddin D. C., *J. Appl. Polym. Sci.*, **1994**, 51(1), 13–20.

9.   Hongjun C., Xiaolie L., Dezhu M., Jianmin W., and Hongsheng T., *J. Appl. Polym. Sci.*, **1999**, 71(1), 93–101.

10.   Gulmine J. V. and Akcelrud L., *Polym. Test.*, **2006**, 25(7), 932–942.

11.   Gulmine J. V., Janissek P. R., Heise H. M., and Akcelrud L., *Polym. Test.*, **2002**, 21(5), 557–563.

12.   DesLauriers P. J., Rohlfing D. C., and Hsieh E. T., *Polymer*, **2002**, 43(1), 159–170.

13.   Qiu L., Chen W., and Qu B., *Polymer*, **2006**, 47(3), 922–930.

14.   Luongo J. P., *J. Polym. Sci.*, **1960**, 42(139), 139–150.

15.   Harvey M. C. and Ketley A. D., *J. Appl. Polym. Sci.*, **1961**, 5(15), 247–250.

16.   Tincul I., Joubert D., and Sanderson R., *Macromol. Symp.*, **2007**, 260, 58–64.

17.   Hong H., Zhang Z., Chung T. C. M., and Lee R. W., *J. Polym. Sci., Part A: Polym. Chem.*, **2007**, 45(4), 639–649.

18.   Santos L. S., *J. Braz. Chem. Soc.*, **2011**, 22(10), 1827–1840.

19.   Shamiri A., Chakrabarti M. H., Jahan S., Hussain M. A., Kaminsky W., Aravind P. V., and Yehye W. A., *Materials*, **2014**, 7(7), 5069–5108.

20.   Kaminsky W., Sperber O., and Werner R., *Coord. Chem. Rev.*, **2006**, 250(1), 110–117.

21.   Gabriel C. and Lilge D., *Polymer*, **2001**, 42(1), 297–303.

22.   Sarzotti D. M., Soares J. B. P., Simon L. C., and Britto L. J. D., *Polymer*, **2004**, 45(14), 4787–4799.

23.   Sarzotti D. M., Soares J. B., and Penlidis A., *J. Polym. Sci., Part B: Polym. Phys.*, **2002**, 40(23), 2595–2611.

24.   Bruaseth I., Soares J. B., and Rytter E., *Polymer*, **2004**, 45(23), 7853–7861.

25.   Reddy S. S. and Sivaram S., *Prog. Polym. Sci.*, **1995**, 20(2), 309–367.

26.   Huang J. and Rempel G., *Prog. Polym. Sci.*, **1995**, 20(3), 459–526.

27.   Starck P., *Polym. Int.*, **1996**, 40(2), 111–122.

28.   Fu Q., Chiu F.-C., McCreight K. W., Guo M., Tseng W. W., Cheng S. Z., Keating M. Y., Hsieh E. T., and DesLauriers P. J., *J. Macromol. Sci. Part B Phys.*, **1997**, 36(1), 41–60.

29.   Kim J. D. and Soares J. B., *Macromol. Rapid Commun.*, **1999**, 20(6), 347–350.

30.   Zhang J., Li B.-G., Fan H., and Zhu S., *J. Polym. Sci., Part A: Polym. Chem.*, **2007**, 45(16), 3562–3569.

31.   Xu J. and Feng L., *Eur. Polym. J.*, **2000**, 36(5), 867–878.

32.   Costeux S., Anantawaraskul S., Wood-Adams P. M., and Soares J. B., *Macromol. Theory Simul.*, **2002**, 11(3), 326–341.

33.   Joubert D. J., Goderis B., Reynaers H., and Mathot V. B. F., *J. Polym. Sci., Part B: Polym. Phys.*, **2005**, 43(21), 3000–3018.

34.   Macko T. and Pasch H., *Macromolecules*, **2009**, 42(16), 6063–6067.

35.   Macko T., Pasch H., and Wang Y., *Macromol. Symp.*, **2009**, 282(1), 93–100.

36.   Cheruthazhekatt S., Mayo N., Monrabal B., and Pasch H., *Macromol. Chem. Phys.*, **2013**, 214(19), 2165–2171.

37.   Macko T., Brüll R., Alamo R. G., Stadler F. J., and Losio S., *Anal. Bioanal.Chem.*, **2011**, 399(4), 1547–1556.

38.   Bunn C. W., *Trans. Faraday Soc.*, **1939**, 35, 482–491.

39.   Gupta P., Wilkes G. L., Sukhadia A. M., Krishnaswamy R. K., Lamborn M. J., Wharry S. M., Tso C. C., DesLauriers P. J., Mansfield T., and Beyer F. L., *Polymer*, **2005**, 46(20), 8819–8837.

40.   Simanke A. G., De Lemos C., and Pires M., *Polym. Test.*, **2013**, 32(2), 279–290.

41.   Hosoda S., *Polym. J.*, **1988**, 20(5), 383–397.

42.   Zhang M., Lynch D. T., and Wanke S. E., *J. Appl. Polym. Sci.*, **2000**, 75(7), 960–967.

43. Kim Y.-M. and Park J.-K., *J. Appl. Polym. Sci.*, **1996**, 61(13), 2315–2324.

44. Hussein I. A. and Hameed T., *J. Appl. Polym. Sci.*, **2005**, 97(6), 2488–2498.

45. Kuwabara K., Kaji H., Horii F., Bassett D. C., and Olley R. H., *Macromolecules*, **1997**, 30(24), 7516–7521.

46. Assumption H., Vermeulen J., Jarrett W. L., Mathias L. J., and van Reenen A., *Polymer*, **2006**, 47(1), 67–74.

47. Flory P. J., Yoon D. Y., and Dill K. A., *Macromolecules*, **1984**, 17(4), 862–868.

48. Kuwabara K., Kaji H., and Horii F., *Macromolecules*, **2000**, 33(12), 4453–4462.

49. Piel C., Starck P., Seppälä J. V., and Kaminsky W., *J. Polym. Sci., Part A: Polym. Chem.*, **2006**, 44(5), 1600–1612.

50. Tincul I., Smith J., and van Zyl P., *Macromol. Symp.*, **2003**, 193(1), 13–28.

51. Tincul I., Joubert D., and Sanderson R., *Macromol. Symp.*, **2007**, 260(1), 58–64.

52. Huff T., Bushman C., and Cavender J., *J. Appl. Polym. Sci.*, **1964**, 8(2), 825–837.

Chapter 5

Preparative temperature rising elution fractionation (prep-TREF) of Ziegler-Natta LLDPE and analyses of the prep-TREF fractions

5.1 Introduction

Temperature rising elution fractionation (TREF) is a widely used fractionation technique for semi-crystalline polyolefins. Several types of polyolefins (linear low density polyethylenes [1], impact polypropylene copolymers and low density polyethylene [2, 3]), have been fractionated through this technique. The studies on fractionated material substantially assist the interpretation of melting behaviour in terms of branch distribution between amorphous and crystalline regions which is not possible with the bulk LLDPE samples, as their chemical composition and molar mass distributions are too complex [4]. Polyolefins are usually mixtures of components with different microstructures [5]. To appreciate the roles of different microstructures in the physical properties of polyolefins, fractions with homogenous microstructures must be obtained. Therefore, in addition to the methods of characterisation discussed in Chapter 4, prep-TREF fractionations were carried out on the EH and EO ZN-LLDPE copolymers.

5.2 Fractionation of bulk samples

Ten ZN-LLDPE samples comprising of sets of EH and EO copolymers with varying comonomer contents were fractionated using prep-TREF. Figures 5.1a-d show the plots of fractions recovered in weight percentage. Prep-TREF findings show an increase in the soluble fractions

(30 °C fractions) for both sets of samples with increase in the comonomer content. This is in agreement with CRYSTAF findings (Section 4.3.4). The 60 °C fractions which are expected to be low in crystallinity also increase in quantity with the same trend in comonomer content. The fractions comprise of copolymer material and have material contributing to the soluble fractions in CRYSTAF. The differences between prep-TREF and CRYSTAF are partly due to the different solvents used in the two types of analyses. 1,2,4-trichlorobenzene (TCB) the solvent used in CRYSTAF analyses is a better solvent for polyolefins as compared to xylene which was used in prep-TREF dissolution and elution steps. Therefore, it is expected that the CRYSTAF soluble fractions contain polymer chains that would otherwise be in the prep-TREF 60 °C fractions.
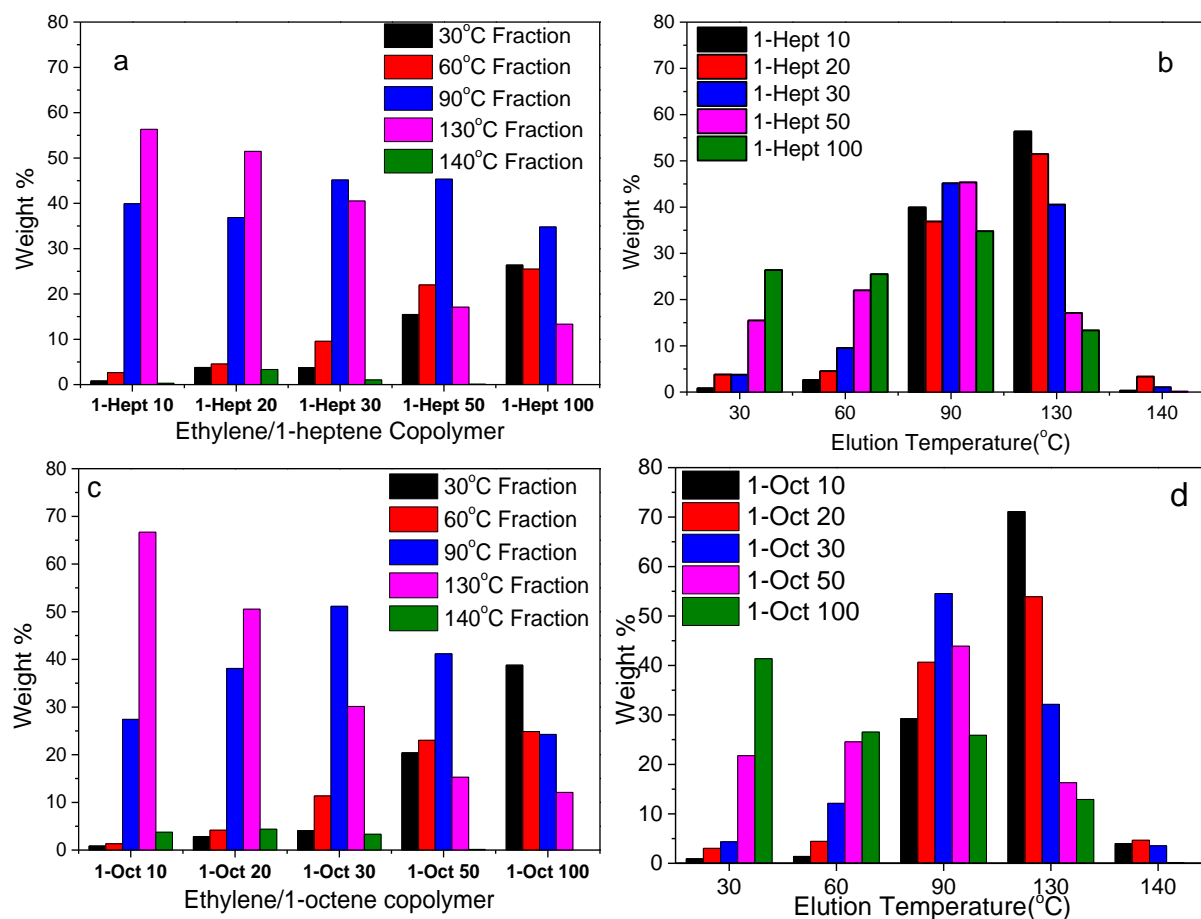
Figure 5.1 **Plots showing prep-TREF fractions obtained from ZN-LLDPE copolymers. Plots of individual resins are shown in (a) and (c). Fractions from different copolymers are compared in (b) and (d).**

The presence of more amorphous material is particularly advantageous when it comes to physical properties such as resin clarity. However, mechanical properties such as tensile strength become reduced with more amorphous material being present. 1-octene appears to be a better comonomer at inducing formation of amorphous material in LLDPE as compared to 1-heptene. (as seen in Section 4.4.3).

These findings are particularly important as they shed light on the distribution of crystalline, semi-crystalline as well as soluble material within a resin. In each resin the dominant fraction is expected to play an influential role in the bulk physical and mechanical properties. For example, 1-Oct 100 (6.4 mol % comonomer) has a soluble fraction of > 40 % and a 60 °C fraction of ≈ 25 %. These fractions will dominate the physical as well as mechanical properties of the resin i.e. density is expected to be low due to the high amount of the comonomer and tensile strength as well as modulus of elasticity will be lower as compared to 1-Oct 10 for example. These effects upon physical and mechanical properties have been presented in Chapter 4.

From the prep-TREF findings, it can also be seen that 1-heptene and 1-octene produce resins with comparable CCD at lower bulk comonomer contents (up to ≈ 3 mol %). Figures 5.2a and b demonstrate this observation.
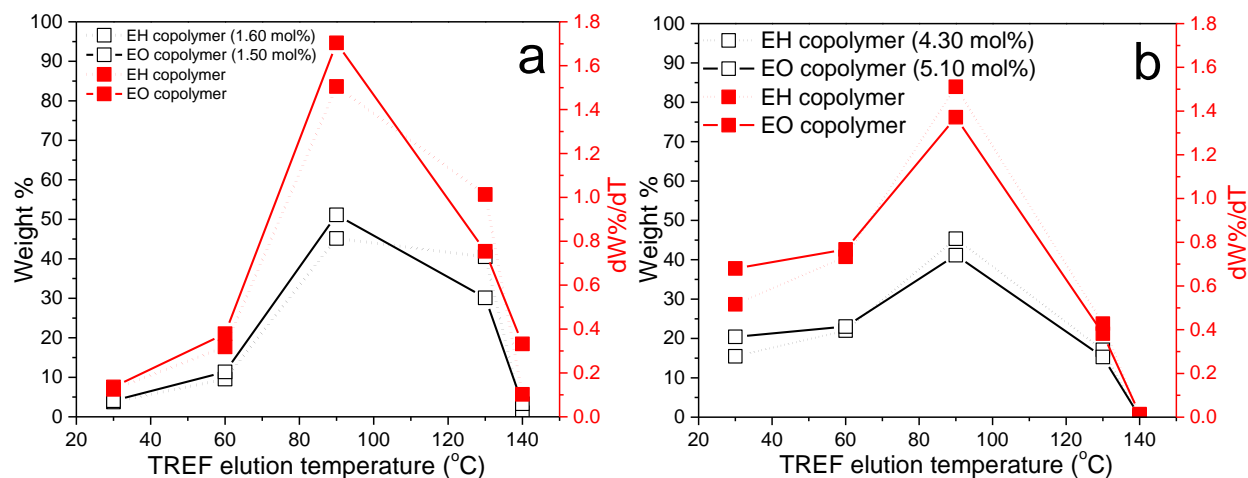
Figure 5.2   Weight % and dW%/dT plots of EH and EO copolymer fractions. Low comonomer resins are compared in (a) and higher comonomer resins in (b).

Resins with close comonomer contents were compared and their fraction weight percentages as well as change in fraction with temperature (dW%/dT) were plotted against prep-TREF elution temperature. It can be seen from these figures that the resins crystalline, semi-crystalline and soluble fractions respond almost similarly to change in comonomer content. Plots of weight % and dW%/dT of individual prep-TREF samples are shown in Figures D.1 and D.2, Appendix D.

Preparative TREF provides a much needed way of fractionating LLDPE samples. With up to 3 g of each sample being fractionated, fractions can be collected and analysed further giving detailed information on the microstructure of these samples [1, 2, 6-9]. After the ZN-LLDPE bulk samples were fractionated, the fractions were analysed using several techniques which are discussed in the following sections.

5.3   ZN-LLDPE prep-TREF fraction analyses

5.3.1   Molar mass (MM) and molar mass distribution (MMD)

Figure 5.3 shows molar mass distributions of prep-TREF fractions and their bulk samples. Analyses of the prep-TREF fractions revealed unimodal distributions in MMD which indicates homogeneity. Only higher comonomer content resins (1-Hept 50, 1-Hept 100, 1-Oct 50 and 1-Oct 100) are shown in the present discussion. The fractions show increasing molar mass with increase in prep-TREF elution temperature. 2D experiments (Figure 4.17b) showed that the copolymer fraction has lower molar mass as compared to polyethylene. The crystallisability of the polymer chains depend mainly on the distribution of the comonomer within the polymer chains [5, 8, 10-17]. The findings however, show that as the crystallisabilities of the fractions increase, the molar mass also increases. The copolymer fractions of lower prep-TREF elution temperatures (30 and 60 °C fractions) have lower molar masses and this is possibly due to higher chances of chain termination due to high comonomer incorporation. It is known that the molar mass of copolymers is influenced by the incorporation of the comonomer which facilitates chain transfer reactions i.e. β-H elimination or chain transfer to aluminium [18, 19]. As a result lower prep-TREF eluting fractions containing more comonomer units have lower molar masses. Higher eluting fractions were found to have higher molar masses and this is also well explained by the low comonomer incorporation.
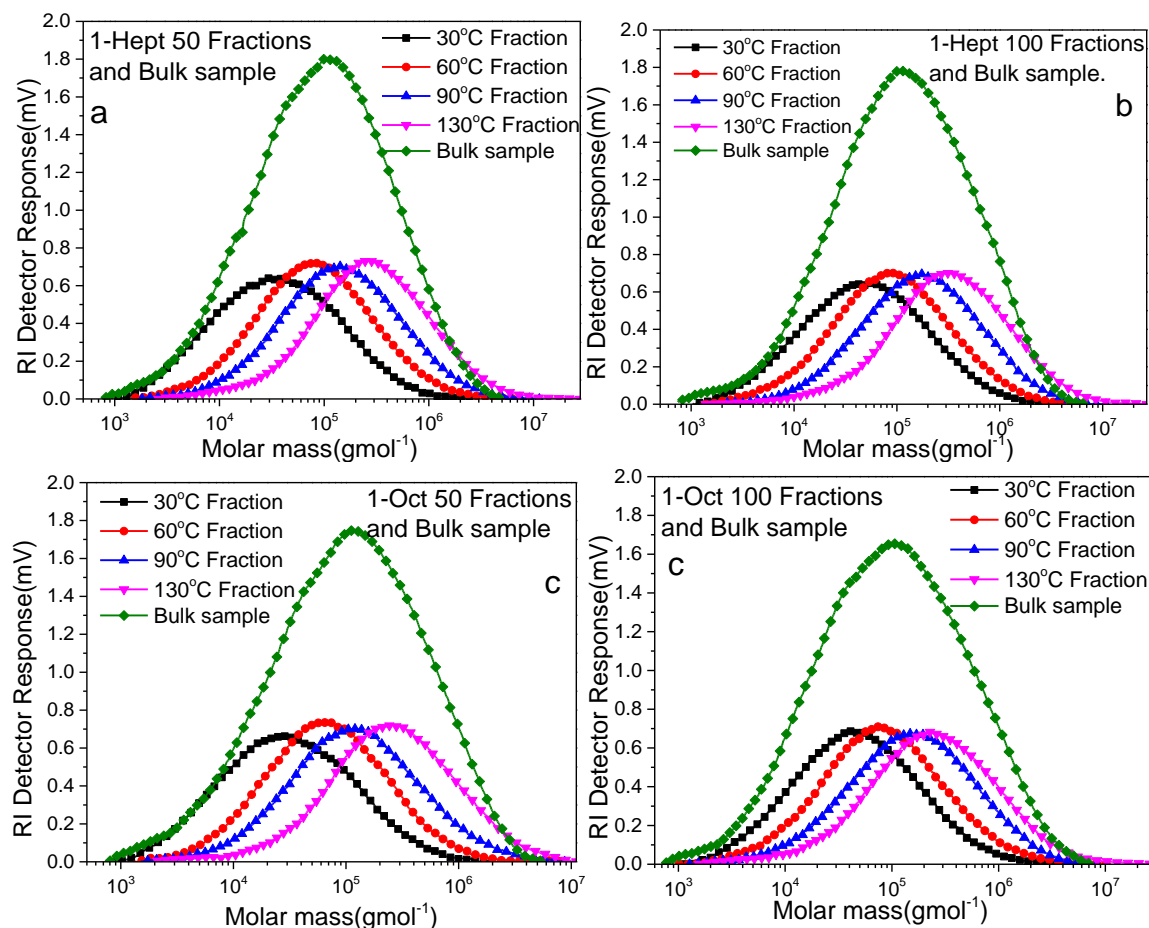
Figure 5.3   Molar mass distributions of ZN-LLDPE copolymers and their prep-TREF fractions.

All prep-TREF fraction MMDs were found to be within those of their bulk samples. This serves only as proof of a successful fractionation. It is known that for typical ZN-LLDPE, comonomer content decreases with increase in molar mass (as shown in Table 2.3). Jorgensen *et al*. [1] found the same result after fractionating a LLDPE resin. They also found that low molar mass fractions contain the highest comonomer content. Mirabella *et al*. [20] found a decreasing trend in short chain branching (SCB) with increase in molar mass in a typical commercial LLDPE sample.

A summary of some of the prep-TREF fractions molar masses and dispersities is given in Table 5.1. The increase in MM with prep-TREF elution temperature can be seen from Table 5.1. It became also interesting to compare the MMDs of fractions collected at similar prep-TREF elution temperatures from bulk samples of differing comonomer content.

Table 5.1   A summary of prep-TREF fractions molar masses and their dispersities.

TREF fraction	M_w [a] (kg mol^{-1})[a]	$Đ$ [a]	TREF fraction	M_w [a] (kg mol^{-1})[a]	$Đ$ [a]
1-Hept 10(60)	38.9	6.57	1-Oct 10(60)	----	----
1-Hept 20(60)	81.1	4.89	1-Oct 20(60)	63.7	4.73
1-Hept 30(60)	101.7	5.11	1-Oct 30(60)	106.7	5.86
1-Hept 50(60)	184.6	5.16	1-Oct 50(60)	148.6	4.77
1-Hept 100(60)	201.5	5.60	1-Oct 100(60)	208.9	6.07
1-Hept 10(90)	179.3	5.37	1-Oct 10(90)	191.8	6.77
1-Hept 20(90)	251.6	5.60	1-Oct 20(90)	216.5	6.52
1-Hept 30(90)	265.7	5.86	1-Oct 30(90)	217.0	5.22
1-Hept 50(90)	327.1	5.62	1-Oct 50(90)	286.3	5.87
1-Hept 100(90)	372.5	5.49	1-Oct 100(90)	336.6	6.09
1-Hept 10(130)	392.4	5.28	1-Oct 10(130)	425.0	5.71
1-Hept 20(130)	475.	5.15	1-Oct 20(130)	482.6	6.17
1-Hept 30(130)	471.8	5.33	1-Oct 30(130)	496.8	7.25
1-Hept 50(130)	617.5	5.79	1-Oct 50(130)	552.4	5.72
1-Hept 100(130)	725.3	6.40	1-Oct 100(130)	578.6	7.40

[a] As determined by HT-SEC

From Figure 5.4a 60 °C prep-TREF fractions show a shift towards higher MM as comonomer content of their bulk samples increase. The same trend was observed with 90 and 130 °C fractions (Figures 5.4b and c respectively). However, the differences in MM decrease as the fraction elution temperature increases. It can be concluded from these findings that the differences in MM are more pronounced at lower prep-TREF elution temperatures.
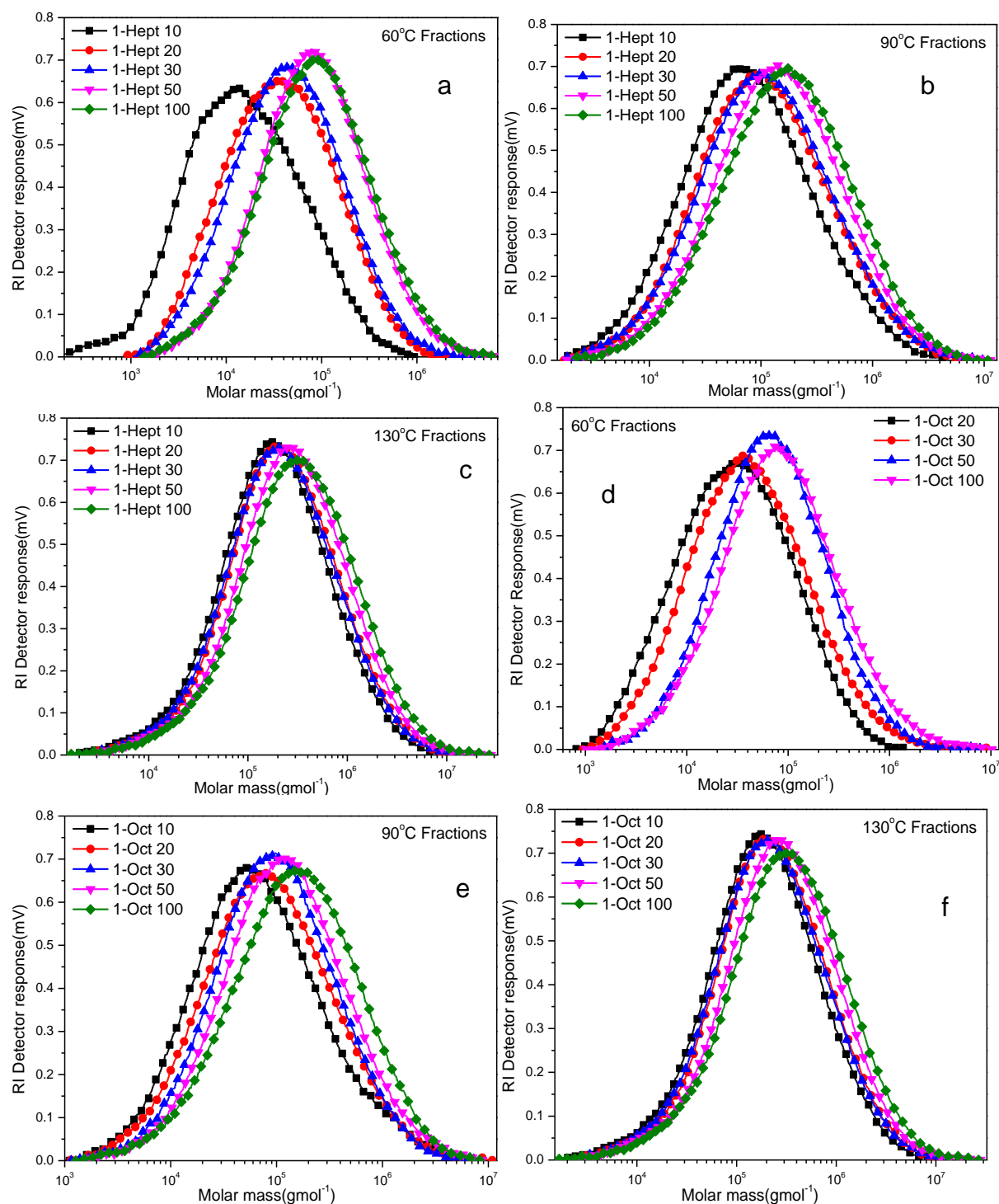
Figure 5.4   **Comparison of molar mass distributions of similar fractions from resins of different comonomer contents.**

Considering the same number of repeat units, copolymer chains with higher comonomer contents will have higher molar masses. The copolymer fractions of similar elution temperatures (say 60 °C) but of different bulk LLDPE origin, will have different comonomer contents. Therefore, when these fractions are compared, the differences in their HT-SEC molar masses are attributed to differences in comonomer contents. Fractions obtained from higher comonomer content resins will have higher molar masses while those obtained from lower comonomer content resins will have lower molar masses. Figure 5.5 shows the variation of comonomer content with the increase in prep-TREF elution temperature as well as the bulk sample comonomer content. The diagram helps to explain what is observed with the prep-TREF fraction molar masses.
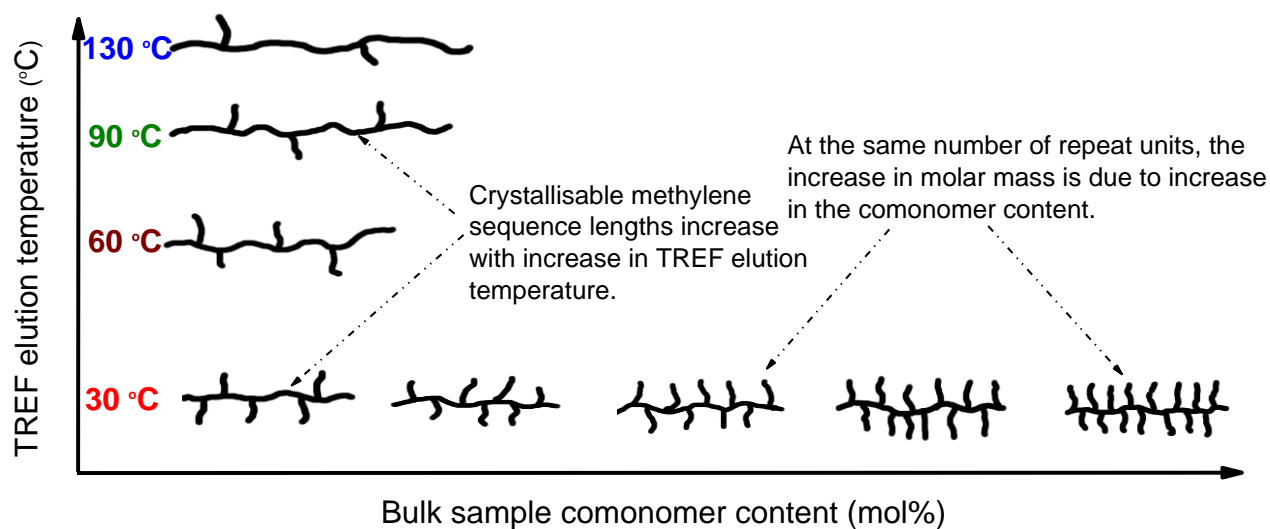
Figure 5.5   Variation of SCB with prep-TREF elution temperature as well the bulk sample comonomer content.

Copolymer chains eluting at higher temperatures have lesser comonomer incorporated which explains their longer crystallisable methylene sequences. Their molar masses are therefore higher as compared to low temperature eluting fractions (e.g. 30 °C fractions). The higher molar mass of the more crystalline fractions as compared to the less crystalline fractions can be related to the polymerisation reactivities of the monomers. Ethylene, due to its higher reactivity, adds to the polymer chain at a faster rate as compared to the bulkier comonomer. Catalyst sites that produce low comonomer content copolymer chains also produce longer chains. The opposite is true for

active sites that can incorporate more comonomer into the copolymer chain. Therefore, the polymer chains having less comonomer incorporated will be longer and as a result have higher molar masses.

HT-SEC information is useful when molar mass heterogeneity within the fractions is considered. In our case, individual fractions showed symmetrical unimodal molar mass distributions meaning the copolymer chains in these fractions are evenly distributed. HT-SEC provides only one dimension of microstructure analyses. In order to have a full understanding of the chemical composition distribution of the fractions, other analyses were also carried out.

5.3.2　FTIR analyses

In the present study, FTIR analyses were quite useful in monitoring changes in the comonomer content as well as changes in crystallinity. Figure 5.6a and b show FTIR spectra of EH (1-Hept 50) fractions and comparison 60 °C fractions respectively. Only EH (1-Hept 50) fractions are discussed as the results of other fractions were similar. As expected, the methyl content within the fractions decreases with increase in prep-TREF elution temperature. This is indicated by the decrease in peak absorbances corresponding to –CH$_3$ stretches at 2960 cm^{-1} (Figure 5.6a). The increase in crystallinity of the fractions (as prep-TREF elution temperature increases) manifests itself as the splitting of the spectral peak in the spectral region of 1480-1463 cm^{-1}. 130 and 140 °C show higher crystallinity while 30 and 60 °C fractions have single peaks indicating significantly lower crystallinity. Spectral peaks at 731 and 719 cm^{-1} also confirm the change in crystallinity.

When fractions collected at the same prep-TREF elution temperature were compared (Figure 5.5b) methyl content within the fractions appeared to be similar indicating almost similar comonomer contents. However, the crystallinity of the prep-TREF fractions was found to be different as shown by the spectral peaks at 731 and 719 cm^{-1}. The peak in the spectral region of 1480-1463 cm^{-1} also revealed differences the fractions. The 60 °C fraction from 1-Oct 10 (0.35 mol %) in Figure 5.6b shows a split peak at 1480-1463 cm^{-1} which is indicative of higher crystallinity. The fraction from 1-Oct 100 (6.4 mol %) shows lower crystallinity in comparison to other fractions eluted at the same prep-TREF temperature. From the FTIR it became necessary to compare further the CCD of the fractions collected at the same prep-TREF elution temperature.
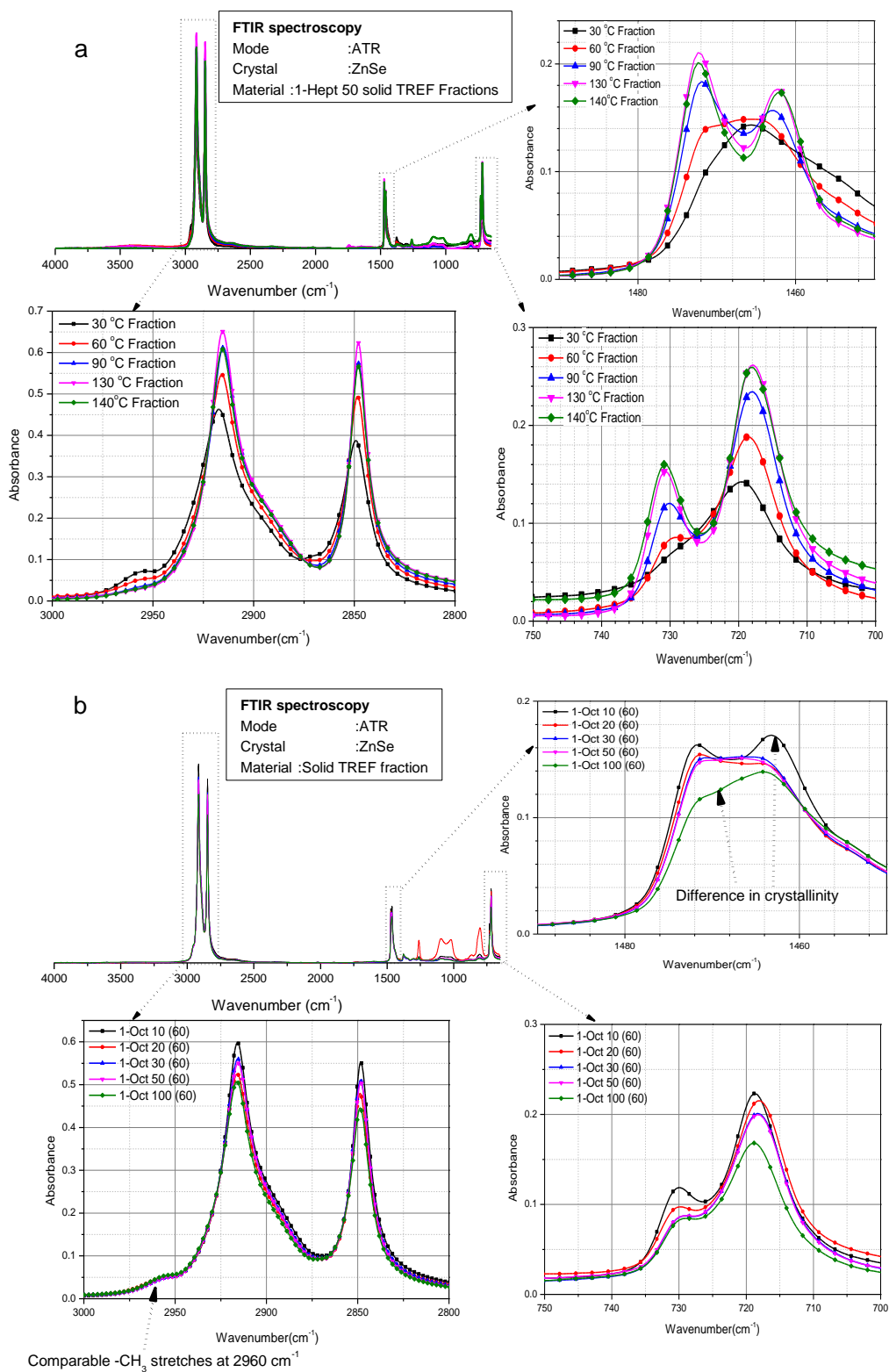
Figure 5.6   FTIR spectra of (a) 1-Hept 50 prep-TREF fractions. 60 °C fractions of EO ZN-LLDPE are shown in (b).

5.3.3   DSC analyses

DSC crystallisation curves of the prep-TREF fractions in comparison to their bulk samples are shown in Figures 5.7a-d and Figures 5.8a-d. Firstly, when the crystallisation exotherms of the prep-TREF fractions are compared to each other, the influence of bulk sample average chemical composition can be noted. Considering 1-Hept 10 (Figure 5.7a) it can be seen that the 90 and 130 °C fractions which form the predominant material in the bulk LLDPE have exotherms that are closely related. As the comonomer content increases (Figures 5.7b through to d), the crystallisation endotherms become more separated.
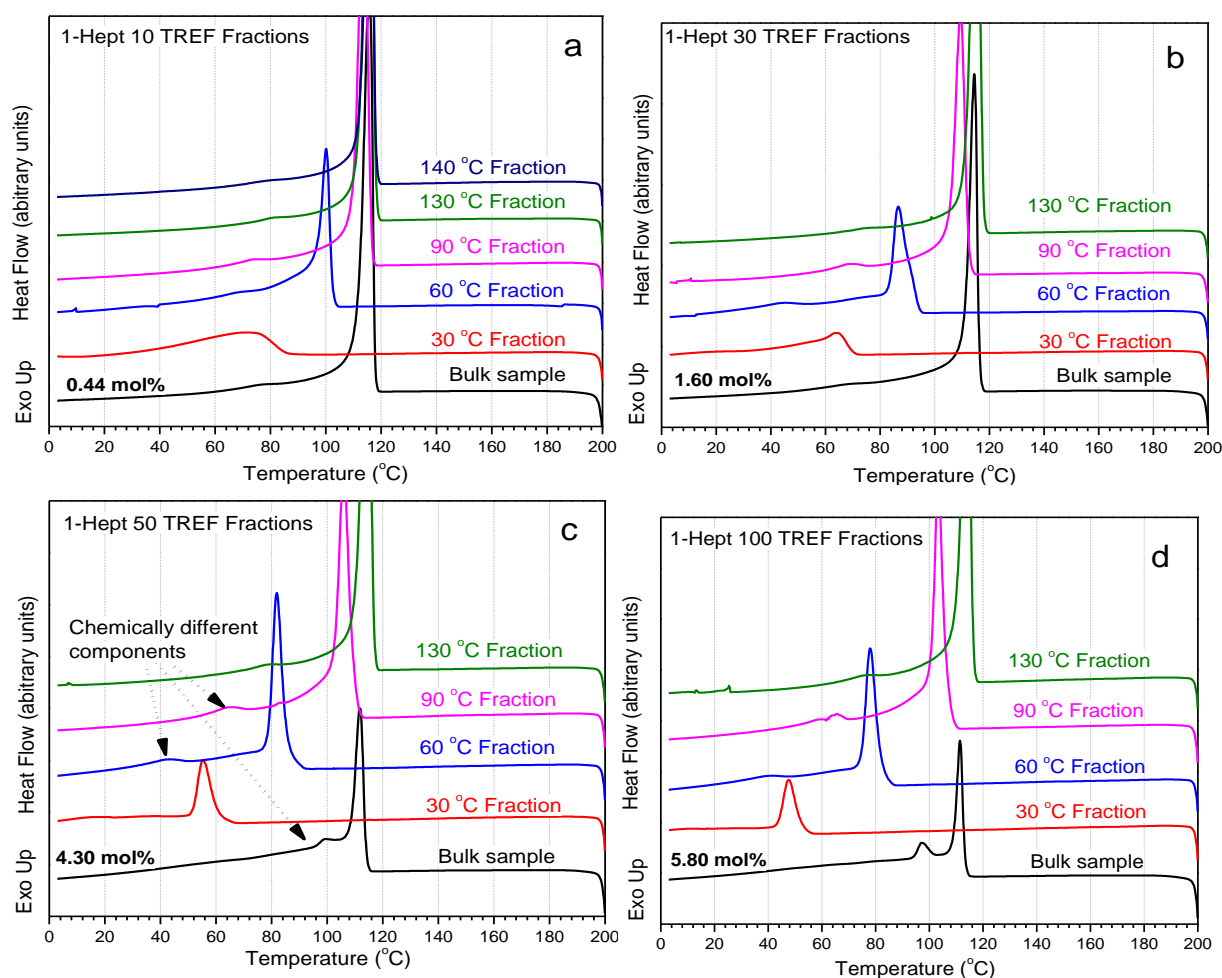
Figure 5.7   DSC crystallisation exotherms of EH copolymers with differing comonomer content in comparison to their prep-TREF fractions. Comonomer contents of the bulk LLDPEs increase from (a) to (d).

Secondly, the soluble fraction (30 °C fraction) shows a crystallisation peak. It would be expected that this fraction be completely amorphous. However, the presence of a crystallisation peak is indicative of methylene sequences of crystallisable length within the fractions. DSC results are in agreement with FTIR findings which indicate differences in crystallinity of the samples in a trend that follows that of their bulk samples. Therefore, a shift in peak melting temperatures for the 60 °C fractions for example, confirms the change in crystallinity of the prep-TREF fractions. The same trend with DSC crystallisation exotherms was observed with EO prep-TREF fractions. Figures 5.8a-d compare the prep-TREF fractions of EO copolymers to their bulk samples. Only four of the five LLDPEs are shown.
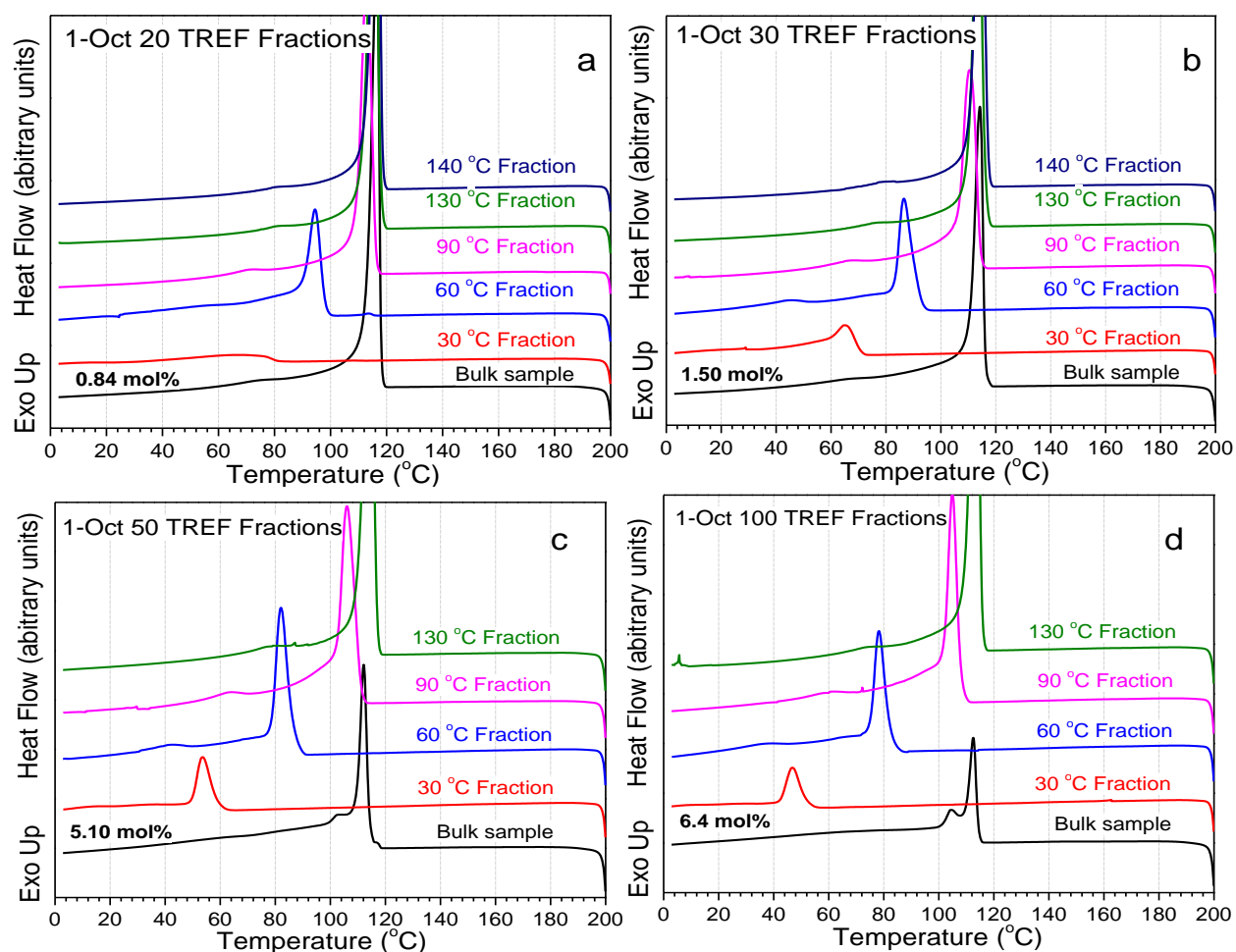
Figure 5.8   **DSC crystallisation exotherms of EO copolymers with differing comonomer content in comparison to their prep-TREF fractions. Comonomer contents of the bulk LLDPEs increase from (a) to (d).**

It is expected that at comparable bulk sample comonomer contents, prep-TREF fractions should have almost similar T_c and T_m. Figure 5.9 compares prep-TREF fractions obtained from EH and EO LLDPE of comparable comonomer contents. Firstly, it is interesting to note that the crystallisation exotherms are comparable with only minor differences being seen. In some cases (e.g. 60 °C fractions, Figures 5.9a-d) the crystallisation exotherms overlap indicating highly comparable chemical compositions and molar masses.
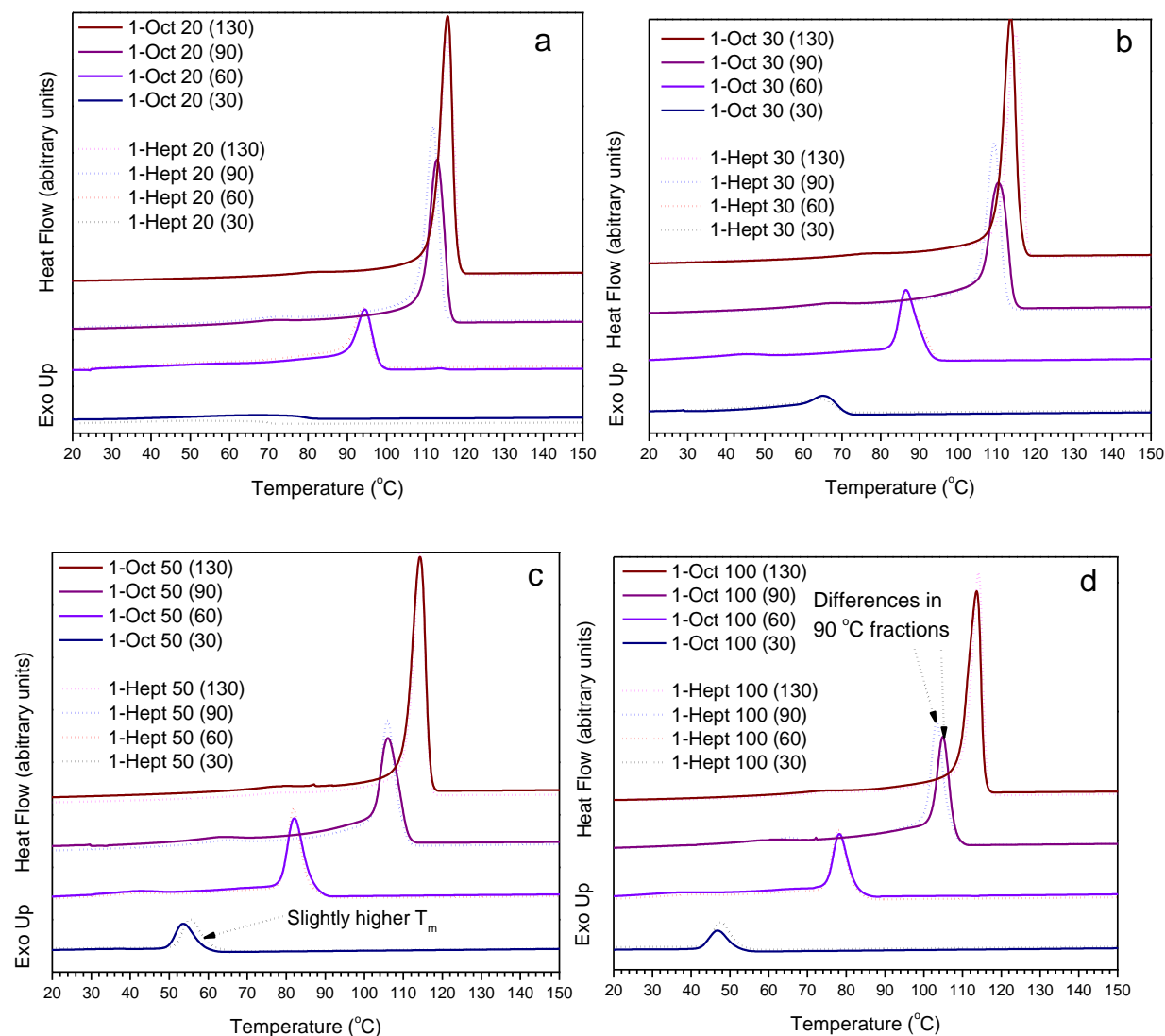
Figure 5.9   Overlays of prep-TREF fraction DSC crystallisation exotherms of EH and EO copolymers with comparable comonomer contents.

Figure 5.9c compares EH and EO copolymers with 4.50 and 5.10 mol % comonomer content respectively. The 30 °C crystallisation exotherm for the EH copolymers is shifted towards higher crystallisation temperatures. This indicates slight differences in the comonomer contents of the fractions. It is assumed that since the EO LLDPE resin has higher comonomer content, its 30 °C fraction has more comonomer as compared to that from the EH copolymer. In addition to that, the crystallisation exotherms of the EH copolymer prep-TREF fractions only show slightly larger curve areas indicating slightly higher crystallinities. From Figures 5.9a, b and d, it can be seen that the main differences in the prep-TREF fractions are in the 90 °C fractions. In all the instances, EH 90 °C fractions show slightly lower T_m, indicating that they have higher comonomer contents. The general trend which is brought out by these findings is that both comonomers (1-heptene and 1-octene) give fractions with similar crystallisation behaviour at similar bulk compositions.

As was seen with MMDs of fractions from LLDPEs with different comonomer contents, DSC crystallisation exotherms show differences even for fractions collected at the similar prep-TREF elution temperatures. Figures 5.10a-d and Figure 5.11 show the DSC crystallisation and melting curves of fractions collected at the same prep-TREF elution temperature from both resins. It can be seen from Figures 5.9a-d that T_m shifts towards lower temperatures as the bulk resin's own comonomer content increases. This finding indicates that the fraction microstructure depends on that of the bulk sample.

The differences in T_m and T_c between the fractions decrease with increase in prep-TREF elution temperature. In the case of EO copolymer fractions (Figures 5.10b and d), 60 °C fractions show a wider variation as compared to the 90 °C fractions. The variation is significantly minimised in the 130 °C fractions (Figure 5.11). The fractions obtained from higher comonomer content resins (e.g. 1-Oct 100 or 1-Hept 100) have higher comonomer contents. The same fractions also have higher MM in comparison to other fractions collected at the same prep-TREF elution temperature.
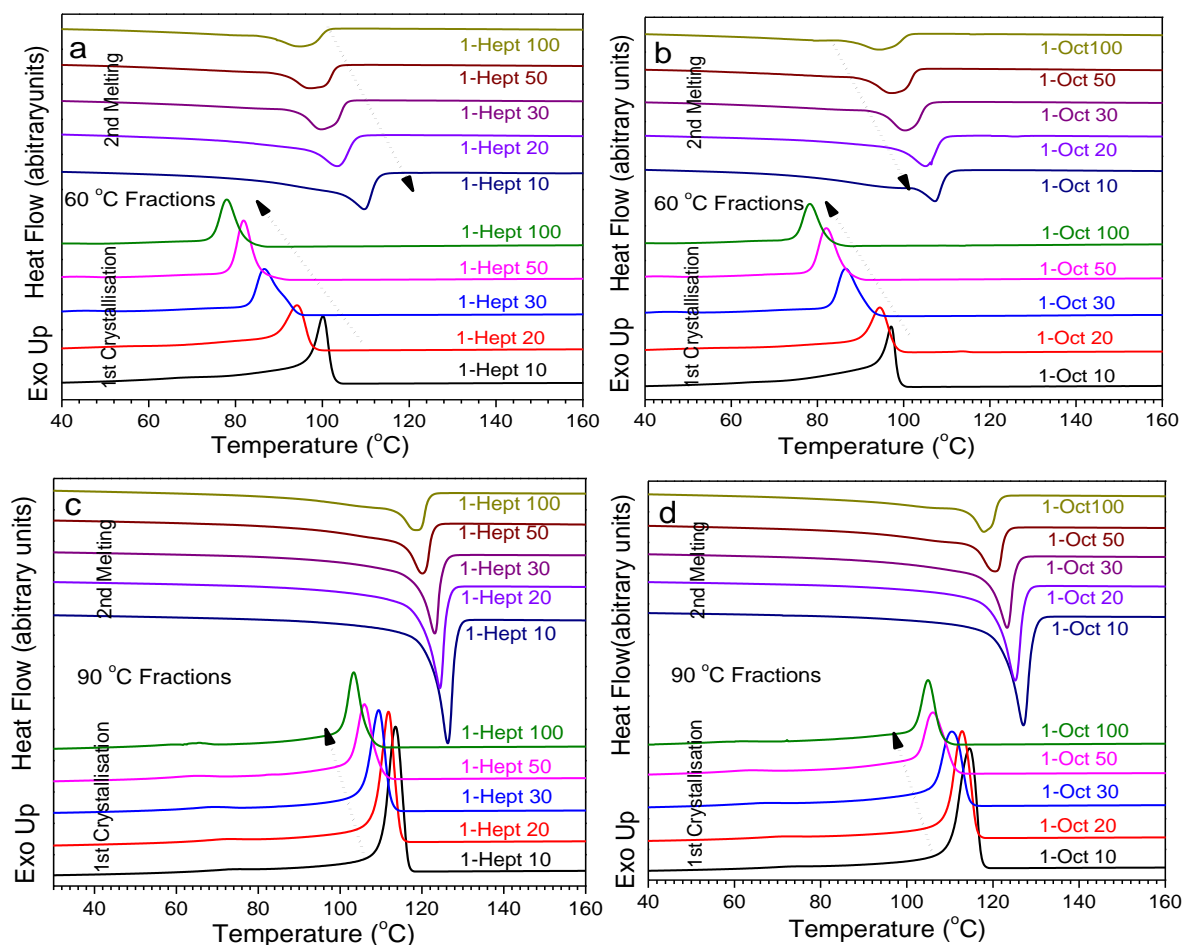
Figure 5.10   A comparison of DSC melting endotherms and crystallisation exotherms of TREF fractions from different bulk samples obtained from the same elution temperature. The arrows indicate the shift in peak temperatures.

As quoted by Xu and Feng [5], Mirabella *et al*. compared the fractionation of high density polyethylene (HDPE), high pressure LDPE (HP-LDPE), and LLDPE and in their study TREF profiles of LLDPE had a trimodal distribution while the others showed a unimodal distribution. A combination of SEC and DSC revealed that polymer chains with low molar mass tended to have more comonomer incorporated and have a broader SCBD. Hosoda [21] also made the same finding when he studied the structural distribution of LLDPE. This is agreement with what is observed from the DSC crystallisation exotherms. As the prep-TREF elution temperature increases, fractions tend to show higher crystallinities as well as narrow DSC crystallisation curves.
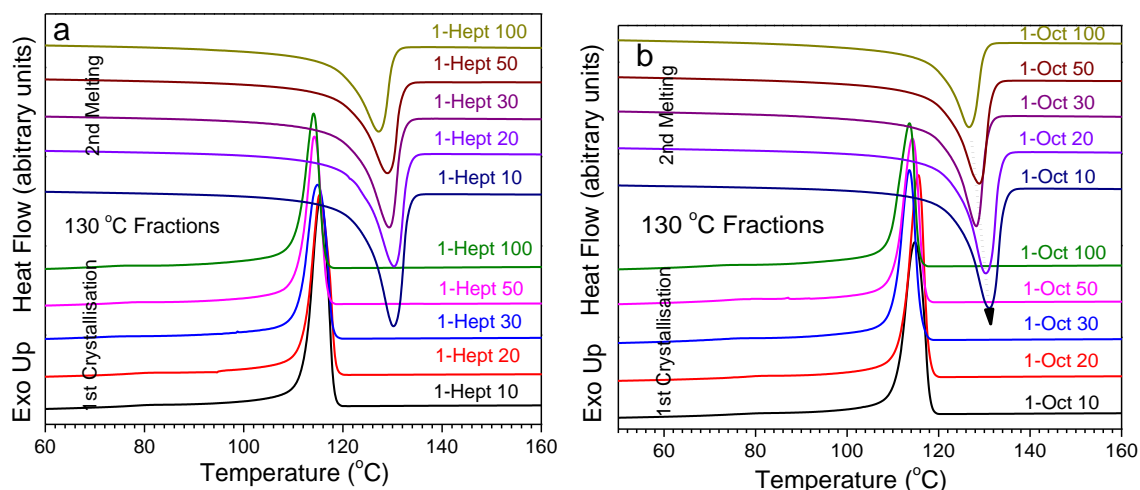
Figure 5.11 **DSC melting endotherms and crystallisation exotherms of the 130 °C prep-TREF fractions of EH (a) and EO (b) LLDPE copolymers. There are smaller differences in T_m and T_c as compared to early eluting fractions.**

Figure 5.12 compares T_m of 60, 90 and 130 °C fractions from both sets of EH and EO resins. It can be seen that the T_m are comparable for LLDPE resins with comparable comonomer contents. T_m also decreases as the comonomer contents of the bulk LLDPE increase.
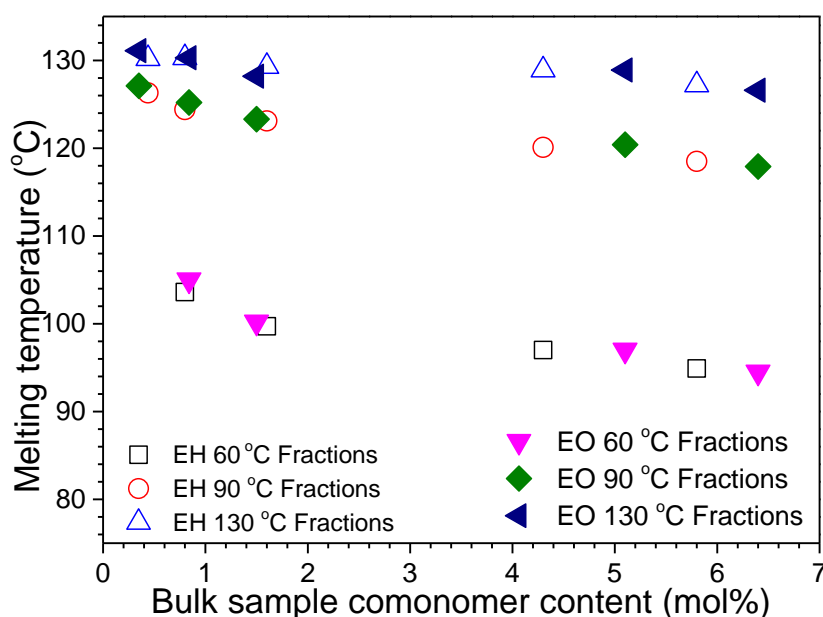
Figure 5.12 **Comparison of melting temperatures of 60, 90 and 130 °C prep-TREF fractions.**

As has been seen with 60 and 90 °C prep-TREF fractions, 130 °C fractions also show differences in crystallinities as indicated by DSC crystallisation curves. In both sets of fractions, crystallinities decrease as the bulk LLDPE comonomer content from which they were obtained increases. In order to confirm the variation in CCD of the prep-TREF fractions obtained at the same temperature, solution ^{13}C NMR analyses were carried out. A summary of the comonomer contents as well as the melting and crystallisation temperatures of 60, 90 and 130 °C fractions are given in Table 5.2 – 5.4. The LLDPE fractions recovered from prep-TREF for the 60 °C elution (1-Hept 10 and 1-Oct 10) were not sufficient in both cases for solution NMR analysis (60 mg required).

Table 5.2   **A summary of 60 °C prep-TREF fractions comonomer content and DSC related data.**

TREF Fraction	[C] mol %[a]	Bulk sample [C] mol %[a]	T_c (°C)[b]	T_m (°C)[b]	X_c (%)[b]
1-Hept 10(60)	----	0.44	101.1	109.6	35.11
1-Hept 20(60)	4.79	0.80	94.1	103.4	29.82
1-Hept 30(60)	5.13	1.60	86.6	99.7	30.24
1-Hept 50(60)	5.86	4.30	81.8	97.0	24.35
1-Hept 100(60)	6.71	5.80	78.0	94.9	22.70
1-Oct 10(60)	----	0.35	97.1	107.2	32.40
1-Oct 20(60)	3.52	0.84	94.4	105.0	29.39
1-Oct 30(60)	5.24	1.50	86.5	100.2	29.67
1-Oct 50(60)	5.84	5.10	82.1	97.0	26.62
1-Oct 100(60)	7.40	6.40	78.2	94.5	22.52

[a] As determined by solution ^{13}C NMR [b] Determined from DSC curves.

Table 5.3   **A summary of 90 °C prep-TREF fractions comonomer content and DSC related data.**

TREF Fraction	[C] mol %[a]	Bulk sample [C] mol %[a]	T_c (°C)[b]	T_m (°C)[b]	X_c (%)[b]
1-Hept 10(90)	0.83	0.44	113.5	126.3	56.67
1-Hept 20(90)	1.08	0.80	111.8	124.4	51.29
1-Hept 30(90)	1.61	1.60	109.4	123.1	50.37
1-Hept 50(90)	1.86	4.30	106.0	120.1	40.82
1-Hept 100(90)	2.23	5.80	103.3	118.5	38.84
1-Oct 10(90)	0.61	0.35	114.5	127.1	54.56
1-Oct 20(90)	0.78	0.84	112.8	125.2	47.89
1-Oct 30(90)	1.54	1.50	110.4	123.3	46.43
1-Oct 50(90)	1.73	5.10	106.1	120.4	44.08
1-Oct 100(90)	2.60	6.40	104.9	117.9	37.35

Table 5.4   **A summary of 130 °C prep-TREF fractions comonomer content and DSC related data.**

TREF Fraction	Bulk sample [C] mol %[a]	T_c (°C)[b]	T_m (°C)[b]	X_c (%)[b]
1-Hept 10(130)	0.44	115.5	130.2	60.91
1-Hept 20(130)	0.80	115.3	130.3	56.87
1-Hept 30(130)	1.60	114.9	129.3	53.16
1-Hept 50(130)	4.30	114.2	128.9	48.88
1-Hept 100(130)	5.80	114.1	127.2	47.59
1-Oct 10(130)	0.35	114.8	131.1	58.13
1-Oct 20(130)	0.84	115.6	130.3	58.4
1-Oct 30(130)	1.50	113.6	128.2	49.90
1-Oct 50(130)	5.10	114.3	128.9	46.67
1-Oct 100(130)	6.40	113.6	126.6	43.23

[a] As determined by solution ^{13}C NMR [b] Determined from DSC curves.

5.3.4   NMR analyses

Solution ^{13}C NMR was carried out on the 60 and 90 °C fractions. The comonomer contents of the prep-TREF fractions were correlated to those of their bulk samples, and linear relationships were obtained for both sets of samples. Comonomer contents of the prep-TREF fractions increased with increase in the bulk LLDPE comonomer content. Figure 5.13 shows the plots of prep-TREF fraction comonomer contents against their respective bulk LLDPE comonomer contents. It can be seen that 60 °C fractions have higher comonomer contents as compared to 90 °C fractions, which is expected as the fractions are collected at different prep-TREF elution temperatures. Interestingly, as was observed with DSC comparisons of the 60 and 90 °C prep-TREF fractions from EH and EO LLDPEs, similar trends in their comonomer contents are observed. The 130 °C fractions are not included in the present discussion as their comonomer contents could not be calculated due to lack of observable branching carbon signals in their spectra. Spectra of two of the 130 °C fractions are shown in Figure B.5, Appendix B.
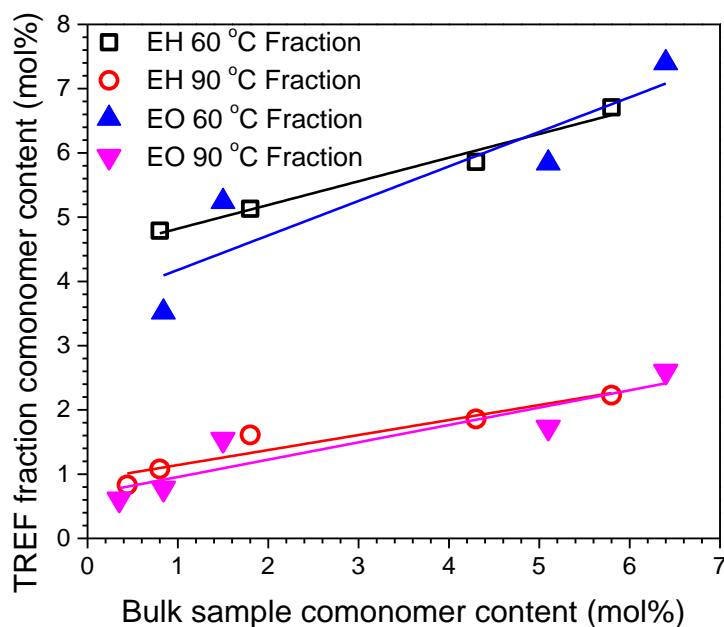
Figure 5.13   Correlation of prep-TREF fraction and bulk LLDPE comonomer contents.

However, FTIR and NMR analyses give only average in formation while the DSC is less sensitive to the presence of minute chemically different polyethylene components. Therefore CCD analyses of the fractions were also carried out using CRYSTAF and HT-HPLC.

5.3.5   CRYSTAF analyses

CRYSTAF is the first step in understanding the chemical composition distribution (CCD) of semi-crystalline polyolefin resins. The spread of copolymer chains over the crystallisable range as well as the soluble material can be observed. Figures 5.14a-d show the differential CRYSTAF curves of 60 and 90 °C fractions. From the Figures 5.14a and b, no observable trend can be seen from the CRYSTAF curves. However, it is surprising that these fractions have a significant amount of soluble material. It must be noted that solvents used for prep-TREF and CRYSTAF are different, hence their solvating power. TCB is a better and thermodynamically stable solvent as compared to xylene which was used in prep-TREF. Therefore slightly higher temperatures are required for dissolution/precipitation with the xylene solvent systems as compared to when TCB is used.
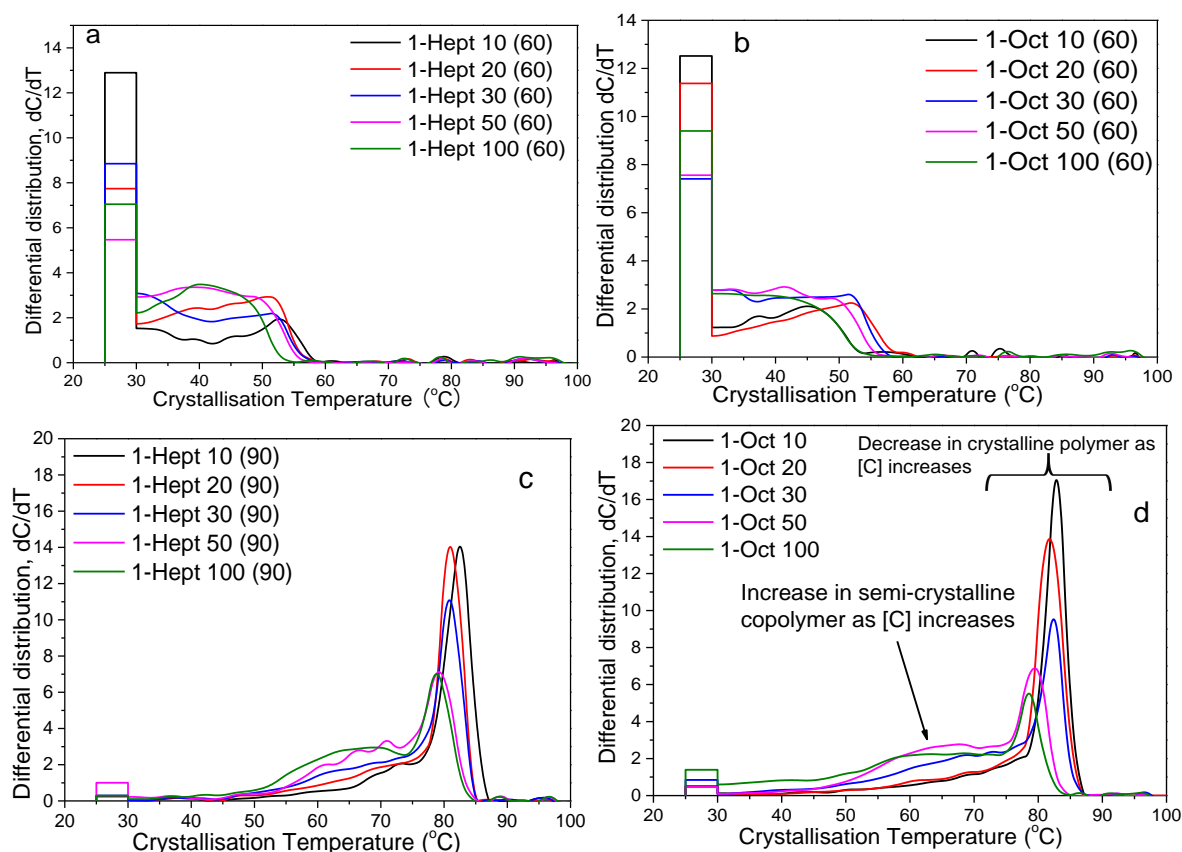
Figure 5.14   Differential CRYSTAF curves of 60 °C (a and b) and 90 °C (c and d) ZN-LLDPE prep-TREF fractions.

In both cases, the 60 °C fractions from the low comonomer content bulk resins exhibit a higher proportion of soluble material. A possible explanation for this observation could be the molar mass effect. As seen from Section 5.3.1, 60 °C fractions from lower comonomer content LLDPEs have the lowest molar masses. Shorter copolymer chains in the 60 °C fractions could be more soluble accounting for the presence of differing amounts of the soluble fraction. Apart from that, there is no clear trend that can be deduced from the different fractions. The lack of material after the 60 °C point signifies absence of copolymer chains of higher crystallinities in the prep-TREF fractions.

On the other hand, 90 °C fractions (Figure 5.14c and d) show an observable change in CCD as the bulk LLDPE comonomer content is changed. Firstly, the fractions from both sets of samples show a shift in the crystallisation peaks towards lower temperatures, which is typical of LLDPEs with higher comonomer contents. Peak crystallisation temperatures change from approximately 85 °C (for 90 °C fractions of 1-Hept 10 and 1-Oct 10) to around 77 °C for fractions of higher comonomer content resins. An increase in the semi-crystalline component can be observed as the prep-TREF fractions' bulk sample comonomer contents increase. The 90 °C fractions clearly demonstrate the differences in CCD of fractions collected at the same prep-TREF elution temperatures. The change in the amount of crystalline material within these fractions supports FTIR (Section 5.3.2) as well as DSC findings (Section 5.3.3). Figure 5.15 compares CRYSTAF profiles of 130 °C fractions from three bulk LLDPE resins.
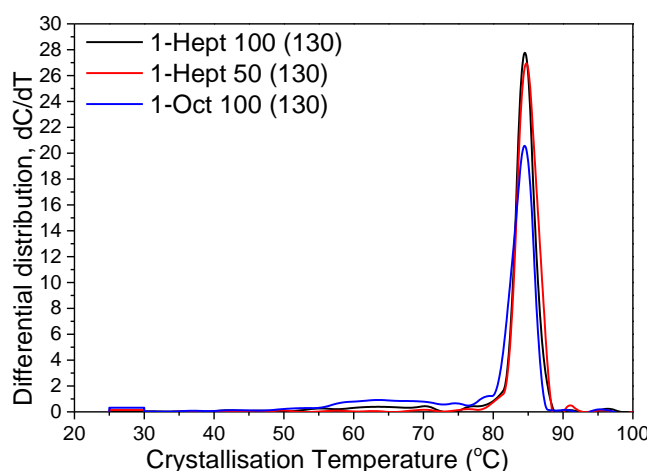
Figure 5.15   CRYSTAF profiles of 130 °C fractions of EH and EO copolymers.

It can be seen that the CCDs of the samples are closely related as compared to those of 60 and 90 °C fractions. The fraction is mainly comprised of the polyethylene homopolymer. HT-SEC (Section 5.3.1) and DSC results also show close similarities in MMD and thermal properties of the high temperature eluting fractions.

Part of the work in the present study is to compare 1-heptene and 1-octene when they are used as comonomers in LLDPE synthesis. Figures 5.16 and 5.17 show the differential CRYSTAF profile overlays of 60 and 90 °C prep-TREF fractions from EH and EO LLDPE resins. When prep-TREF fractions collected at similar elution temperatures from EH and EO copolymers of comparable comonomer contents were compared, minor differences in the CRYSTAF profiles were observed. Notable differences observed in the 60 °C prep-TREF fractions are in the CRYSTAF soluble fraction. However, these differences do not form a recognisable pattern leading to the conclusion that experimental conditions in prep-TREF and experimental errors in CRYSTAF contribute to the differences.

From Figure 5.17, it can be seen that 90 °C prep-TREF fractions show highly similar CRYSTAF profiles, with small differences being observed at higher bulk LLDPE comonomer contents. The polymerisation process is statistical in nature hence the level of heterogeneity in terms of comonomer distribution is expected to be high at higher comonomer contents. The fractions from higher comonomer contents show slightly higher soluble CRYSTAF fractions. This can be attributed to the effects of co-precipitation as the copolymer fractions may be trapped together with the homopolymer fractions during the crystallisation step in prep-TREF. Therefore, differences in the 90 °C prep-TREF fraction CRYSTAF profiles of higher comonomer LLDPE resins can be attributed to the high heterogeneity brought about by increasing comonomer content.
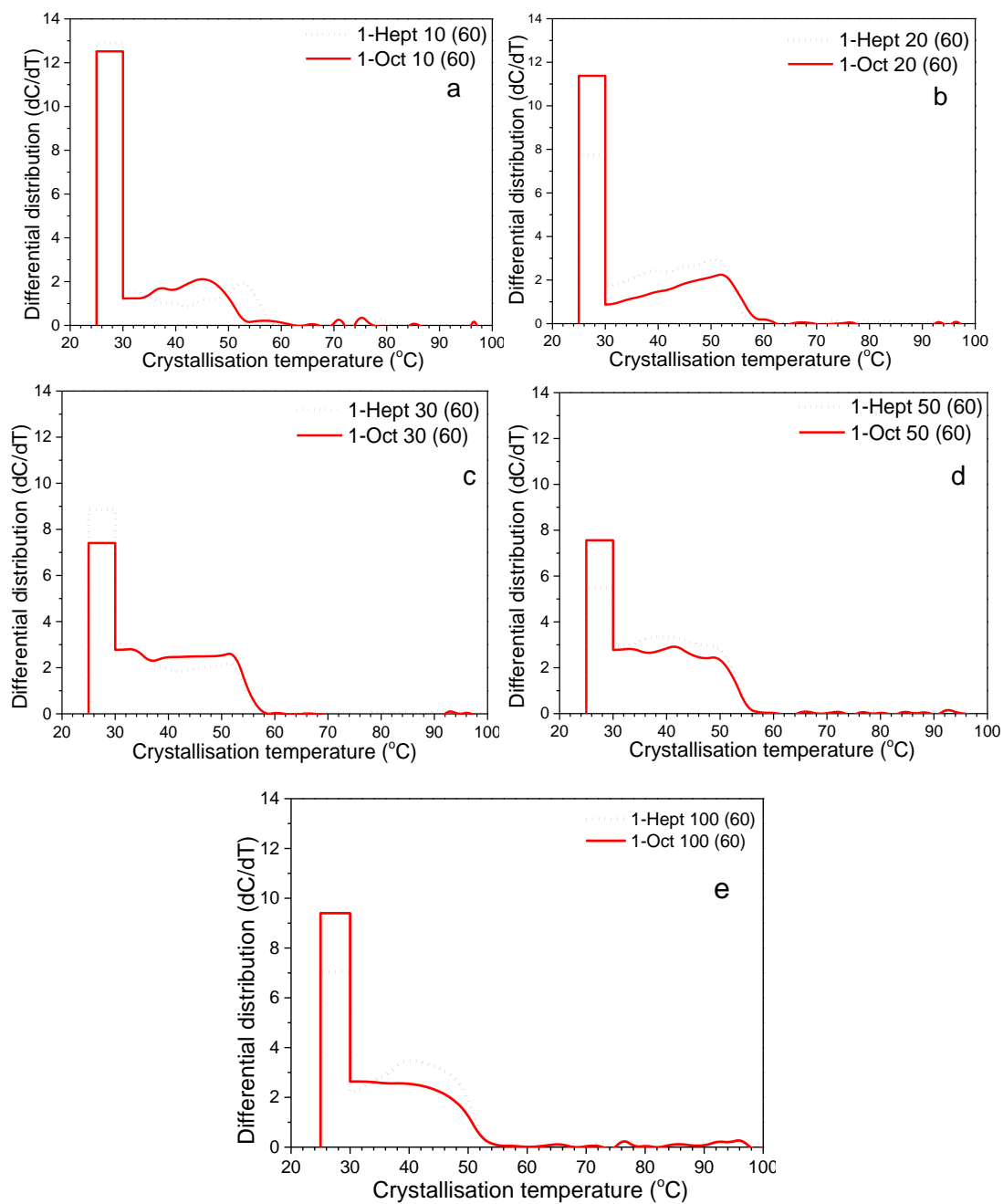
Figure 5.16 **Comparisons of the differential CRYSTAF profiles of 60 °C EH and EO LLDPE prep-TREF fractions. The comonomer contents of the bulk LLDPE resins increase from (a) to (e).**
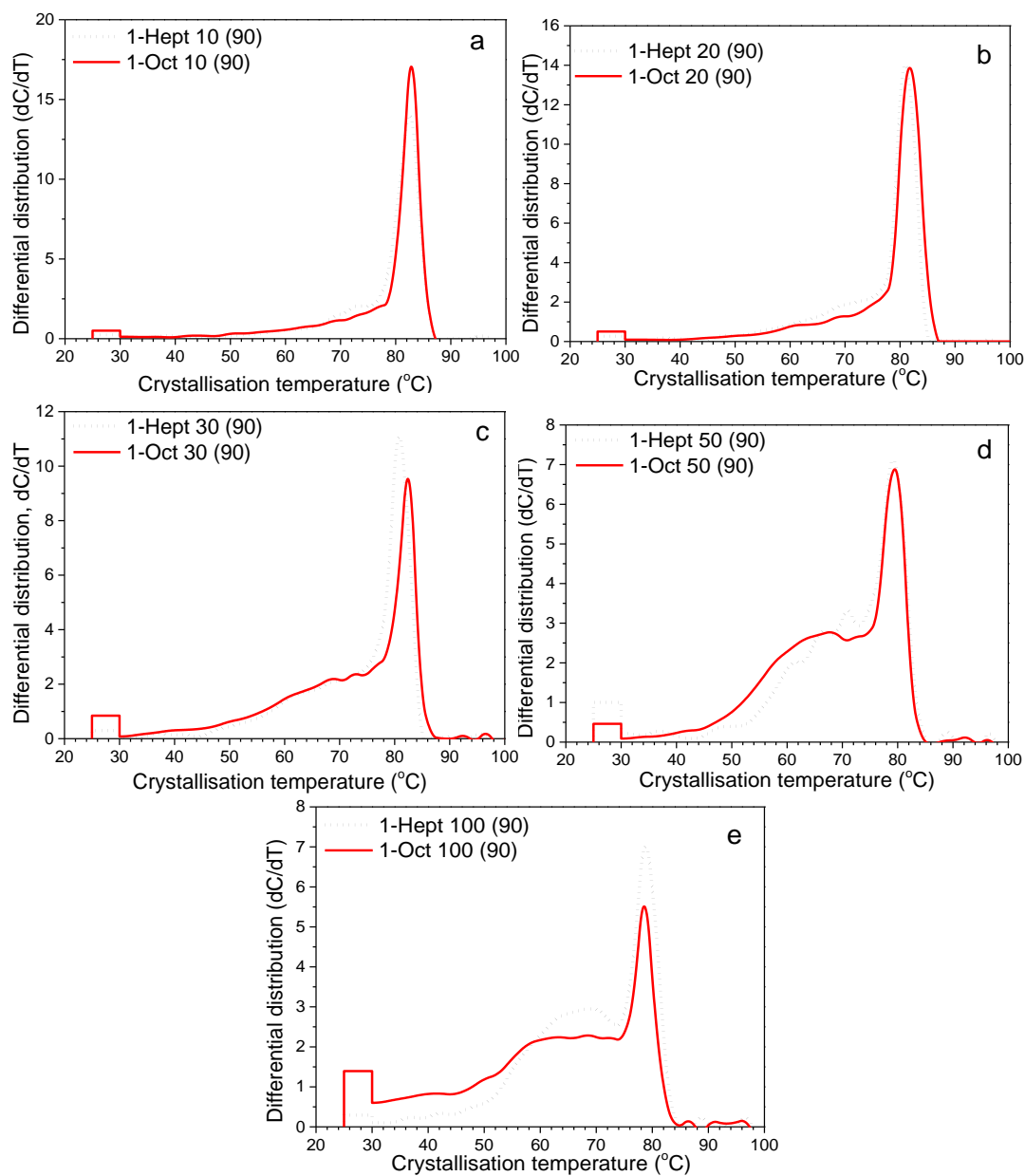
Figure 5.17   Comparisons of differential CRYSTAF profiles of 90 °C EH and EO LLDPE prep-TREF fractions. The comonomer contents of the bulk LLDPE resins increase from (a) to (e).

5.3.6   HT-HPLC analyses

Another important technique for CCD analyses as previously stated in chapter 2 (Section 2.65) is HT-HPLC. Due the small amount of material recovered for some fractions such as the 30 and 140 °C from prep-TREF, this method becomes ideal as only 3 – 4 mg are required for analysis.
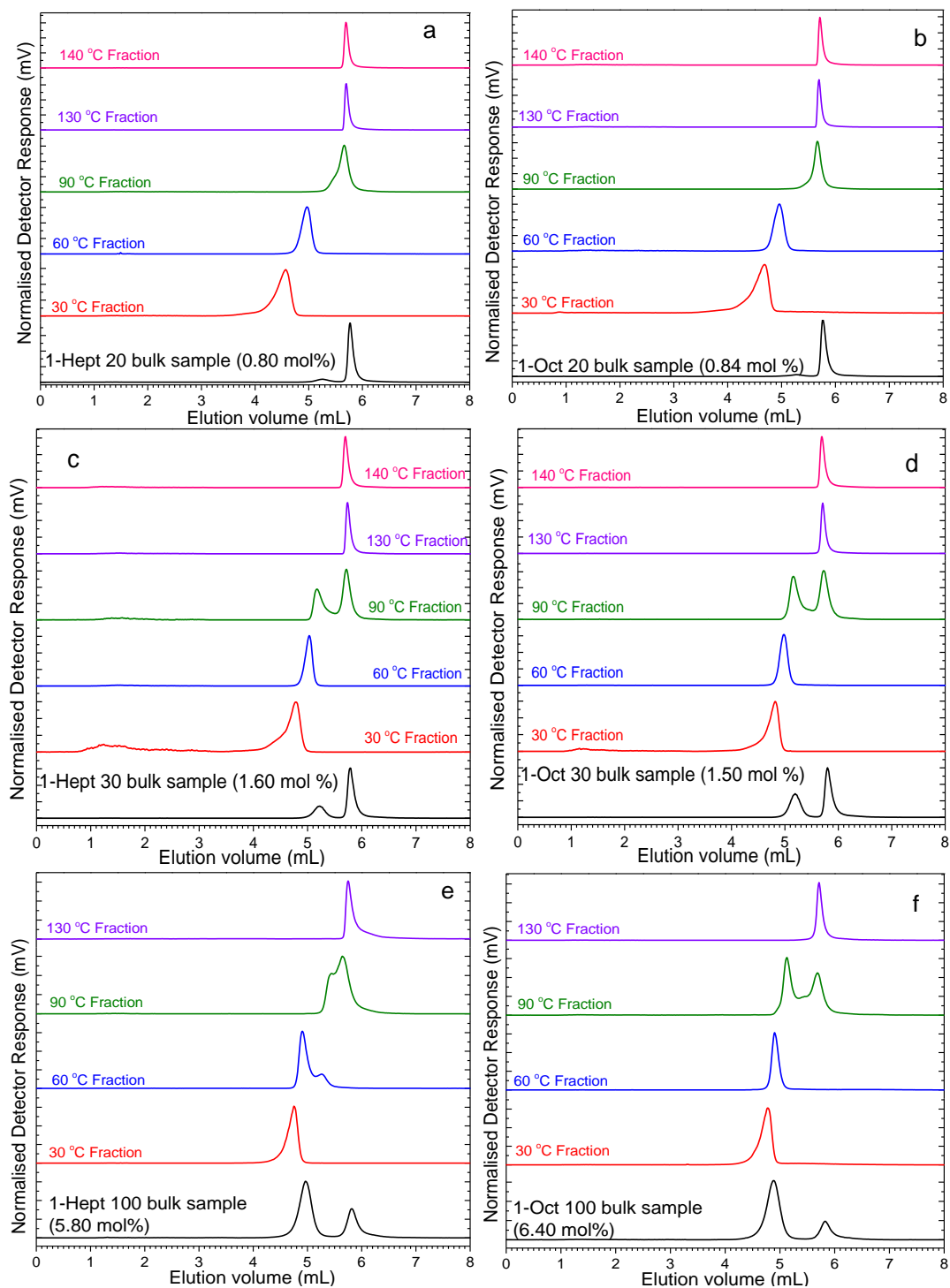
Figure 5.18   HT-HPLC chromatograms of prep-TREF fractions in comparison to their bulk LLDPE resins. EH copolymers are shown in (a), (c) and (e) while EO copolymers are shown in (b), (d) and (f).

Figures 5.18a-f show the HT-PHLC chromatograms of prep-TREF fractions in comparison to their bulk resins. Figures 5.18 a and b compare the low comonomer resin fractions from EH and EO copolymers respectively. Firstly, as the prep-TREF elution temperature increases, the retention volumes (V_r) of the chromatogram peaks increase. This can be explained by the change in chemical composition of the fractions as they become more comprised of copolymer chains with longer uninterrupted methylene sequences. Therefore, van der Waals forces of interaction with the Hypercarb column also increase, leading to longer retention times. The 30 °C fractions elute after the start of the gradient (2.8 mL) indicating that their polymer chains have methylene sequences that are long enough to interact with the Hypercarb column.

Apart from the increase in retention time it can be observed from Figure 5.18a and b that lower eluting fractions have broader CCDs as compared to higher eluting fractions. This also explains well the differences observed in DSC analyses. Hosoda [21] also found high heterogeneity with fractions obtained at lower prep-TREF elution temperatures. Shirayama *et al.* [22] found that the SCBD of low molar mass fractions (similar to 30 °C fractions in the present study) was broader. HT-HPLC results are also in agreement with the Stockmeyer bivariate distribution [16] which suggests that a broader composition distribution is expected for chains with lower average molar mass.

As elution temperature increases, the chemical composition distribution of the fractions become narrower as illustrated in Figure 5.18. The diagrams also show that the bulk LLDPE chemical composition influences that of the prep-TREF fractions. At lower bulk LLDPE comonomer contents, more fractions tend to have V_r closer to that of the bulk sample main peak (Figure 5.1.8a and b). This finding is in good agreement with what was observed with DSC crystallisation peaks (Figure 5.7 and Figure 5.8). The 90 °C fractions from higher comonomer content resins showed marked heterogeneity in CCD. This was seen as the bimodality of the chromatograms especially for fractions of higher comonomer content resins. The fraction appeared to be in the intermediate region between the polyethylene homopolymer and copolymer fractions.
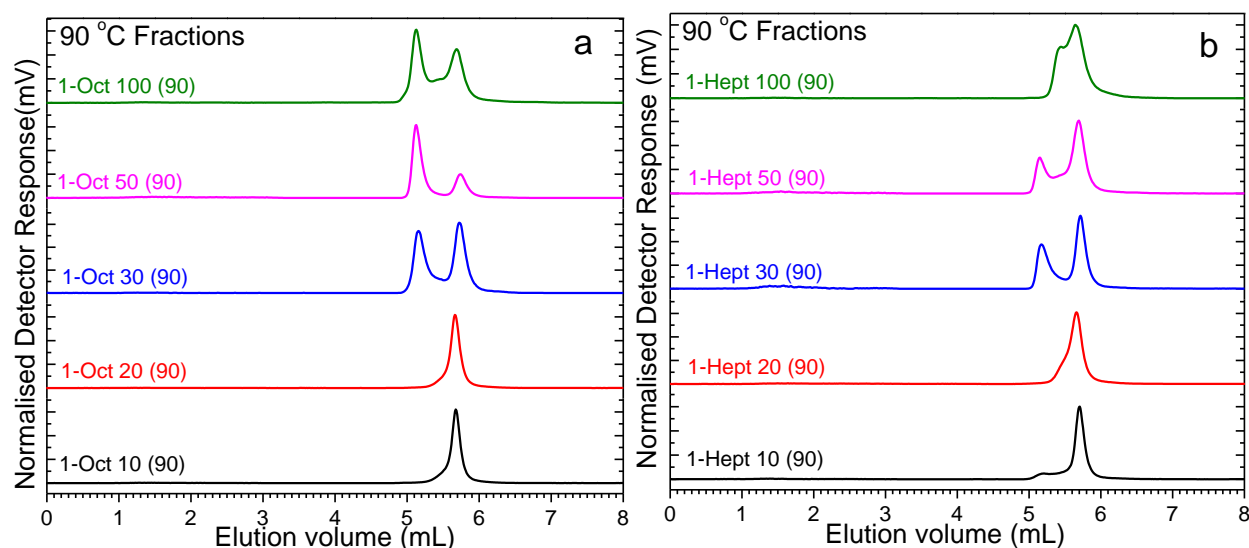
Figure 5.19   HT-HPLC chromatograms of 90 °C prep-TREF fractions showing high chemical composition heterogeneity in fractions obtained from higher comonomer content LLDPE resins.

Figures 5.19a and b show the HT-HPLC chromatograms of the 90 °C prep-TREF fractions of EH and EO copolymers. From the comparison, it can be clearly seen that the heterogeneity in the fractions increases with increase in bulk sample comonomer content. HT-HPLC proved to be a better tool at bringing out CCD heterogeneity as compared to DSC and CRYSTAF. CRYSTAF analyses on the 90 °C fractions (Figure 5.16 and 5.17) are confirmed by HT-HPLC findings which show that chemical composition heterogeneity is responsible for the differences in differential CRYSTAF profiles at higher bulk sample comonomer contents.

Considering the 90 °C fractions of 1-Hept 50 and 1-Oct 50, it can be seen that their chemical compositions are different. 1-Oct 50 (90) is comprised mostly of the lower eluting copolymer and less of the late eluting fraction. The opposite is true for 1-Hept 50 (90), which has more of the late eluting fraction. These differences in material can be crucial at the macroscopic level in influencing physical and mechanical properties. This finding also shows that HPLC can be a powerful tool in monitoring co-crystallisation as it can separate polymer chains according to CCD rather than crystallisabilities.

5.4   Conclusions

For the first time preparative temperature rising elution fractionations on a large number of LLDPE copolymers with varying comonomer type as well as comonomer content were carried out. Two sets of five EH and EO LLDPE copolymers were fractionated using prep-TREF. Weight % recovery of prep-TREF fractions revealed similarities in both EH and EO copolymers at low comonomer contents (< 3 mol %) while differences in the soluble/amorphous fraction could be seen at higher comonomer contents (> 3 mol %).

Analyses of the prep-TREF fractions with HT-SEC revealed unimodal molar mass distributions in all the fractions. Molar masses also increased with prep-TREF elution temperature, an indication of higher eluting fractions having longer chains and lower comonomer incorporation. Interestingly, when molar mass distributions of prep-TREF fractions collected at the same elution were compared, molar mass differences were observed. Fractions molar masses increased with increase in the comonomer content of their bulk LLDPEs, an indication of side chains having an effect on the hydrodynamic volume (V_h).

The comparisons of EH and EO prep-TREF fractions revealed close similarities in DSC crystallisation as well as melting behaviour. Minor differences were, however, seen with some of the fractions, and this was attributed to experimental errors as well as slight differences in comonomer contents of the bulk samples. Differences in prep-TREF fractions collected at similar elution temperatures were also confirmed by DSC through their differences in T_m and crystallinity (X_c).

Solution ^{13}C NMR revealed that the comonomer contents of the fractions collected at similar prep-TREF elution temperatures from LLDPE resins of different comonomer contents are also different. A further correlation of the fractions' comonomer contents to those of their bulk LLDPEs, showed a linear relationship which indicated that higher comonomer bulk samples give fractions with higher comonomer contents. The comonomer contents of the EH and EO 60 and 90 °C fractions were comparable at roughly similar comonomer contents of their bulk samples, which was further evidence of close similarity of the two types of copolymers.

A detailed chemical composition distribution comparison of EH and EO copolymer prep-TREF fractions by CRYSTAF showed highly comparable profiles at lower comonomer content resins (< 3 mol %). Minor differences in the chemical composition distributions of 60 and 90 °C fractions were observed at higher bulk resin comonomer contents. HT-HPLC confirmed the heterogeneous nature of 90 °C with good separation of the copolymer fraction components.

5.5   References

1.   Jorgensen J. K., Larsen A., and Helland I., *e-Polymers*, **2010**, 10(1), 1596–1612.

2.   Cheruthazhekatt S., Pijpers T. F. J., Mathot V. B. F., and Pasch H., *Macromol. Symp.*, **2013**, 330(1), 22–29.

3.   De Goede E., Mallon P., and Pasch H., *Macromol. Mater. Eng.*, **2010**, 295(4), 366–373.

4.   Zhou X. and Hay J. N., *Eur. Polym. J.*, **1993**, 29(2–3), 291–300.

5.   Xu J. and Feng L., *Eur. Polym. J.*, **2000**, 36(5), 867–878.

6.   Xue Y., Fan Y., Bo S., and Ji X., *Eur. Polym. J.*, **2011**, 47(8), 1646–1653.

7.   Karbashewski E., Kale L., Rudin A., Tchir W. J., Cook D. G., and Pronovost J. O., *J. Appl. Polym. Sci.*, **1992**, 44(3), 425–434.

8.   Pasch H., De Goede E., and Mallon P., *Macromol. Symp.*, **2012**, 312(1), 174–190.

9.   Luruli N., Heinz L. C., Grumel V., Brüll R., Pasch H., and Raubenheimer H. G., *Polymer*, **2006**, 47(1), 56–66.

10.   Pasch H., Malik M. I., and Macko T., *Adv. Polym. Sci.*, **2013**, 251, 77–140.

11.   Xu J., Feng L., Yang S., Yang Y., and Kong X., *Eur. Polym. J.*, **1998**, 34, 431–434.

12.   Anantawaraskul S., Soares J. B. P., and Wood-Adams P. M., *J. Polym. Sci., Part B: Polym. Phys.*, **2003**, 41(14), 1762–1778.

13.   Anantawaraskul S., Sottesakul S., Siriwongsarn E., and Soares J. B. P., *Macromol. Symp.*, **2013**, 330(1), 123–131.

14.   Mncwabe S., Luruli N., Marantos E., Nhlapo P., and Botha L., *Macromol. Symp.*, **2012**, 313-314(1), 33–42.

15.   Starck P., *Polym. Int.*, **1996**, 40(2), 111–122.

16.   Soares J. B. P. and Hamielec A. E., *Polymer*, **1995**, 36(8), 1639–1654.

17. Anantawaraskul S., Soares J. B. P., and Wood-Adams P. M., *Fractionation of Semicrystalline Polymers by Crystallization Analysis Fractionationand Temperature Rising Elution Fractionation*, in *Polymer Analysis Polymer Theory*, Springer, **2005,** 1–54.

18. Quijada R., Dupont J., Miranda M. S. L., Scipioni R. B., and Galland G. B., *Macromol. Chem. Phys.*, **1995**, 196(12), 3991–4000.

19. Byun D.-J. and Kim S. Y., *Macromolecules*, **2000**, 33(6), 1921–1923.

20. Mirabella F. M. and Ford E. A., *J. Polym. Sci., Part B: Polym. Phys.*, **1987**, 25(4), 777–790.

21. Hosoda S., *Polym. J.*, **1988**, 20(5), 383–397.

22. Shirayama K., Okada T., and Kita S. I., *J. Polym. Sci., Part A: Polym. Chem.*, **1965**, 3(3), 907–916.

Chapter 6

Conclusions and recommendations

6.1   Summary

The main aim of the study was to investigate the microstructure of EH and EO resins, with the intention of getting detailed information on the similarities and differences of the two types of resins. This was achieved through the use of various advanced analytical as well as fractionation techniques. The correlation of such information to that obtained from mechanical and physical analyses will be useful in deciding whether 1-heptene can be used instead of 1-octene in the manufacture of commercial LLDPE.

6.2   Conclusions

LLDPE resins with different comonomer contents were successfully synthesised. Ziegler-Natta LLDPE resins containing comparable 1-heptene and 1-octene contents were obtained from SASOL. Metallocene LLDPE was locally synthesised via a semi-batch process.

HT-SEC analyses were carried out on the bulk samples and symmetrical unimodal molar mass distributions on all EH and EO copolymers were obtained. This indicated uniform distribution of copolymer chains in all the resins. The type of the comonomer and its content did not have any significant influence on the bulk sample molar masses or their dispersities.

DSC analyses revealed changes in bulk LLDPE T_m and T_c upon comonomer incorporation, which were comparable for both sets of EH and EO copolymers. Crystallinity determinations also revealed close similarities in the effects of 1-heptene and 1-octene on bulk resin melting properties. In both sets of copolymers, heterogeneous fractions were observed at almost similar comonomer contents ($\approx$ 4.30 mol % in EH and 5.10 mol % in EO copolymers). The deconvoluted DSC crystallisation curves showed presence of three main fractions which differed in T_m and crystallinity. Differences in crystallinity were also confirmed by FTIR.

Chemical composition analyses through CRYSTAF also confirmed the presence of three main fractions from each of the LLDPE samples. Theses fractions were identified as being soluble (contains amorphous copolymer chains), semi-crystalline and crystalline. Both EH and EO copolymers showed the same trend (increase in soluble fractions and decrease in the crystalline fractions) with increase in the comonomer content. A comparison of EH and EO CRYSTAF profiles at higher comonomer contents revealed differences in the soluble fractions at higher comonomer contents. This was attributed to the slightly better ability of 1-octene in inducing formation of soluble/amorphous polyethylene as compared to 1-heptene. However, the differences could have been more influenced by the slightly higher comonomer contents of EO resins. Metallocene resins showed similar trends in CRYSTAF profiles as was seen with Ziegler-Natta LLDPE.

Further analyses of CCD with HT-HPLC revealed the presence of a copolymer fraction as well as a polyethylene fraction. These fractions were observable in all EH and EO copolymers except those with the lowest comonomer content (0.35 mol % EO and 0.44 mol % EH copolymers). In both sets of LLDPEs, the copolymer peak increased in size (a shift towards lower elution volumes was also observed) with increase in the comonomer content while the polyethylene peak decreased in size. A correlation of the polyethylene peak areas to bulk sample comonomer content also showed a linear relationship which was comparable to that observed from CRYSTAF analyses.HT-2D-LC showed that the copolymer fraction had lower molar masses in comparison to the polyethylene homopolymer fraction.

Prep-TREF fractionations of the ten EH and EO LLDPE copolymers were successfully carried out. Through prep-TREF fractionation it was confirmed that 1-octene is marginally better at reducing the resin crystallinity as compared to 1-heptene. However, the abilities of the two comonomers in influencing change in crystalline fractions were comparable. Only slight differences in the soluble and semi-crystalline fractions were noticeable. For both sets of EH and EO resins, soluble material increased while crystalline fractions decreased which was in good agreement with CRYSTAF and HT-HPLC findings. In order to achieve the same ratio of soluble/crystalline material in EH and EO LLDPEs, slightly higher amounts of 1-heptene have to be used.

Analyses of prep-TREF fractions with HT-SEC showed unimodal distributions in molar masses. Molar masses increased with prep-TREF elution temperature. In addition, molar masses of the fractions collected at similar prep-TREF elution temperatures increased as their bulk LLDPE comonomer contents increased. Higher comonomer content resins gave fractions with higher molar masses, and this was attributed to the effect of the comonomer content on molar mass.

Studies on the thermal properties of the prep-TREF fractions revealed two important findings. Firstly, it was shown through correlation of T_m and T_c of the fractions to their bulk sample comonomer contents that fraction microstructures are dependent on those of their bulk LLDPEs. Secondly, it was revealed that fractions of EH and EO resins of comparable comonomer contents have highly comparable crystallisation exotherms indicating almost similar microstructures. This was a highly significant finding as comparison of prep-TREF fractions allows for a closer look at the microstructures of the two types of resins.

Solution ^{13}C NMR confirmed the chemical composition dependency of the prep-TREF fractions on that of their bulk LLDPEs. A correlation of prep-TREF fraction comonomer content showed that if the comonomer content of the bulk LLDPE is high, the fraction comonomer content will also be high. Such a dependency has never been observed before with prep-TREF.

CRYSTAF and HT-HPLC were used to compare the chemical compositions of the fractions from different resins. At lower bulk sample comonomer contents, the 60 and 90 °C CRYSTAF profiles of EH and EO TREF fractions were highly comparable. However, at higher bulk sample comonomer contents minor differences in the CRYSTAF profiles were observed. HT-HPLC showed that the chemical compositions of the mid eluting TREF fractions (90°C) were heterogeneous in CCD and this was prevalent at higher comonomer contents. The type of comonomer did not have any influence on the heterogeneity of the fractions as similar trends were observed for both sets of EH and EO prep-TREF fractions.

Mechanical properties of the bulk samples were successfully determined. At low comonomer contents (up to about 3 mol %) the resins showed close similarities in tensile properties and Young's modulus. At higher comonomer contents (> 3 mol %) differences in the tensile strength and Young's modulus were observed. EO copolymers showed reduced tensile strength and modulus in comparison to EH copolymers. This was attributed to the slightly higher

soluble/amorphous fraction in EO copolymers which was a result of 1-octene's better ability to reduce the copolymer crystallinity.

It was seen that mechanical properties of EH and EO copolymers are highly dependent on the microstructure of the bulk resins. In addition, the amorphous fractions also play an important role in the mechanical properties of the LLDPE material. 1-heptene can therefore be a good substitute for 1-octene at low comonomer contents (< 3 mol %). Slightly higher amounts of 1-heptene may have to be used in order to induce formation of more amorphous/soluble material for higher comonomer content resins.

6.3   Recommendations

➢ Other physical properties such a clarity tests and performance may be conducted on the blown films of ethylene/1-heptene and ethylene/1-octene copolymers to compare the effectiveness of 1-heptene in reducing haziness since outward appearance also plays a role when consumers are taken into account. Recent studies have compared properties of LLDPE blown films of 1-hexene and 1-octene with good results [1, 2].

➢ Successive self-annealing DSC has been used successfully [3] for the fractionation and analysis of LLDPE resins. After prep-TREF fractionation, it becomes extremely difficult to fractionate further the obtained copolymer fractions. Therefore, prep-TREF fractions can be analysed using this technique to help understand why the chemical composition of similar TREF fractions varies with the bulk sample chemical composition. Depending on sample quantities, mechanical analyses such as micro hardness tests can also be performed on the 90 °C prep-TREF fractions to help understand the differences in microstructure.

➢ Crystallisation elution fractionation (CEF) is a new technique of polyolefin analysis [4-6]. It can be equipped with IR detectors which can detect methyl group concentrations. It would be interesting to compare the CEF profiles with CRYATAF profiles for the same copolymers as well as establish the comonomer distribution in the soluble, semi-crystalline and crystalline fractions.

➢ Terpolymers of ethylene with 1-octene and 1-heptene are an interesting alternative. As seen from the present study 1-heptene is as effective in changing the chemical

composition of LLDPE as 1-octene when comonomer content is varied. These terpolymers would therefore considerably cut on quantities of 1-octene required for LLDPE while maintaining similar physical properties. Therefore, an investigation of terpolymers containing ethylene, 1-heptene and 1-octene can be carried out at different monomer ratios.

6.4   References

1.   Kim Y.-M. and Park J.-K., *J. Appl. Polym. Sci.*, **1996**, 61(13), 2315–2324.

2.   Zhang X. M., Elkoun S., Ajji A., and Huneault M. A., *J. Plast. Film Sheeting*, **2004**, 20(1), 43–52.

3.   Mathot V. and Pijpers M., *Polym. Bull.*, **1984**, 11(3), 297–304.

4.   Monrabal B., Sancho-Tello J., Mayo N., and Romero L., *Macromol. Symp.*, **2007**, 257(1), 71–79.

5.   Monrabal B. and Romero L., *Macromol. Chem. Phys.*, **2014**, 215(18), 1818–1828.

6.   Cheruthazhekatt S., Mayo N., Monrabal B., and Pasch H., *Macromol. Chem. Phys.*, **2013**, 214(19), 2165–2171.

Appendix A   Molar mass data
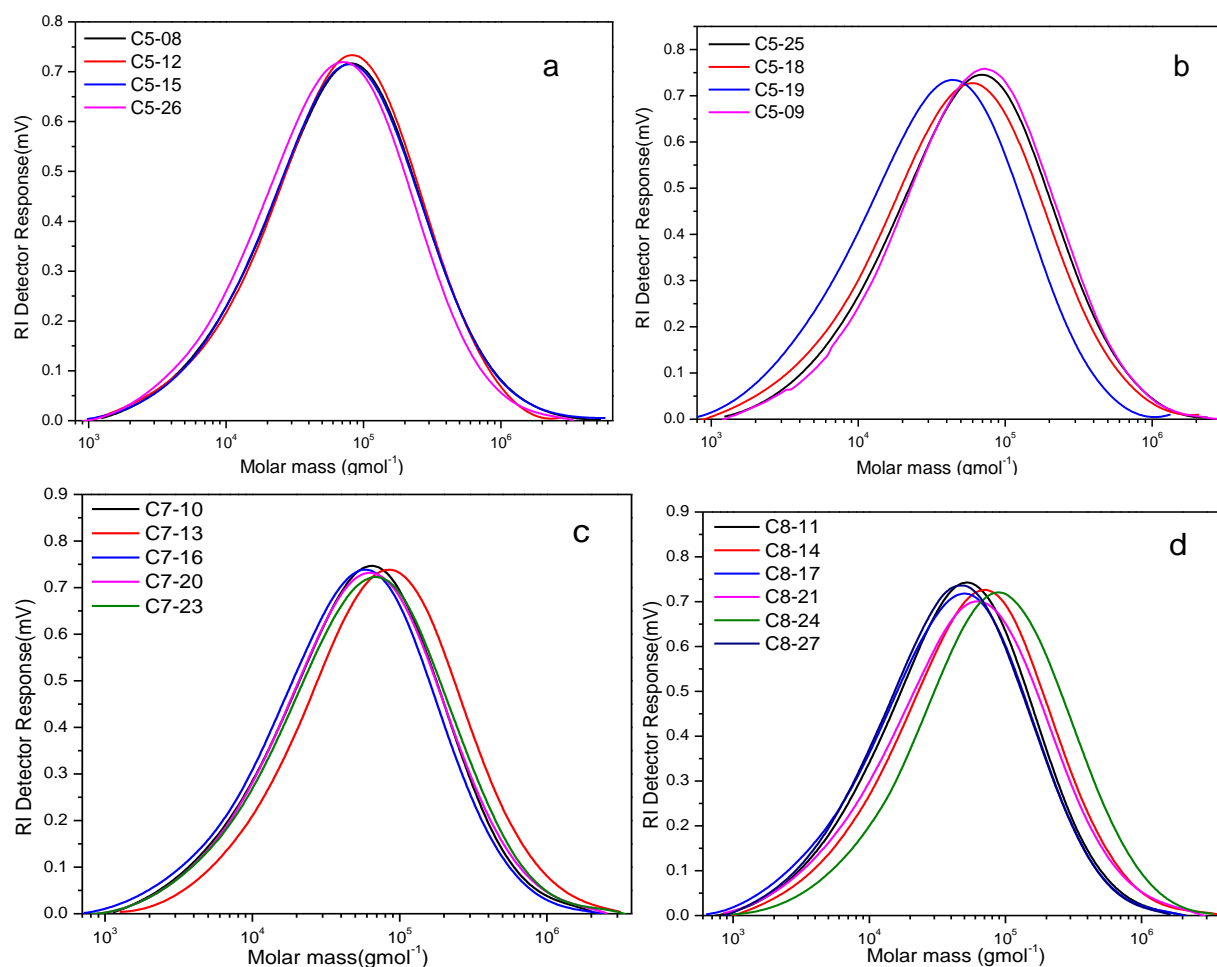
Figure A.1   **Molar mass distributions of low molar mass (68 – 160 kgmol^{-1}) ZN-LLDPE resins. Ethylene/1-pentene copolymers are shown in (a) and (b) while ethylene/1-heptene and ethylene/1-octene are shown in (c) and (d) respectively.**

Table A.1   Summary of ethylene/1-pentene copolymer properties (Set A)*

Sample	α-Olefin used(mL)	Yield (g)	Comonomer content (mol %)	M_w (× kg mol^{-1})	D	T_m (°C)	T_c (°C)	X_c (%)
C5-09	10	28.96	0.69	119.1	4.2	126.6	115.3	59.8
C5-25	20	29.89	1.75	116.1	4.5	125.0	113.8	53.4
C5-18	30	40.75	3.16	103.7	4.9	124.1	112.5	42.4
C5-19	40	29.24	4.50	68.4	4.4	122.9	112.5	37.5

*Set A LLDPE resins have slightly lower molar masses as compared to those of set B.

Table A.2   Summary of ethylene/1-pentene copymer prperties (Set B)*

Sample	α-Olefin used(mL)	Yield (g)	Comonomer content (mol %)	M_w (× kg mol^{-1})	D	T_m (°C)	T_c (°C)	X_c (%)
C5-08	10	40.23	0.92	154.6	5.3	126.6	115.1	58.4
C5-12	20	23.00	1.90	140.0	4.9	125.0	113.3	51.4
C5-15	30	37.20	2.93	158.5	5.6	124.1	112.2	45.6
C5-26	50	24.92	4.03	129.0	5.0	123.7	111.9	35.6

*Set B LLDPE resins have slightly higher molar masses as compared to those of set A.

Table A.3   Summary of ethylene/1-heptene low molar mass ZN-LLDPE properties.

Sample	α-Olefin used(mL)	Yield (g)	Comonomer content (mol %)	M_w (× kg mol^{-1})	D	T_m (°C)	T_c (°C)	X_c (%)
C7-10	10	40.85	0.32	108.3	4.6	128.5	117.0	61.1
C7-13	20	64.28	0.78	153.9	4.7	127.8	116.1	54.7
C7-16	30	43.51	1.74	98.3	4.9	126.5	115.2	48.3
C7-20	40	68.03	2.58	115.4	4.8	125.6	114.7	43.0
C7-23	50	60.56	2.52	123.4	5.0	125.3	114.0	41.2

Table A.4   Summary of ethylene/1-octene low molar mass ZN-LLDPE properties.

Sample	α-Olefin used(mL)	Yield (g)	Comonomer content (mol %)	M_w ($\times$ kg mol^{-1})	D	T_m (°C)	T_c (°C)	X_c (%)
C8-11	10	35.14	0.46	89.3	4.6	129.3	117.2	69.1
C8-14	20	64.32	0.59	126.0	5.2	127.7	116.4	55.6
C8-17	30	61.34	1.50	84	5.1	126.8	116.3	53.0
C8-21	40	72.43	1.70	118.0	5.7	126.5	115.5	46.7
C8-24	50	18.6	1.37	163.5	5.1	126.3	114.8	49.7
C8-27	50	62.08	2.44	82.4	4.5	126.0	115.4	43.4

Appendix B   NMR data
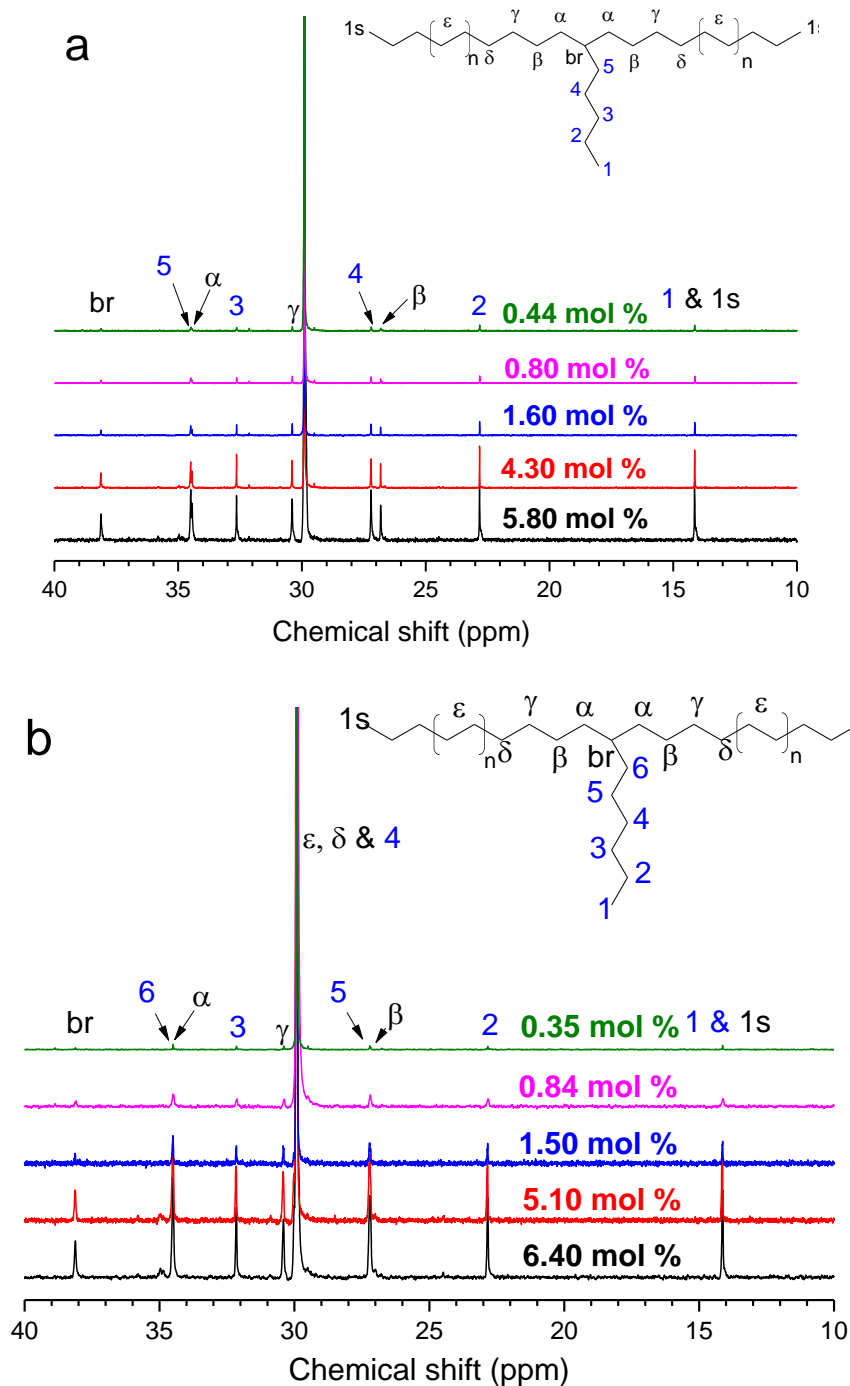
Figure B.1   Solution ¹³C NMR spectra of high molecular weight ZN-LLDPE resins. EH copolymers are shown in (a) and EO copolymers in (b).
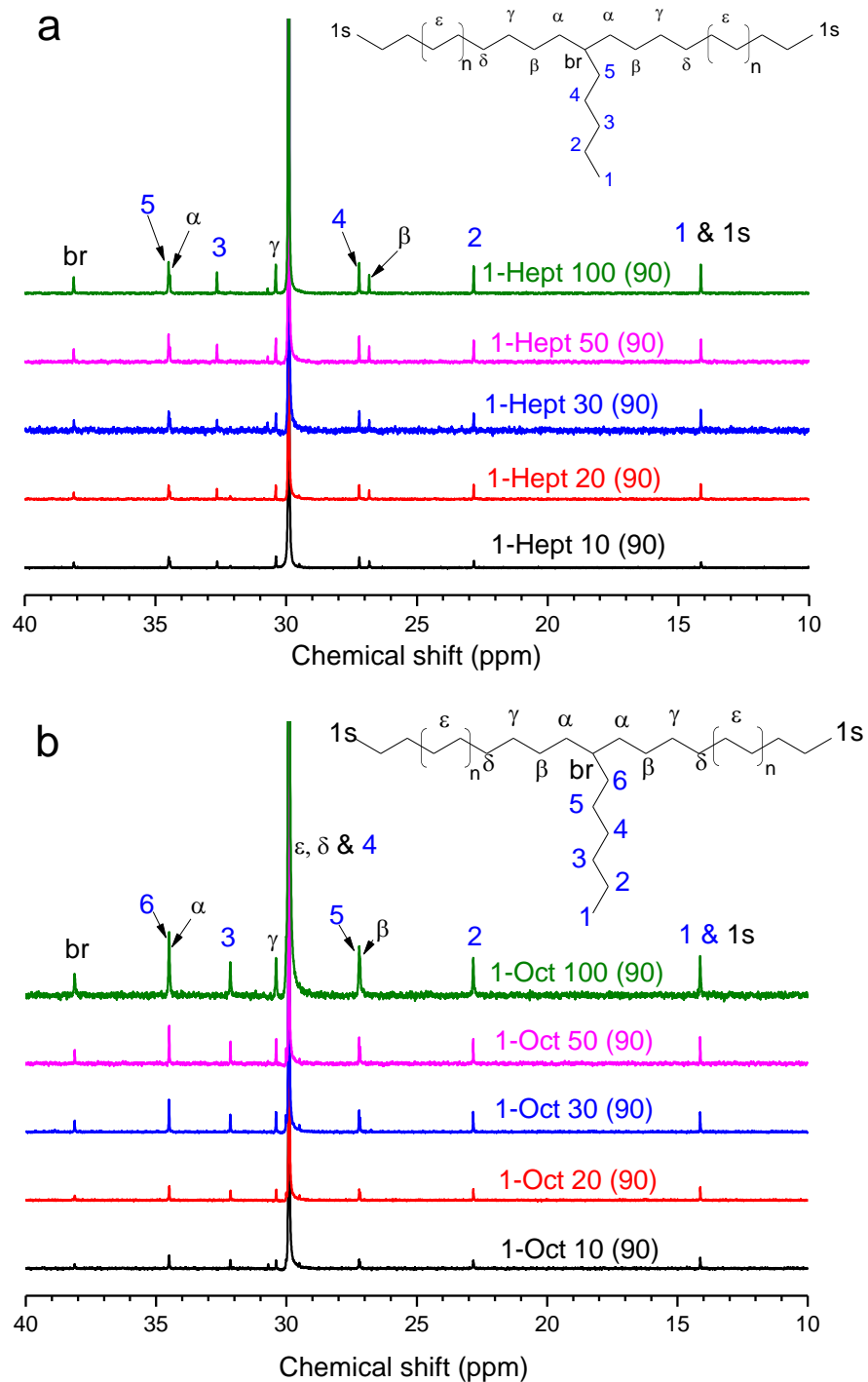
Figure B.2 **Normalised solution ^{13}C NMR spectra of 90 °C fraction of EH (a) and EO (b) copolymers showing increase in spectral signals with increase in the bulk sample comonomer contents.**
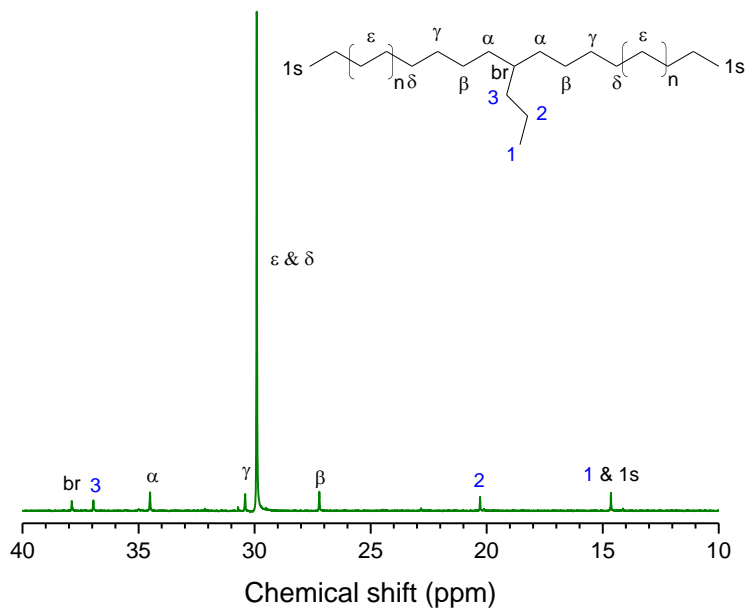
Figure B.3   Solution ^{13}C NMR spectrum of C5-26.
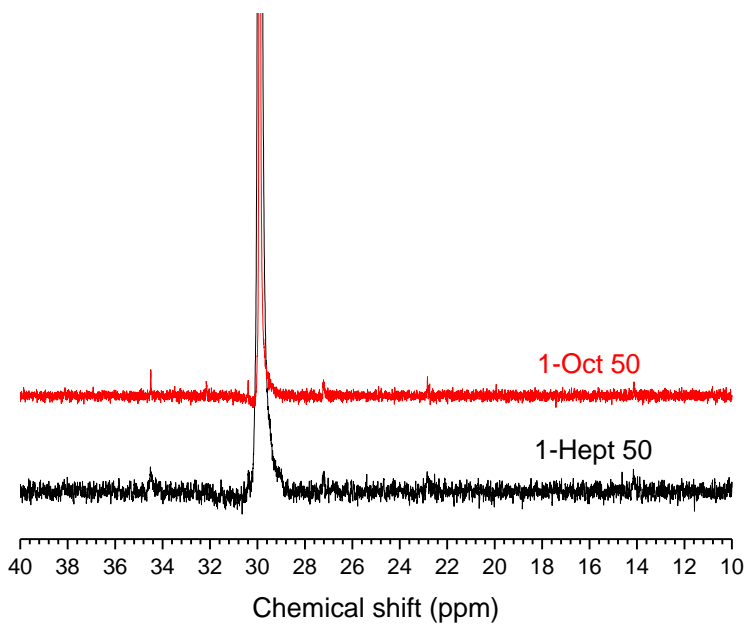
Figure B.4   Normalised solution ^{13}C NMR spectra of 130 °C fractions from 1-Oct 50 and 1-Hept 50.

Appendix C   DSC data
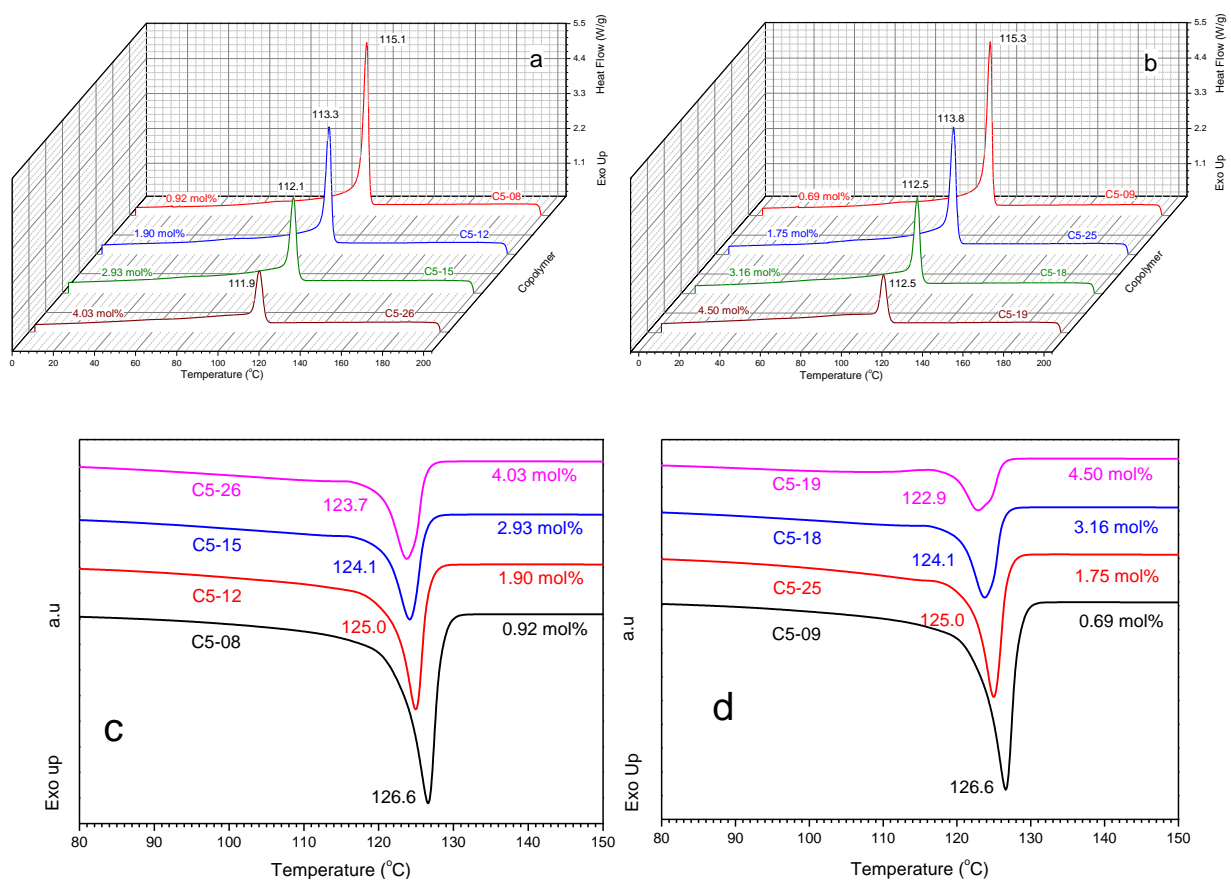
Figure C.1   **DSC crystallisation curves (a and b) and melting endotherms (c and d) for low molar mass ZN-LLDPE ethylene/1-pentene copolymers.**
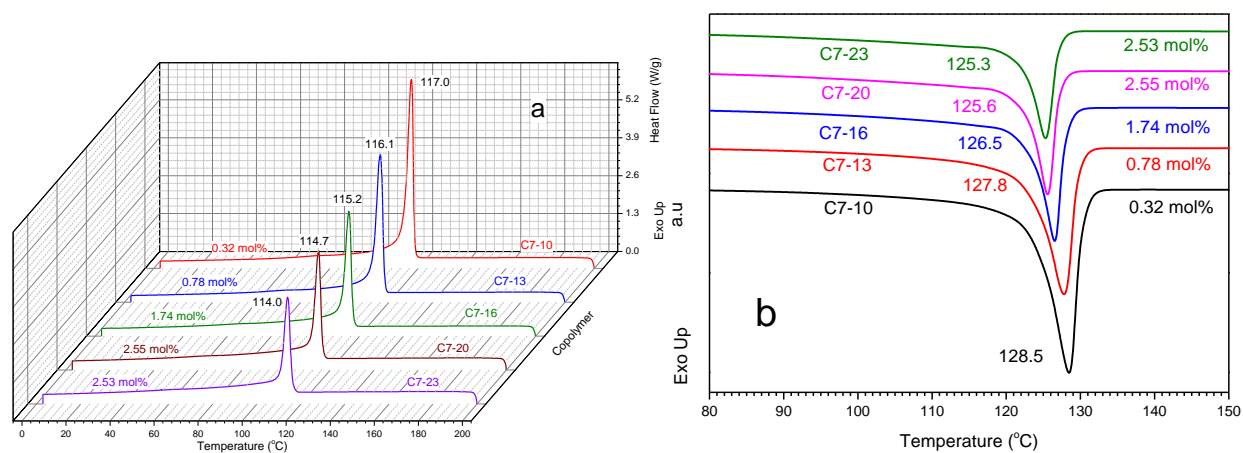
Figure C.2   **DSC crystallisation curves (a) and melting endorthems (b) of low molar mass ZN-LLDPE ethylene/1-heptene copolymers.**
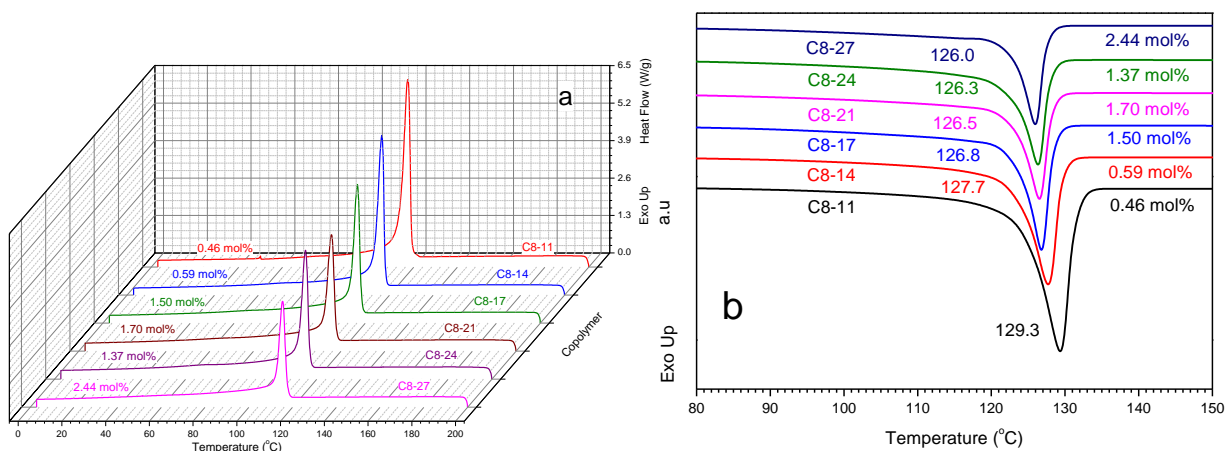
Figure C.3   **DSC crystallisation curves (a) and melting endotherms (b) of low molar mass ethylene/1-octene ZN-LLDPE.**

130
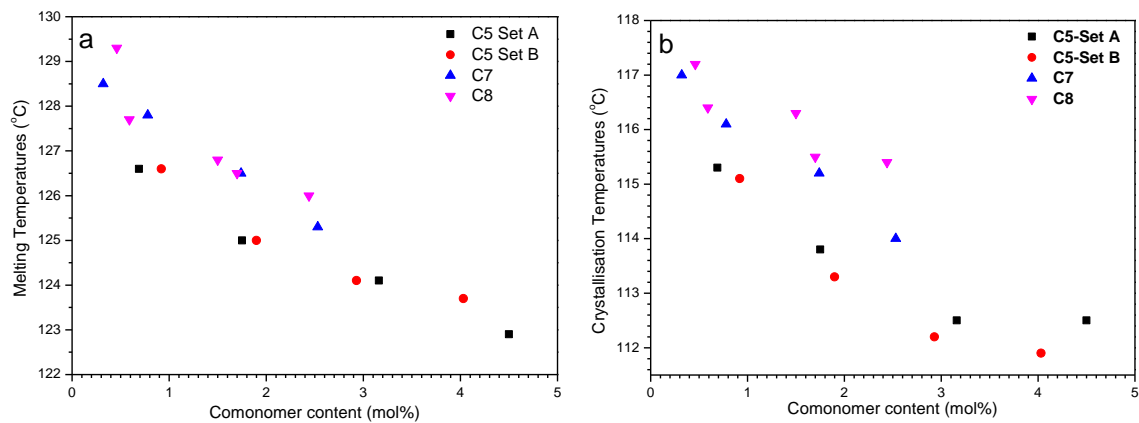
Figure C.4   Plots showing the variation of melting temperatures (a) and crystallisation temperatures (b) of low molar mass ZN-LLDPE with increase in comonomer content.

Appendix D   TREF data
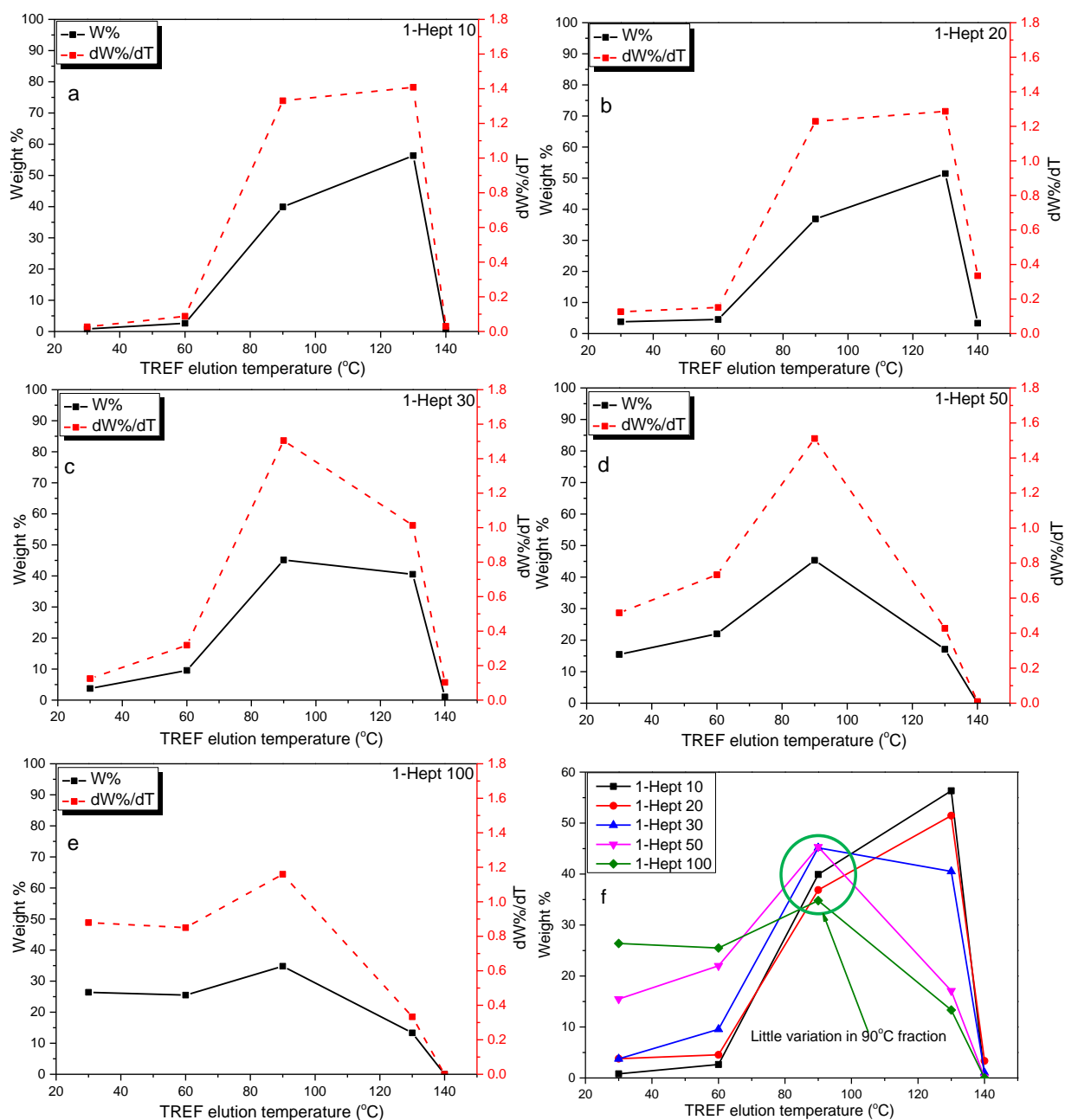
Figure D.1   Plots of weight % and dW%/dT against prep-TREF elution temperature (a-e) and a comparison of the weight % of ethylene/1-heptene high molar mass ZN-LLDPE copolymers (f).
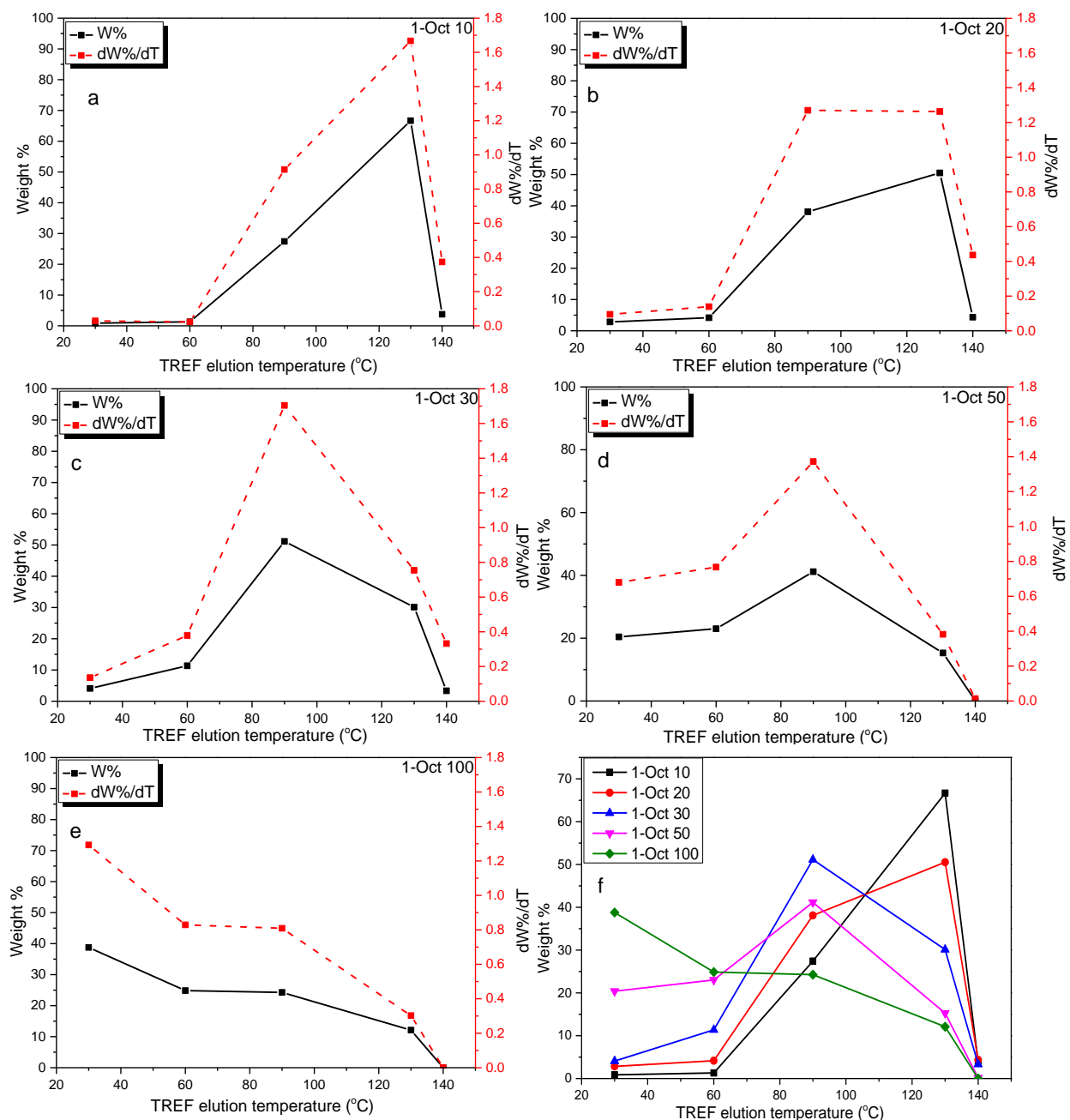
Figure D.2   Plots of weight % and dW/dT against TREF elution temperature (a-e) and a comparison of the weight % of ethylene/1-octene high molecular weight ZN-LLDPE copolymers (f).

Appendix E   Mechanical properties

Table E.1   **Summary of mechanical properties of high molecular weight Ziegler-Natta polyethylene, ethylene/1-heptene and ethylene/1-octene samples.**

Sample Name	[C] mol %	[C] weight %	Tensile Strength (MPa)	Young's modulus (MPa)	Stiffness ($\times 10^3$ Nm)
1-Hept 10	0.44	1.52	29.82±0.47	530.3±30.4	104.4±6.0
1-Hept 20	0.80	2.75	25.71±0.41	442.1±17.1	85.1±4.7
1-Hept 30	1.60	5.39	21.12±0.34	310.4±19.4	59.4±2.8
1-Hept 50	4.30	13.59	12.71±0.34	137.3±13.8	25.8±2.6
1-Hept 100	5.80	17.73	11.73±1.01	83.16±9.2	15.7±1.7
1-Oct 10	0.35	1.39	36.28±0.70	618.0±81.5	114.4±17.6
1-Oct 20	0.84	3.28	31.86±3.11	527.2±38.6	96.4±7.1
1-Oct 30	1.50	5.74	19.25±0.88	274.4±19.24	49.9±3.5
1-Oct 50	5.10	17.70	9.36±0.63	96.6±4.1	18.3±0.7
1-Oct 100	6.40	21.48	7.06±0.55	53.32±5.0	10.1±0.9
Polyethylene (ZN)	0	0	38.32±2.88	890.6±48.0	182.4±15.2
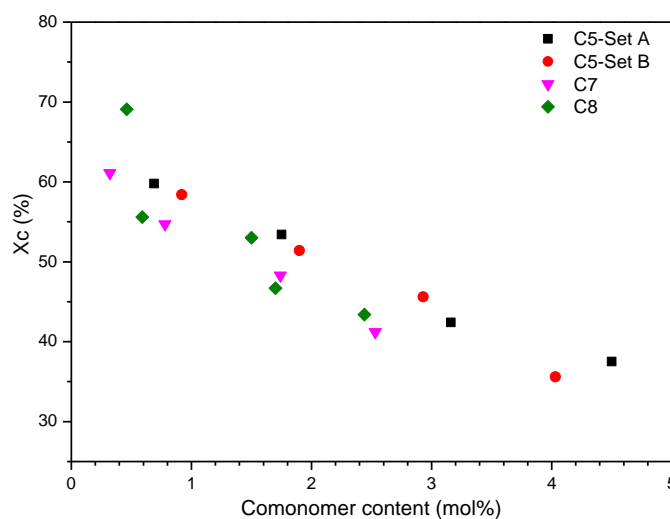
Figure E.1   **Effect of short chain branching on the crystallinity of low molar mass ZN-LLDPE.**
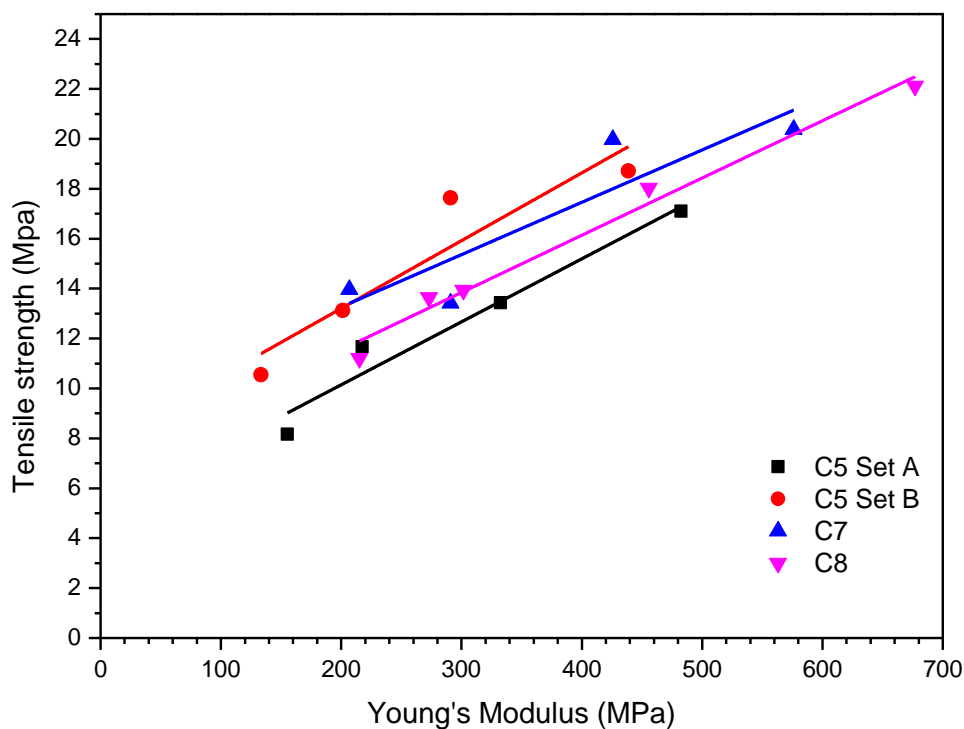
Figure E.2   **Relationship between tensile strength and Young's modulus for low molar mass ZN-LLDPE copolymers.**
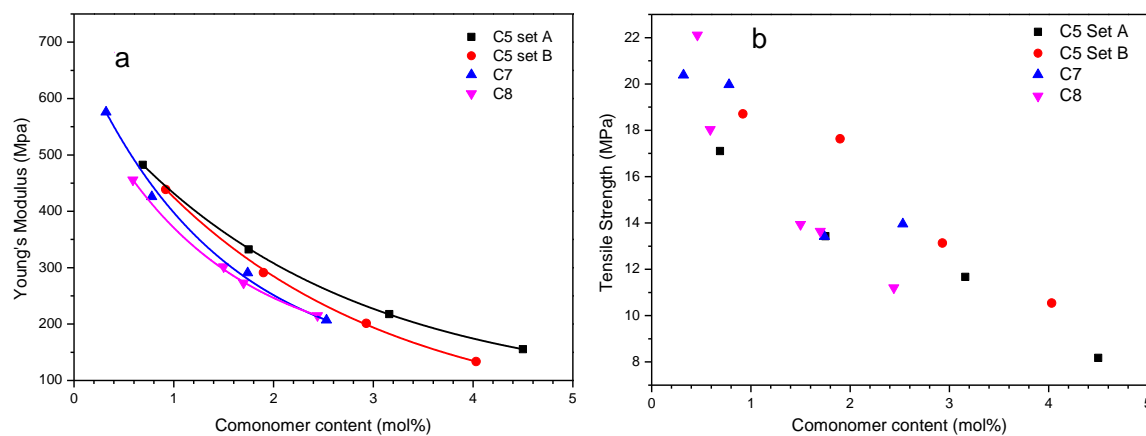
Figure E.3   **Variation of Young's modulus (a) and tensile strength (b) of low molar mass ZN-LLDPE with increase in comonomer content.**

Appendix F   Metallocene LLDPE polymerisations

Table F.1   **Comonomer used, yield comonomer content and DSC related data of ethylene/1-pentene m-LLDPE.**

Sample[a]	α-Olefin used (mL)	Comonomer used (mol %)	Yield (g)	Catalyst Activity*	T_m (°C)	T_c (°C)	X_c (%)
1-P-1	1	0.89	19.93	1.70	129.9	116.7	61.6
1-P-2	2	1.77	21.34	1.82	128.7	115.6	61.2
1-P-4	4	3.54	23.73	2.02	128.1	116.3	60.4
1-P-6	6	5.31	23.62	2.01	126.5	115.1	51.5
1-P-8	8	7.08	24.66	2.10	126.0	114.4	47.7
1-P-10	10	8.85	27.55	2.35	123.9	112.1	41.6
1-P-15	15	13.28	23.31	1.99	123.8	112.3	36.2
PE (M)	0	0	18.00	1.53	131.6	117.6	69.6

*($\times 10^3$ kg Polymer/mol Zr h)

[a] Polymerisation time = 2 hours, Total volume of toluene = 120 mL, Ethylene pressure = 800 KPa, Temperature 75 °C, Catalyst {Dichloro[rac-ethylene bis(indenyl)] Zirconium}= 5.87 μmol

Table F.2   **Comonomer used, yield comonomer content and DSC related data of ethylene/1-heptene m-LLDPE.**

Sample	α-Olefin used (mL)	Comonomer used (mol %)	Yield (g)	Catalyst activity *	T_m (°C)	T_c (°C)	X_c (%)
1-H-1	1	0.69	19.89	1.69	129.8	116.5	64.1
1-H-2	2	1.38	19.91	1.70	128.4	116.0	57.2
1-H-4	4	2.75	20.57	1.75	127.1	114.9	55.7
1-H-6	6	4.13	22.06	1.88	126.8	115.0	53.3
1-H-8	8	5.51	23.46	2.00	126.5	114.6	46.7
1-H-10	10	6.89	25.05	2.13	124.5	113.0	43.1
1-H-15	15	10.32	25.97	2.21	123.6	112.7	33.5

*($\times 10^3$ kg Polymer/mol Zr h)

Table F.3   **Comonomer used, yield comonomer content and DSC related data of ethylene/1-octene m-LLDPE.**

Sample	α-Olefin used (mL)	Comonomer used (mol %)	Yield (g)	Catalyst Activity*	T_m (°C)	T_c (°C)	X_c (%)
1-O-1	1	0.62	17.71	1.51	128.6	115.0	58.8
1-O-2	2	1.24	18.54	1.58	128.5	116.0	58.1
1-O-4	4	2.50	16.56	1.41	125.4	113.3	51.8
1-O-6	6	3.75	23.49	2.00	126.7	115.0	50.0
1-O-8	8	5.00	22.99	1.96	127.0	115.1	49.7
1-O-10	10	6.24	25.27	2.15	126.5	114.7	46.8
1-O-15	15	9.37	29.85	2.54	122.8	111.7	37.0

*($\times 10^3$ kg Polymer/mol Zr h)